

2019 年度  
博 士 論 文

酪農学園大学大学院  
酪農学研究科 食生産利用科学専攻 博士課程  
環境リモートセンシング研究室

Tsedendamba Purevsuren

**2019 School Year**

**Doctor Thesis:**

北東アジアにおけるダスト輸送について  
----ゴビ砂漠地域におけるダストの発生、  
分布とその輸送の事例研究

**Dust transportation of Northeast Asia:  
A case study of dust emission,  
distribution and transport from Gobi  
Desert region**

**21633003 ツェデンダンバ プレブスレン  
Tsedendamba Purevsuren**

**Supervisor: Prof. Hoshino Buho  
Graduate School of Dairy Science  
Rakuno Gakuen University**

## Table of Content

Abstract .....	1
Introduction .....	4
Aeolian dust .....	4
Dust source.....	7
Main Sources.....	10
Physical and chemical features of dust source soils.....	11
Mineralogy of dust particles .....	12
Dust source in East Asia .....	12
Study objectives.....	14
Chapter 1 Specific features of desert zone in Mongolia .....	16
1.1 Introduction .....	16
1.2 Geographic distribution of desert steppe zone and desert zone .....	16
1.3 Grassland ecosystem of desert steppe region.....	17
1.4 Climatic conditions of the Gobi region.....	18
1.5 Current climate change .....	19
Chapter 2 Relationship between vegetation coverage and dust storms over the Gobi area.....	21
2.1 Introduction .....	21
2.2 Study area.....	22
2.3 Material and methods.....	24
2.4 Result .....	26
2.4.1 Changes in mean NDVI, dust storm and precipitation in study area during 2000-2013.....	26
2.4.2 Relations between NDVI, Soil moisture and elevation in spring 2013... ..	28
2.5 Conclusion.....	29
Chapter 3 Overview of dust storms in Mongolia.....	30
3.1 Introduction .....	30
3.1.1 Distribution of number days with dust storms and dusty day.....	32
3.1.2 Distribution of number of dusty days .....	33

3.1.3 Annual and daily variations of dust storms.....	34
3.1.4 Duration of dust storms .....	35
3.1.5 Dust storm in Central Asia.....	38
3.2 Result .....	39
3.2.1 Duration of dust storm of Gobi area .....	39
3.2.1.1 Data and methods .....	39
3.2.2.2 Maximum duration day of dust storm .....	40
3.3 Discussion.....	41
3.4 Conclusion .....	41
Chapter 4 Northeast Asian dust transport: A case study of a dust storm event from 28 March to 2 April 2012 .....	42
4.1 Introduction .....	42
4.2 Materials and methods .....	43
4.2.1 Description of dust event .....	43
4.2.2 Surface dust concentration data.....	44
4.2.3 LiDAR Monitoring data for AD-Net (The Asian Dust and Aerosol Lidar Observation Network) .....	47
4.2.4 Meteorological data .....	48
4.2.5 Trajectory method.....	48
4.3 Result.....	49
4.3.1 Number of dusty days, its trend and PM <sub>10</sub> concentration of spring season at Dalanzadgad, Sainshand and Zamyn-Uud stations, Mongolia .....	49
4.3.2 North East Asian dust transport: A case study .....	52
4.3.2.1 Meteorological condition .....	52
4.3.2.2 Dust concentrations of PM <sub>10</sub> in the source areas.....	54
4.3.2.3. Dust concentrations of PM <sub>10</sub> in downwind areas .....	56
4.3.2.4 Vertical distribution of dust by LiDAR measurements and transport trajectories .....	58
4.3.2.5 Dust transport by Air Mass Trajectories .....	60
4.4 Discussion .....	62
4.5 Conclusions .....	63
Chapter 5 Overview of Regime shift .....	64
5.1 Introduction .....	64

5.2.1 The study area.....	66
5.2.2 Methods and Materials .....	66
5.2.2.1 Normalized Difference Vegetation Index (NDVI) .....	66
5.2.2.2 Hovmoller diagrams .....	66
5.2.2.3 Identification of vegetation growth period.....	66
5.3 Results and Discussion .....	67
5.3.1 Detection environmental regime shift .....	68
5.3.2 Dust emission and transportation effects on Regime shift .....	71
Chapter 6 Summary .....	74
Acknowledgments .....	76
References .....	77
北東アジアにおけるダスト輸送について---ゴビ砂漠地域におけるダスト の発生、分布とその輸送の事例研究 .....	89
7. Publication and Presentation .....	92
7.1 Publication.....	92
7.2. Presentation .....	94

Table 1. Selected meteorological station.....	24
Table 2. Correlation coefficients various parameter (dust storm, precipitation, NDVI) .....	27
Table 3. Average duration in a dust storm (a drifting dust) occurrence (h).....	36
Table 4. Selected meteorological station (Gobi).....	39
Table 5. Dust monitoring stations in Mongolia. (Source: National Agency for Meteorology and Environmental Monitoring, Mongolia) .....	45
Table 6. Dust monitoring stations in China. (Source: China National Environmental Monitoring Center) .....	45
Table 7. Dust monitoring stations in Korea (Source: Korea Meteorological Administration).....	45
Table 8. Dust monitoring stations in Japan. (Source: Ministry of the Environment, Japan) .....	46

Figure 1. A schematic illustration of the three distinct phases of Aeolian dust: entrainment, transport and deposition. Atmospheric conditions (flow patterns, precipitation and turbulence), soil characteristics (texture, aggregation and moisture) and land-surface properties (roughness elements and vegetation) control the erosion process (modified from Shao 2000)..... 5

Figure 2. Hot spots of dust sources; according to (Engelstaedter et al., 2007) ..... 7

Figure 3. An illustration of creep, saltation and suspension of soil particles during an erosion event. Saltation is further classified into pure and modified saltation and suspension is further divided into short-term and long-term suspension (modified from Shao, 2008) ..... 9

Figure 4. Distribution of USGS land covers that are taken as first guess mask for potentially dust productive areas; data of the U.S. Geological Survey..... 10

Figure 5. Long term mean TOMS AI averaged over 1984–1990 and location of 131 dust hot spots with coded regional designation; according to (Engelstaedter et al., 2007) ..... 11

Figure 6. Mean dust concentration (averaged over time) for Asia. Data used for this graph are derived from visibility observations from 27 May 1998 to 26 May 2003. Main deserts in region are enumerated: 1 Taklamakan (Tarim Basin); 2 Gurbantunggut (Junggar Basin); 3 Kumutage; 4 Tsaidam Basin; 5 Badain Juran; 6 Tengger; 7 Ulan Buh; 8 Hobq; 9 Mu Us; 10 Gobi and 11 Thar. Four regions of frequent dust events, i.e., the Tarim Basin, Inner Mongolia, the Gobi region and the Indian Subcontinent, are denoted with A, B, C and D, respectively (Shao and Dong, 2006) ..... 13

Figure 7. Routes of the cold air outbreaks and the dust transport patterns in China (source Sun et al., 2001)..... 14

Figure 8. Geographic distribution of annual mean air temperature 1960-1990 (Munkhbat and Natsagdorj , 2013, MARCC, 2014)..... 18

Figure 9. Geographic distribution of mean annual precipitation 1960-1990 (Munkhbat and Natsagdorj, 2013, MARCC, 2014)..... 19

Figure 10. Location of the study area ..... 22

Figure 11. Study sites..... 23

Figure 12. Relationship between mean NDVI and dust storm in spring 2000-2013

.....	26
Figure 13. Relationship between mean NDVI and precipitation in spring 2010-2013	27
.....	27
Figure 14. Comparison of NDVI (A), soil moisture measurements (B) and elevation (C) in Sainshand	28
.....	28
Figure 15. Distribution of number of days with dust storms observed in Mongolia	32
.....	32
Figure 16. Distribution of number of days with drifting dust observed in Mongolia	33
.....	33
Figure 17. Distribution of number of dusty days observed in Mongolia.	33
.....	33
Figure 18. Average number of days with dust storms between 1960 and 1989.	34
.....	34
Figure 19. Average duration of a dust storm (time interval) in the Gobi.	37
.....	37
Figure 20. In order to indicate dust storm dispersion through desert zone of the Central Asia, a Map was developed by using data base on climate information of China Meteorological Administration and Meteorological Services of Mongolia.	38
.....	38
Figure 21. (a) Dust monitoring stations in Northeast Asia and (b) DEMs (digital elevation models) in the southern part Mongolia retrieval using NASA's Shuttle Radar Topography Mission (STRM Data product)	46
.....	46
Figure 22. Locations of the AD-Net light detection and ranging (LiDAR) stations	47
.....	47
Figure 23. Number of dusty days at Dalanzadgad, Sainshand and Zamyn-Uud between 1999-2016.	50
.....	50
Figure 24. Monthly average datasets of PM <sub>10</sub> at Dalanzadgad, Sainshand and Zamyn-Uud in March and April between 2009-2017.	50
.....	50
Figure 25. Sea level pressure (hPa) by contour and 10-m wind vectors using the.	52
.....	52
Figure 26. Time series variations of dust concentration of PM <sub>10</sub> at stations in Mongolia, 2012.	55
.....	55
Figure 27. Time series variations of dust concentration of PM <sub>10</sub> at stations in China, 2012.	55
.....	55
Figure 28. Time series variations of dust concentration of PM <sub>10</sub> at stations in Korea, 2012.	56
.....	56
Figure 29. Time series variations of dust concentration of PM <sub>10</sub> at stations in Japan, 2012.	57
.....	57
Figure 30. The Mie LiDAR extinction coefficients of non-spherical aerosol (dust) and spherical aerosol in Sainshand (a), Seoul (b), Hedo (c) from 28 March to 2	

April, 2012 (Note: Time (UTC) in the horizontal axis and height in the vertical axis. The black circles indicate suspected dust observation) .....	59
Figure 31. Forward and backward air mass trajectories using the NOAA HYSPLIT model: a) forward from Zamyn-Uud, Mongolia, b) backward from Hohhot, China, c) backward from Seoul, Korea d) backward from Hedo, Japan .....	61
Figure 32. Hovmoller diagrams of monthly precipitation (left) and monthly NDVI (right) VGP along the E90° – E117.5° longitude .....	67
Figure 33. Environmental regime shifting in North China, during 2003-2013. (a) shows that the concept of relationship between precipitation and vegetation, (b) shows that the concept of regime shift, (c) precipitation anomaly and (d) NDVI anomaly of the study area.....	69

## Abstract

Mongolia is one of the severe arid to the south and with cold and mountainous regions to the north and west. Over Gobi Desert and steppe, arid and semi-arid regions, often occur the natural disasters such as dust storm. This study aims to examine the relationship between Normalized Differential Vegetation Index (NDVI) and dust storm observations in Mongolia during 2000 to 2013. The results reveal that a correlation between dust storm and vegetation cover reasonable negative relationship, the  $r$ -value was -0.5. For the analysis, we examined correlation between the precipitation and the NDVI. Dust storm occurrence had increased with decreasing of annual precipitation in spring. The most degraded area was southwest region of the Gobi with the least precipitations. The distribution and transport of windblown dust in the North-East Asia that occurred in the North East Asia from 28 March to 2 April 2012, was investigated. Data of particulate matter less than 10 micrometers ( $PM_{10}$ ) near the surface and LiDAR measurements from the ground up to 18 km was used in the study. A severe dust event originated over the southern Mongolia and northern China on March 29, and the wide-spread dust moved from the source area southeastward toward Japan next few days. Maximum of  $PM_{10}$  during the dust storm event were 2 times higher in comparison with normal atmospheric condition. Windblown dust was reaching to Japan Islands after 2 days from the originating area. Heights of dust vertical distribution by LiDAR measurements were with a thickness of 1 to 2 km in the lower layer of atmosphere and getting higher to the great distances from the source areas.

In the Chapter 1 of Introduction, I study about the specific features of desert zone and climate change in Mongolia. During the last 60 years the annual mean air temperature has increased 1.56 °C. The winter temperature has increased 3.61°C and the spring-autumn temperature 1.4-1.5°C. The country's average precipitation between 1940-1998 has increased by 6%. However, the spring precipitation decreased by 17%. The spring dryness occurs mainly in May. The rapid increase in temperature and considerable decrease in precipitation in the spring sowing period have significant negative impacts on dust storm outbreak.

In the Chapter 2, purpose to examine the relationship between NDVI and meteorological data in Mongolia during 2000 to 2013 in Gobi Desert, Mongolia. In all sites, there were positive correlation between NDVI and precipitation between May to

August, 2000-2013. Dust storm occurrence had increased with decreasing of precipitation in spring. Comparing Spring's NDVI and previous summer precipitation. We assume that summer precipitation becomes the limiting factor for the vegetation growth. The dust storm occurred during 2000-2013 are depended on precipitation of last summer and the vegetative coverage.

In the Chapter 3, focusing on spatial and temporal distribution of dust events over Mongolia based on the results of previous research. We examined the association maximum duration day of dust storms occurred in March from 2000 to 2014 in Gobi, Mongolia. Maximum duration day of dust storm was observed at 12.04 hour from March 29-30, 2012 in Zamyn-Uud station.

In the Chapter 4, purpose to investigate the effects of long-distance transport from dust events occurring in Mongolia by cross-examining the elevated level of particulate matter in neighboring countries. An Asian dust event occurring from 28 March to 2 April, 2012 was analyzed by ground observations of  $PM_{10}$ , dust vertical spread by AD-Net LiDAR measurements and dust transport by air mass trajectories using the NOAA HYSPLIT model. The main results shown:

a). Climatological data of dusty days show that the number of dusty days at only Zamyn-Uud, Mongolia has an increasing trend; b). A low-pressure system and its cold front resulted in strong winds that transported dust from the source area across Northeast Asia at the end of March and the beginning of April, 2012. The dust storm also created an increase in  $PM_{10}$  particles in the dust source area as well as in the downwind areas. Dust concentration of  $PM_{10}$  near the surface is higher in the source areas of the Gobi Desert in Mongolia and China and less in the downwind areas during transport such as in Korea and Japan; c). LiDAR measurements showed that dust vertical diffusion in the atmosphere is lower in the source area during the dust storm period and increases in the downwind areas especially when transported across far distances. The trajectories of air mass confirmed that dust can be transported from the dust source areas in Mongolia and China to the Korean Peninsula and Japan.

In the Chapter 5, shown the previous study result of ecosystem regime shifting of Mongolian plateau. According to the major theoretical finding when it comes to regime shifts is that ecosystems recover slowly from small perturbations in the vicinity of tipping points. The provided water condition such as rainfall is one of the most important factors for vegetation especially in arid regions.

Chapter 6 shows main conclusion of precipitation was a determinant of vegetation productivity in arid regions and a driving force for ecosystem change. The frequency of dust storms is increasing in the spring when annual average precipitation is decreasing, and it is found that the occurrence of dust storms in spring is highly dependent on the summer precipitation in the previous year. In the Gobi Desert, where dust storms occur, the frequency of dust storms increases as the wind speed increases, and critical wind speed is 6.5 m/s (a constant threshold. It was also confirmed that the dust storm generated in the Gobi Desert reached the Japan in just two days via Seoul in northern China, and the PM<sub>10</sub> concentration reached more than twice the normal level.

# Introduction

## Aeolian dust

Dust can be defined as a suspension of solid particles in a gas or as a deposit of such particles. Dust particles larger than about 20  $\mu\text{m}$  in diameter settle back to the Earth's surface quite quickly but smaller particles can remain in suspension in the air unless washed out by rain.

Soil materials that are transported very long distances in the atmosphere are mostly smaller than 10  $\mu\text{m}$  in diameter ( $d$ ) and many are smaller than 2  $\mu\text{m}$  (Pye, 1987). Dust is type of aerosol, related to, but distinct from, smokes, mists, fumes and fogs. Smokes are generally composed of smaller particles than dusts (mostly smaller 1  $\mu\text{m}$ ) and result from burning or condensation of supersaturated vapours. Mists and fogs are suspensions of liquid droplets formed by atomization or vapour condensation. Like smokes, mists consist of very high concentrations of small particles. If the particle concentration is high enough to reduce visibility significantly, it is referred to as fog. Mixtures of smoke and fog, and by-products of their chemical interactions, are termed smog. Smog is type of air pollution. Smog usually forms when smoke from pollution mixes with fog.

Atmospheric dust particles originate from several different sources. There are several dust types of dust such as soil dust, cosmic dust, volcanic dust, industrial dust, and so on, while the dust, and so on, while the dust treated in this study is soil dust.

Wind erosion is a process of wind-forced movement of soil particles. This process has the distinct phases of particle entrainment, transport and deposition (Figure. 1). It is a complex process because it is affected by many factors which include atmospheric conditions (e.g. wind, precipitation and temperature), soil properties (e.g. soil texture, composition and aggregation), land-surface characteristics (e.g. topography, moisture, aerodynamic roughness length, vegetation and non-erodible elements) and land-use practice (e.g. farming, grazing and mining). During a wind-erosion event, these factors interact with each other and, as erosion progresses, the properties of the eroded surface can be significantly modified (Shao, 2000).

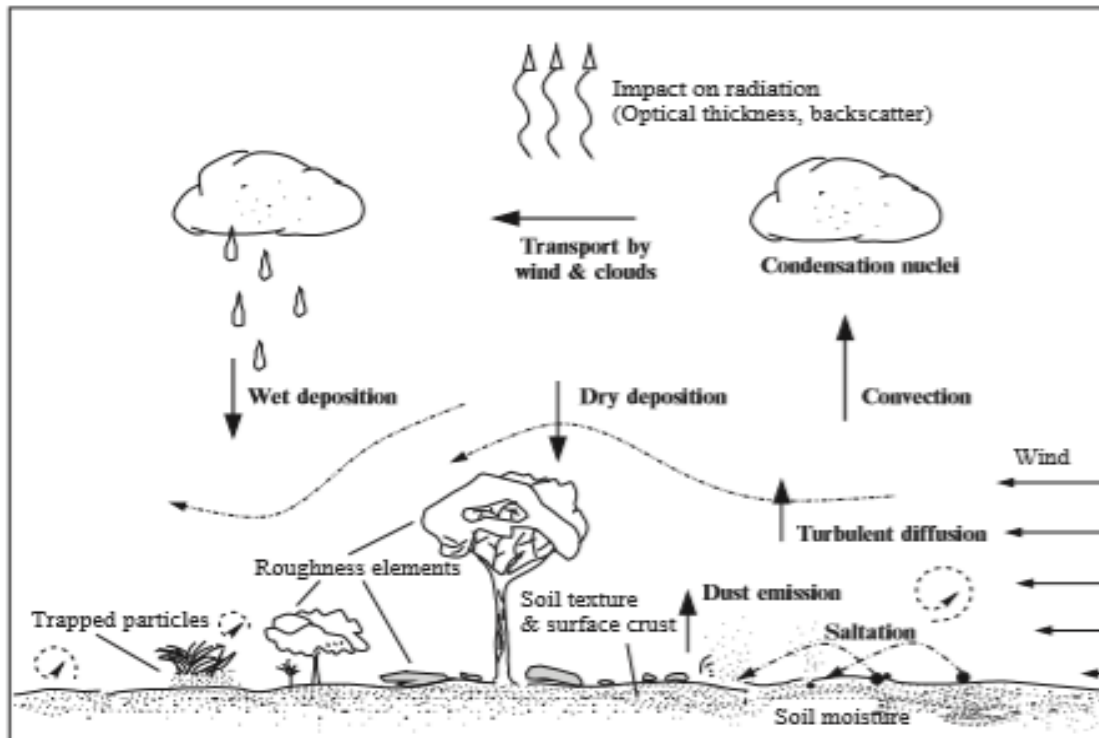


**Figure 1.** A schematic illustration of the three distinct phases of Aeolian dust: entrainment, transport and deposition. Atmospheric conditions (flow patterns, precipitation and turbulence), soil characteristics (texture, aggregation and moisture) and land-surface properties (roughness elements and vegetation) control the erosion process (modified from Shao 2000)

A life of the aeolian dust has three distinct phases: (1) the entrainment of particles by wind shear at surface (“produced” or “eroded”), (2) the transport of particles in the atmosphere by advection and turbulent diffusion (“borne by wind” or “airborne”), and (3) the deposition of particles through dry and wet removal (“deposited”) (Figure. 1). The phase discussed in this study is the first one (i.e., “produced” or “eroded”). This phase of entrainment is called “Aeolian dust outbreak” or “dust outbreak”. Soil particles are crudely divided into four categories referred to as gravel ( $2000 \mu\text{m} < d < 2 \text{ m}$ ), sand ( $63 < d < 2000 \mu\text{m}$ ), silt ( $4 < d < 63 \mu\text{m}$ ) and clay ( $d < 4 \mu\text{m}$ ) (Shao, 2000). Silt and clay particles are commonly called dust. The particle size distribution in the surface soil is one of important keys in the process of aeolian dust. The difference of particle size is important in the discussion of radiative forcing and dust transport. Coarse dust particles ( $31\text{-}62 \mu\text{m}$ ) can travel up to 320 km from their source, medium dust particles ( $16\text{-}31 \mu\text{m}$ ) can travel up to 1600 km, and fine dust particles ( $16 \mu\text{m}$ ) can be transported globally. Dust storms evacuate material from desert surfaces, then deposit it elsewhere and thus contribute to various geomorphological phenomena like desert depressions, wind-fluted bed forms and stone

pavements. In general, they play an important role in the denudation of desert surfaces.

Dust is a type of aerosol with one of the highest atmospheric mass loadings on a global scale. Dust storms are natural phenomena; and they can result in severe ecology and environment problems. Many scientists have studied how dust storms impact human life, society and the economy, and climate change (Kwon et al., 2002; Chen et al., 2004; Park et al., 2005).

Sandy dunes that exist in wide valleys of the Gobi Desert represent favorable soil conditions for dust and sandstorm events. Muddy brown soil with a 70–80 cm deep loose dust layer is abundant in the Gobi and in the southward direction, the soil in the Gobi becomes drier and areas of bare soil and saline soil become larger. Sandy brown soils are distributed mostly over vast hollows with lakes between the Altai and Khangai mountains and southern parts of the Dornogobi Aimag in the southeastern region of the country. Vegetation coverage is sparse over 20–30% of the soil in the Gobi (desert steppe) and 10–15% in the desert (Tsegmed, 1969).

When winds are strong, large amounts of sand and dust are emitted from arid soils into the atmosphere and then transported downwind, affecting areas in the vicinity of dust sources but also regions hundreds to thousands of kilometers away. Drought and wind contribute to the emergence of dust storms, as do poor farming and grazing practices or inadequate water management by exposing the dust and sand to the wind.

Satellite data analysis by Prospero et al., (2002) indicated that most major dust sources are located in arid regions in topographic depressions where deep alluvial deposits have been accumulated. Dust sources include small-scale structures ("hot spots") that substantially contribute to global dust emissions. One of the uncertainties related to sources is the contribution of dust due to human activities. Mahowald et al., (2010) have shown that dust load may have doubled in the 20th century over much of the world due to anthropogenic activities. Recently, Ginoux et al., (2012) mapped dust sources based on satellite observations making distinction between natural, anthropogenic and hydrologic dust sources, where the anthropogenic sources contributes with 25% to global dust emissions.

A factor of a significant influence on dust emissions and dust impacts to society and environment is the dust grain size distribution. The coarse particles are primarily deposited near the source regions, but finer particles can be transported over distances of intercontinental scales. Dust is removed from the atmosphere through gravitational

sedimentation and turbulence, and through scavenging in precipitating clouds. Mineral composition is another important dust feature. Recent work on detailed global mineralogy of arid soils (Nickovic et al., 2012; Journet et al., 2014) provides appropriate input for studying processes affected by the dust mineralogy, such as radiation, health, cloud formation and marine productivity.

Multi-scale meteorological processes are involved in dust emission and transport. Driving meteorological conditions, which control the structure of the dust horizontal and vertical distribution, are cyclones and fronts, low-level jets, haboobs and dust devils and plumes. A more realistic representation of the effects of the smaller-scale meteorological features in dust models is one of the key challenges for the future (e.g. Knippertz and Todd, 2012; Vukovic et al., 2014).

## Dust source

There are a number of countries, which are affected on a regular basis by major dust storms either directly from local sources or indirectly from wind driven events. In the Northern Hemisphere, the main sources of dust are the Sahara Desert, the Middle East, the Gobi Desert in Mongolia and the western desert regions of the United States of America. In the Southern Hemisphere, the main sources of dust are the in land desert regions of Australia. A search of the literature using Scopus and Google Scholar reveals that the most publications are from China, followed by a significant number from the USA. Australia and the Middle East are also very active in dust research (Figure 2).

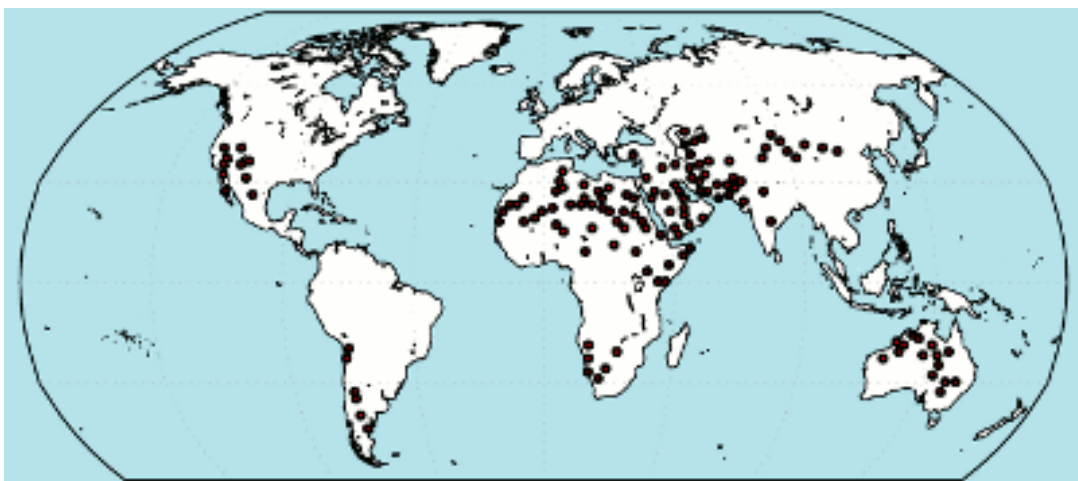


**Figure 2.** Hot spots of dust sources; according to (Engelstaedter et al., 2007)

Research into dust storms covers a wide range of perspectives including the

mechanism of dust storm formation (Barenblatt et al., 1974, Prospero et al., 2002a), transportation (Kurosaki et al., 2003), Littmann (1991), (Shao and Wang, 2003), and soil characteristics, and the climate (Bryant, 2013; Wang et al., 2015) and effect on human health (Mu et al., 2011) and sand movement (Luvsandendev and Jamiyanaa, 2001), climatology (Tuvdendorj, 1973 and Natsagdorj et al., 2002).

The process of the uptake of sand and dust particles from the soil depends on the near-surface dynamics (Goudie et al., 2006). It is controlled by the wind intensity, the soil wetness, the soil texture and the land cover. It has the lowest value for disturbed soils, followed by sand dunes, alluvial and aeolian deposits, disturbed playa soils, skirts of playas, playa centers and highest for desert pavements (Goudie et al., 2006). It also increases with the size of the particles, because they are heavier and therefore more difficult to lift up due to gravity. If the particles are pretty small the threshold wind value is high, since it has to break rather strong cohesion force keeping small particles together.

Within the uptake process there are three modes of aeolian particle motion identified (Bagnold et al., 1954 ), which are also shown in the diagram below (Figure 3) :

- creep: the largest particles are moving by rolling motion.
- saltation: particles in the size range from 70-500  $\mu\text{m}$  are hopping.
- suspension: the smallest particles are wafting due to turbulent diffusion.

1. Surface creep: this mechanism operates when light winds roll large particles along the surface.

2. Saltation: this process of removing particles from the surface involves a series of bombardments and collisions that move particles horizontally and vertically. Initially, downward movement is stronger than upward. The saltation process continues if the particles that moved upward return to the surface and collide with other particles. This mechanism is the dominant process involved in removing particles from the surface; other processes can take over depending on atmospheric conditions (Shao et al., 2008).

3. Suspension: this is the mechanism by which small, fine particles are transported into the atmosphere and advected horizontally under favourable atmospheric conditions. For particles to become suspended and to continue moving upwards, wind speeds must be strong enough to support the weight of the particles. Winds generate turbulence, which

lofts the particles through vertical mixing (Zender, 2004). Horizontal advection depends on synoptic dynamics, which can disperse particles over thousands of kilometres (Zender, 2004). Together, vertical turbulence and horizontal advection, which usually occur in an unstable atmosphere, can transport particles far from their source region on scales as large as the continental scale.

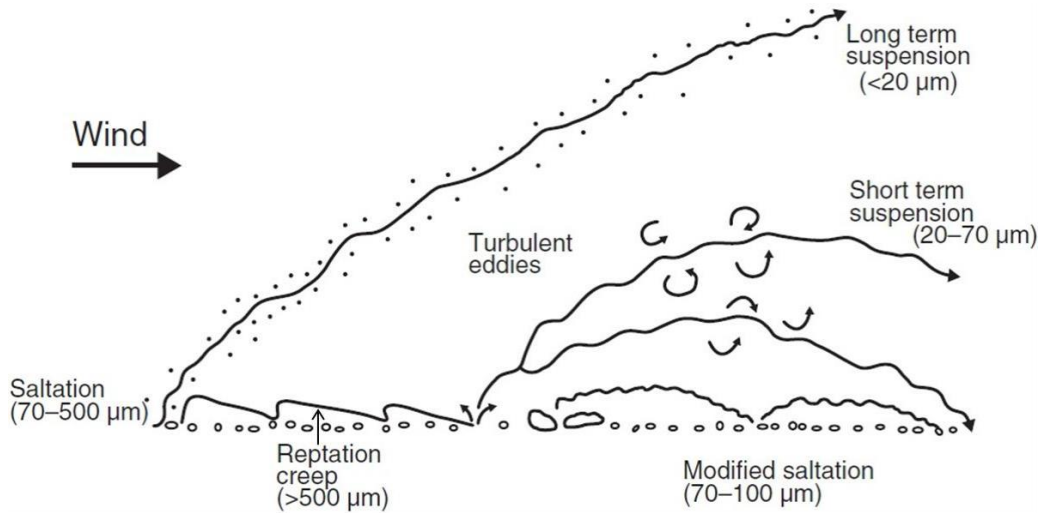


**Figure 3.** An illustration of creep, saltation and suspension of soil particles during an erosion event. Saltation is further classified into pure and modified saltation and suspension is further divided into short-term and long-term suspension (modified from Shao, 2008)

Saltation is the dominant mechanism for the uptake of dust particles by wind from the surface (Goudie et al., 2006). Further, it leads to the so-called process of saltation bombardment or sandblasting to produce fine dust aerosols . (Gomes et al., 1990; Shao et al., 1993; 2008; Grini et al., 2002). After emission, dust particles are carried up from the source by turbulent diffusion and vertical advection. They are also transported by horizontal advection. They can be transported further away from the source region in the free atmosphere under the influence of strong winds. Through the process of dust dispersion, which is driven by synoptic dynamics, trans-continental scales can be easily achieved.

The dust particles are removed out of the atmosphere by sedimentation (gravitational settling) and dry and wet deposition. The lifetime of the particles/the removal processes is dependent on the particle size (Jickels et al., 2001). Their original size ranges from sub-microns to scales of about 40 μm (Tegen et al.,1994). Particles with a diameter smaller

than 1  $\mu\text{m}$  have a life time around 2-3 weeks. In contrast, larger particles like sand and large silt have a live time of several hours (Tegen et al., 1994).

## Main Sources

Dust sources are associated with arid regions (mostly topographically low) characterized by little rainfall (annual rainfall under 200–250 mm, Prospero et al., 2002). Moreover, these areas are often affected by human impacts (e.g. agricultural activity, etc.) (Prospero et al., 2002). Another important factor controlling dust emission at the source areas is the vegetation cycle. The dust storm frequency is highest in desert/bare ground (Engelstaedter et al., 2003). It is inversely correlated with the leaf area index, which describes the density of the vegetation. The emissions of dust are correlated with the vegetation types of the areas considered. The diagram below shows six land cover types from which dust potentially could be released to the atmosphere (Figure 4).

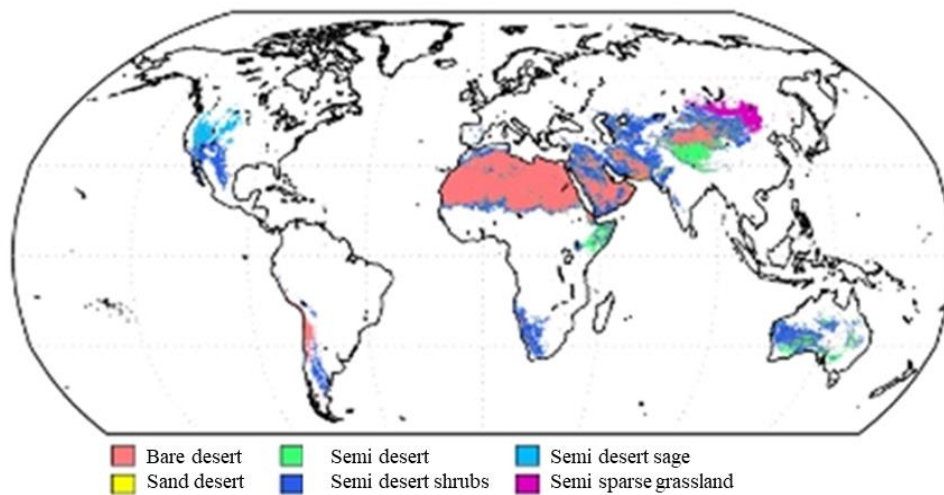


**Figure 4.** Distribution of USGS land covers that are taken as first guess mask for potentially dust productive areas; data of the U.S. Geological Survey

The largest dust source region in the world is North Africa (heat low regions of the Sahara), (Engelstaedter et al., 2006). The most intense source region in North Africa is the Bodélé Depression (northern Chad). It may be responsible for up to 18% of global dust emissions (Todd al., 2007). Other main source regions are the Middle East, Central and South Asia. The emitted dust from these regions is also most persistent (Prospero et al., 2002).

According to Engelstaedter et al., (2006) hotspots in regions classified by the United

Nations Environmental Programme (1992) as hyper-arid, arid and semi-arid based on an aridity index of annual precipitation over potential evapotranspiration available at 1° resolution. This results in the exclusion of some falsely identified dust hotspots because of the TOMS AI's sensitivity to biomass burning aerosols. One hotspot was excluded as the TOMS AI annual dust cycle calculated for subsequent analysis had missing values. The application of this results in the identification of 131 dust hot spots (Figure 5).

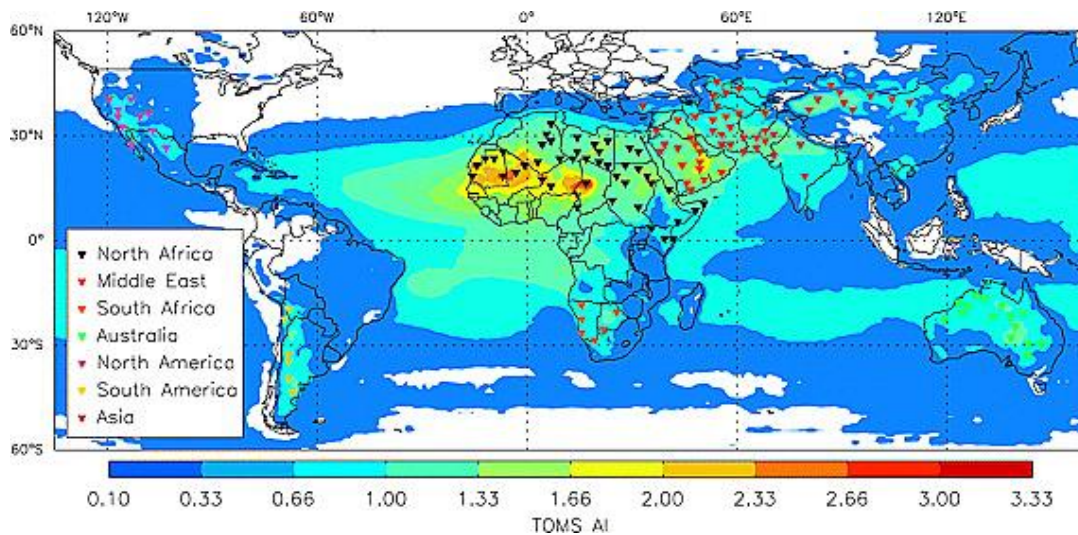


**Figure 5.** Long term mean TOMS AI averaged over 1984–1990 and location of 131 dust hot spots with coded regional designation; according to (Engelstaedter et al., 2007)

### **Physical and chemical features of dust source soils**

The emission of mineral particles underlies a large daily variability controlled by the meteorology (Moulin et al., 1998, Zubler et al., 2001, Todd et al., 2007). The dust mobilization is more active during daytime than night time (Yue et al., 2009).

This can potentially be explained by a peak of dust burden and the dry deposition in the late afternoon. In addition, a clear seasonal cycle exists with its maximum during the dry season (Zubler et al., 2001) especially in the Sahara desert and central Asia (Yue et al., 2009).

The emission varies in time and space depending on atmospheric and surface conditions (Shao et al., 2006). However, many sources are point sources which result in wide spread dust weather (Shao et al., 2006), therefore it is quite difficult to describe the emission process in atmospheric dust models.

Mineral dust aerosols have complex nonspherical shapes and varying composition (Kalashnikova et al., 2004). They are generally a highly heterogeneous mixture (Buseck et

al., 1999). The composition of mineral particles is dependent on the source region (Aston et al., 1973). Whereas dusts in the Atlantic northeast trades resulting from dust sources in Africa are dominated by kaolinite, are dusts in the northeast monsoons of the northern Indian Ocean resulting from the Rajasthan desert dominated by illite (Aston et al., 1973).

### **Mineralogy of dust particles**

Dominant minerals in arid soils are illite, kaolinite, smectite, calcite, quartz, feldspar, hematite and gypsum. *Phyllosilicates* (illite, kaolinite and smectite) makes up the largest chemical weathering minerals in sedimentary rocks (Claquin et al., 1999).

The crust of the Earth constitutes approximately 90 percent of phyllosilicates and *Tectosilicates* (quartz, feldspar; three dimensional framework of silicate).

Mineral dust aerosol affects the atmospheric radiation budget through absorption and scattering of incoming solar radiation, and absorption and reemission of outgoing long-wave radiation. Several works have indicated the relevance of the absorbing properties of mineral dust (Kaufman et al., 2001; Moulin et al., 2001; Haywood et al., 2003). However, it is not clear the degree in which mineral dust cools or warms the atmosphere (IPCC, 2013).

### **Dust source in East Asia**

In Central and Eastern Asia, the major source regions are the Tarim Basin (Taklimakan Desert) in western China, the upper reach of the Yellow River (Gobi Desert) in southern Mongolia and northwestern China, the east part of Inner Mongolia, and the northern part of the Indian Subcontinent (Figure 6, Sun et al., 2001).

The Gobi (Region B) is another region of frequent dust events. The highest frequency (about 15%) is recorded near the China-Mongolia border. The dust-affected region in Mongolia is mainly the Gobi Desert region the southern part. The highest dust-storm frequency occurs at the southern side of the Altai Mountains, the Ulaan-nuur area and the Zamyun-Uud area (Natsagdorj et al., 2003). The highest mean annual number of dust-storm days of 34.4 is recorded at Zamyun-Uud (Middleton, 1991). Another region of high dust frequency is the Great Lakes Depression to the northwest of Mongolia.

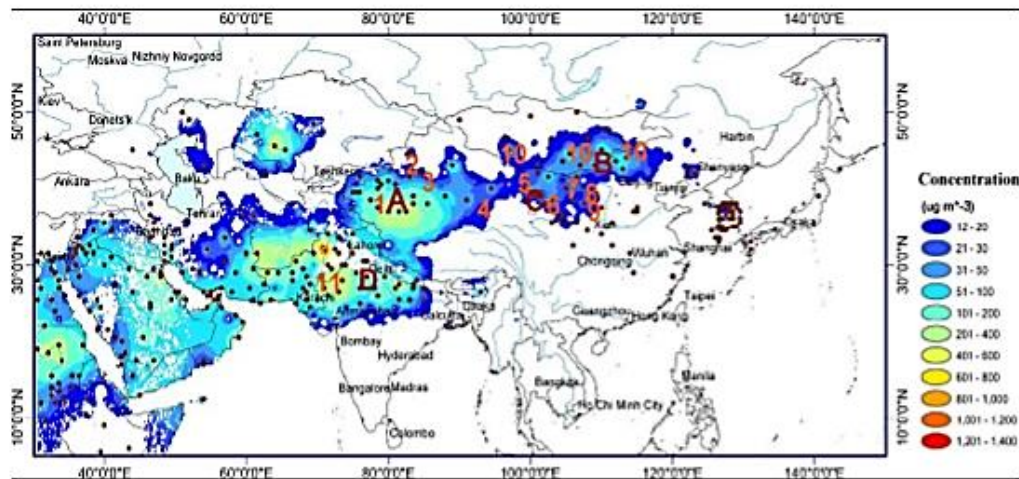


**Figure 6.** Mean dust concentration (averaged over time) for Asia. Data used for this graph are derived from visibility observations from 27 May 1998 to 26 May 2003. Main deserts in region are enumerated: 1 Taklamakan (Tarim Basin); 2 Gurbantunggut (Junggar Basin); 3 Kumutage; 4 Tsaidam Basin; 5 Badain Juran; 6 Tengger; 7 Ulan Buh; 8 Hobq; 9 Mu Us; 10 Gobi and 11 Thar. Four regions of frequent dust events, i.e., the Tarim Basin, Inner Mongolia, the Gobi region and the Indian Subcontinent, are denoted with A, B, C and D, respectively (Shao and Dong, 2006)

According to study three following geographical characteristics are essential for the dust event outbreak in East Asia: (1) frequent synoptic disturbances in spring, (2) complicated distribution of land cover types, and (3) frequent snow covers in early spring. In this section, the relations among the aeolian dust outbreak, these three geographical characteristics and massive topography in East Asia are described (Kurosaki and Mikami, 2004).

Frequent synoptic disturbances in spring It is well known that strong winds cause dust event outbreaks when synoptic disturbances pass over the regions around the Gobi Desert (Figure 7), (Watts, 1969; Pye, 1987; Littmann, 1991; Goudie and Middleton, 1992; Sun et al., 2001; Youlin, 2001; Gao et al., 2002; Qian et al., 2002). These synoptic disturbances derive from Altai-Sayan lee cyclogenesis indicated by Chen et al., (1991).

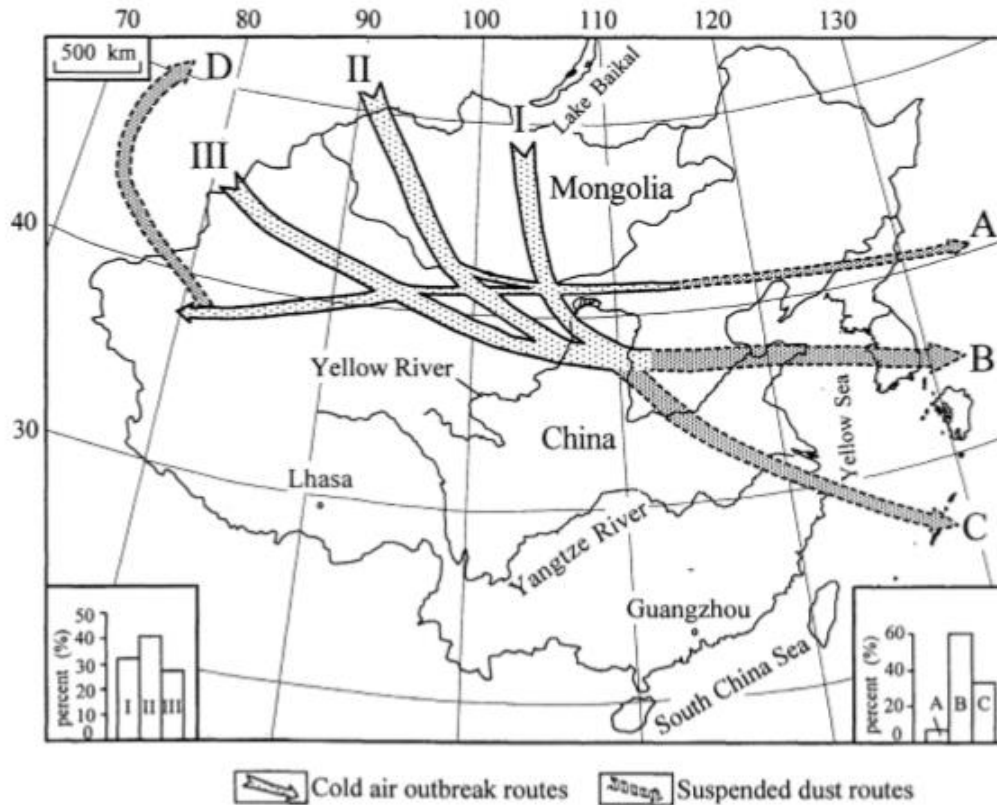


**Figure 7.** Routes of the cold air outbreaks and the dust transport patterns in China (source Sun et al., 2001)

## Study objectives

This study focuses on the aeolian dust outbreak in Mongolia, which it is important to understand the impact of aeolian dust on the Earth's climate. Aeolian dusts are generated by strong winds, while land surface conditions largely affect the aeolian dust outbreaks. In increasing number of observational and modeling studies are investigating about the relationship between atmospheric mineral dust aerosol levels and radiative forcing (see, for example, Zhu et al., 2007; Helmert et al., 2007; Prasad et al., 2007; Derimian et al., 2007; Yue et al., 2010) but it remains a major research priority, not least because of the possibility that dust aerosols could be an accelerant of aridity trends (Han et al., 2008a). In past decades, dust storms originating from the arid regions in central Asia have become more powerful and more frequent (Qiu and Yang 2000). Asian dust has advanced rapidly in the past decades (Iwasaka, 2006; Shao and Dong, 2006).

Mongolia is one of the severe arid to the south and with cold and mountainous regions to the north and west. Over Gobi Desert and steppe, arid and semi-arid regions,

often occur the natural disasters such as dust storm.

In Chapter 2, our study purpose to examine the relationship between Normalized Differential Vegetation Index (NDVI) and meteorological data in Mongolia during 2000 to 2013 in Gobi desert, Mongolia.

In Chapter 3, focusing on spatial and temporal distribution of dust events over Mongolia based on the results of previous research (Natsagdorj, 2003).

This study aims to examine the association maximum duration day of dust storms occurred in March from 2000 to 2014 in Gobi, Mongolia.

In Chapter 4, the purpose of this study is to investigate the effects of long-distance transport from dust events occurring in Mongolia by cross-examining the elevated level of particulate matter in neighboring countries. With temporal variations and dust transport in Northeast Asia, we have used analyses of PM<sub>10</sub> concentration, back trajectory, and AD-Net LiDAR measurements at various locations during the period of 28 March to 2 April 2012.

In the Chapter 5, focusing on the previous study result of ecosystem regime shifting of Mongolian plateau.

# **Chapter 1 Specific features of desert zone in Mongolia**

## **1.1 Introduction**

The Gobi Desert is a large desert region in Asia. It covers part of northern and northwestern China, and of southern Mongolia. The desert basins of the Gobi are bounded by the Altai Mountains and the grasslands and steppes of Mongolia on the north, by the Taklamakan Desert to the west, by the Hexi Corridor and Tibetan Plateau to the southwest, and by the North China Plain to the southeast. The Gobi is notable in history as part of the great Mongol Empire, and as the location of several important cities along the Silk Road. The Gobi is a rain shadow desert, formed by the Tibetan Plateau blocking precipitation from the Indian Ocean reaching the Gobi territory.

## **1.2 Geographic distribution of desert steppe zone and desert zone**

### **Desert steppe zone**

Desert steppe occupies a large band, more than 20 percent of Mongolia's area, extending across the country between the steppe and desert zones. This zone includes the Depression of the Great Lakes, the Valley of the lakes, and most of the area between the Khangai and Altai mountain ranges, as well as the eastern Gobi area. The zone includes many low-lying areas, soils with salt pans, and small ponds. The climate is arid with frequent droughts and annual precipitation of 4-5 inches (100-125 mm), and frequent strong winds and dust storms strongly influence the area vegetation. Still, many nomadic herders of Mongolia occupy this zone.

### **Desert Zone**

The Gobi is one of the great deserts in the world, occupying much of southern Mongolia and northeastern China and composing the northern part of Central Asian deserts. Starkly beautiful, the expanses of the fabled Gobi are rugged and inhospitable. Vegetation is sparse here, and the zone displays a remarkable variety, from rocky mountain massifs to the flat pavement-like areas of the super-arid desert, from poplar-fringed oases to vast out wash plains and areas of sand dunes. These areas provide habitat for many threatened species of Mongolia, including the wild camel, Gobi bear, and wild ass. Climate is extreme. Precipitation may fall only once every two to three years and averages less than 4 inches (100 mm.) annually. Temperatures climb as high as 104° F (40° C) in summer, and fall as

low as 104° F (- 40° C) in winter. During the spring and fall, dangerously strong winds buffet the area with dust storms and wind-speeds up to 140 km/h.

### **1.3 Grassland ecosystem of desert steppe region**

A total of 854 species of plant are registered in grassland of Mongolia. Desert steppes have communities with a specific composition and structure; they distribute in the extreme south of the steppe region neighboring the desert. They occur 20% of total area country, by altitude 1000-2200 m above sea level. Desert steppes have 6-15 species on 100 m<sup>2</sup> plot, it is lowest number of species comparing other steppe sub-types. Total cover in desert steppe communities in the most favorable years is 20-30%, but in dry years, this declines to 5–7%. In the desert steppes dominate feather-grass species (*Stipa gobica*, *S. glareosa*, *Cleistogenes songorica*), bunch-onions (*Allium polyrhizum*), and semi-shrubs (*Anabasis brevifolia*, *Salsola passerina*, *Eurotia ceratoides*, *Reaumuria soongorica*, *Ajania achilleoides*).

Desert steppe is dominated by grasses, herbs, and shrubs. Among them *Stipa gobica*, *Chenopodium acuminatum*, *Allium mongolicum*, *Caragana microphylla*, *Poa* sp. are dominant species in desert steppes zone.

The pasture productivity, dominant species and type, length of growing season and phenology are different for each of these natural zones. The pasture productivity, for instance, ranges between 320 and 760 kg/ha in mountain steppes (Olziikhutag, 1989).

## 1.4 Climatic conditions of the Gobi region

According to “Mongolia Assessment Report on Climate change” (MARCC, 2014) in Mongolia, annual mean temperature is 8°C to -8°C, the winter average is -15°C to -30°C and summer average is 10°C to 26.7°C. Annual mean air temperature is -4°C in the Altai, Khangai, Khentei and Khuvsgul mountainous region and - 6°C to - 8°C in the large river valleys, +2°C in the desert steppe region and 6°C in southern Gobi region (Figure 8).

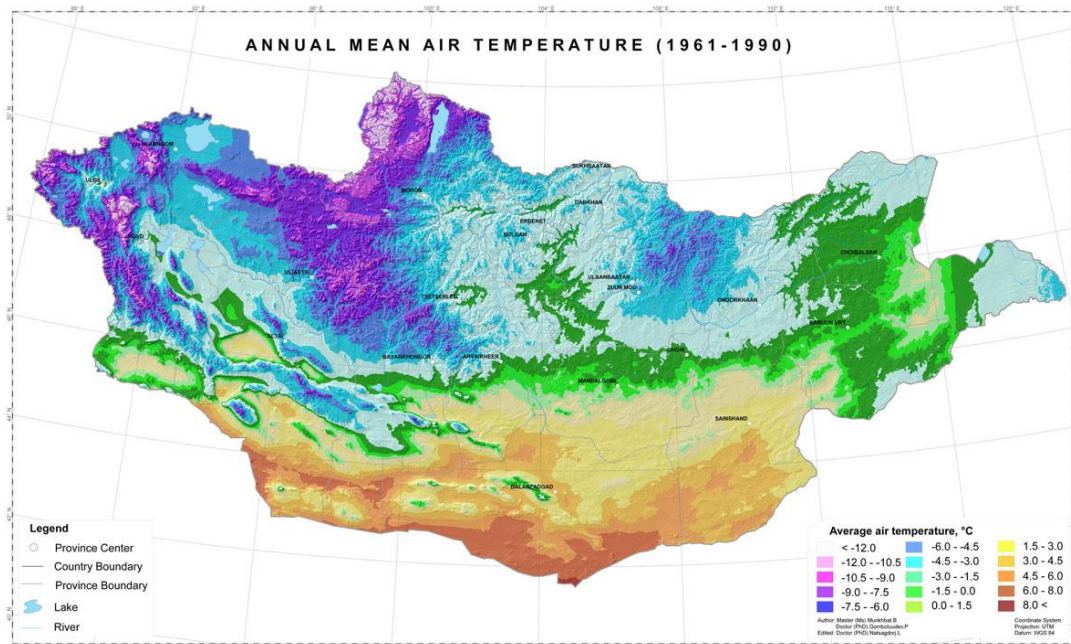


**Figure 8.** Geographic distribution of annual mean air temperature 1960-1990 (Munkhbat and Natsagdorj , 2013, MARCC, 2014)

The annual mean temperature of 0°C line is roughly located at the northern boundary of desert-steppe, Gobi region of Mongolia along the northern latitude of 46°. In addition, permafrost is distributed in areas where the annual mean air temperature is lower than – 20°C.

The Mongolian climate is characterized by long and cold winters, cool summers, small amounts of precipitation, high temperature fluctuations and a relatively high number of sunny days. The annual mean precipitation is 300-400 mm in the Khangai range, Khentei, Khuvsgul mountain regions, 250–300 mm in Mongol Altai and forest-steppe region, 150-250 mm in steppe region and 150-50 mm in Gobi desert region. Precipitation generally decreases from the north to the south and from the east to the west, however land contours play significant role for its distribution (Figure 9).

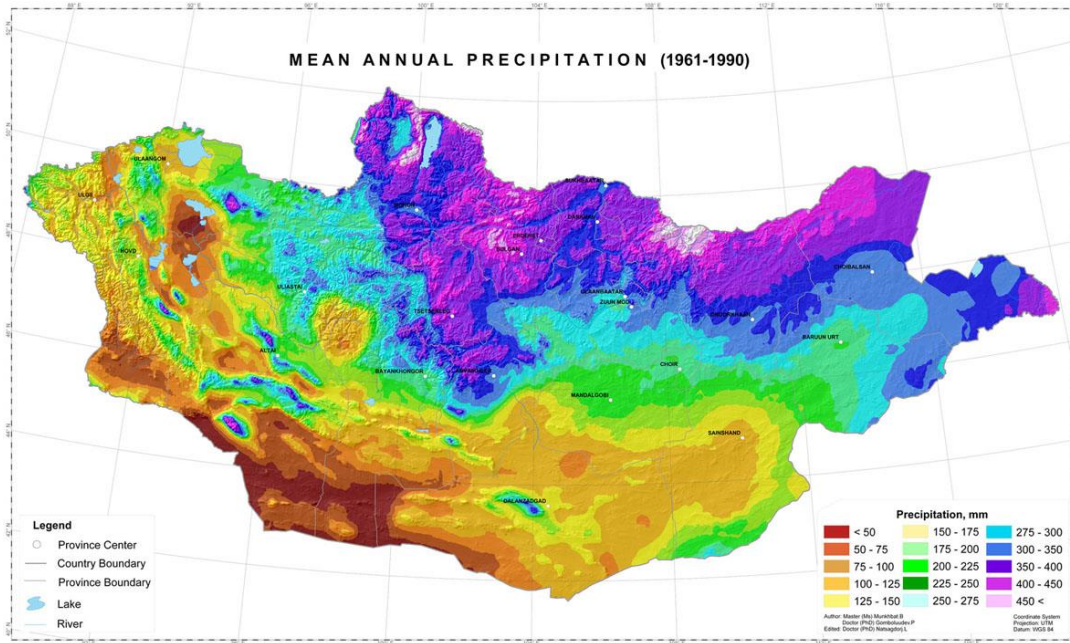


**Figure 9.** Geographic distribution of mean annual precipitation 1960-1990 (Munkhbat and Natsagdorj, 2013, MARCC, 2014).

About 85 per cent of annual precipitation falls as rain in warm season (April to September) and 50-60% of this amount happens in July and August alone. Even though the precipitation amount is little, its intensity per unit of time is high. During winter (November-March) about 10 mm of snow falls in the desert, 20-30 mm in the mountains and the Uvs lake depression and 10-20 mm in the other regions. Accordingly, the number of days with snow cover is about 150 in the mountain region, 100-150 days in the forest-steppe, 50-110 days in the Dornod steppe and the steppe zone, 50 days and less in the Gobi-desert.

The average depth of snow cover is not much: about 5 cm in mountains (the maximum is over 30), 2-5 cm in the steppe (the maximum is 15-20 cm). Gobi region sees many years without snow cover.

## 1.5 Current climate change

During the last 40 years, Mongolia's ecosystems have clearly changed as a result of climate change and human activities. Examples include desertification, soil erosion, and water resources and bio-diversity degradation. During the last 60 years the annual mean air temperature has increased 1.56°C. The winter temperature has increased 3.61°C and the spring-autumn temperature 1.4-1.5°C. In contrast, the summer temperature has decreased 0.3°C. Particularly in March, May, September and November, the temperature has

increased rapidly. Summer cooling occurs predominantly in June and July. The country's average precipitation between 1940-1998 has increased by 6%. However, while summer precipitation increased by 11%, spring precipitation decreased by 17%. The spring dryness occurs mainly in May. There are not many changes in the precipitation in April and a little increase in the precipitation in May. The rapid increase in temperature and considerable decrease in precipitation in the spring sowing period have significant negative impacts on crop growth, (MARCC, 2014).

The Mongolian scientist L. Natsagdorj has studied seasonal changes in precipitation in winter and autumn has increased by 5.2 to 10.75% and spring and summer precipitation has decreased by 9.1 to 3.0%.

Pasture growth begins in late April and biomass peak is usually reached in August. Mongolian livestock obtains over 90% of its annual feed intake from the annual pastures.

Pasture yields are strongly affected by climate and weather conditions. The main pasture ecological zones are desert steppe and desert.

## **Chapter 2 Relationship between vegetation coverage and dust storms over the Gobi area**

### **2.1 Introduction**

Dust storm is meteorological phenomenon common in Gobi desert of Mongolia, the Taklamakan Desert of northwest China and other arid and semiarid regions. Dust storm are offer serious hazards to the human health, animal husbandry and pasture. Its occurrences are more significant in urban areas where the soil erosion is caused by human related activities.

Dust storm occurs when soil and air are in dry condition and relative humidity average is 20-40% in Mongolia.

## 2.2 Study area

For the study purpose 8 sites were selected in Sainshand, Mongolia (Figure.10, Figure.11). Sainshand is the capital of Dornogovi Province in Mongolia. It is located in the eastern Gobi desert steppe. The distance from Ulaanbaatar, the capital of Mongolia, is about 413 kilometer (km) in a straight line.

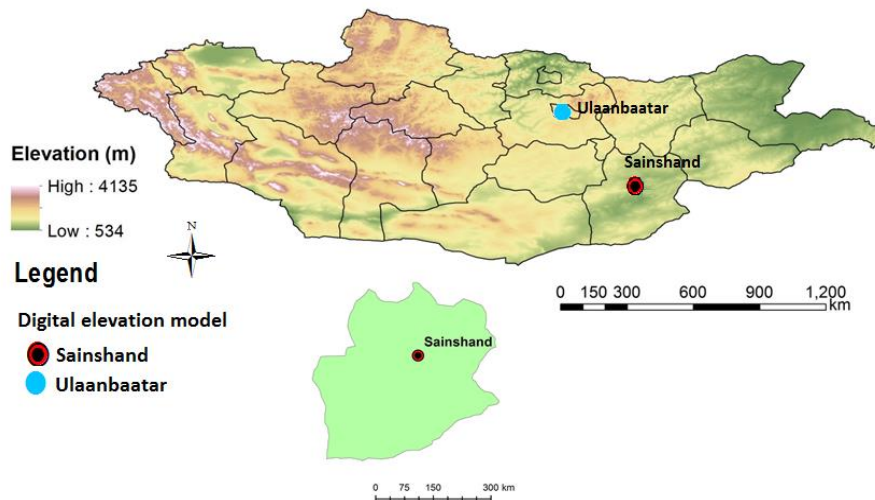
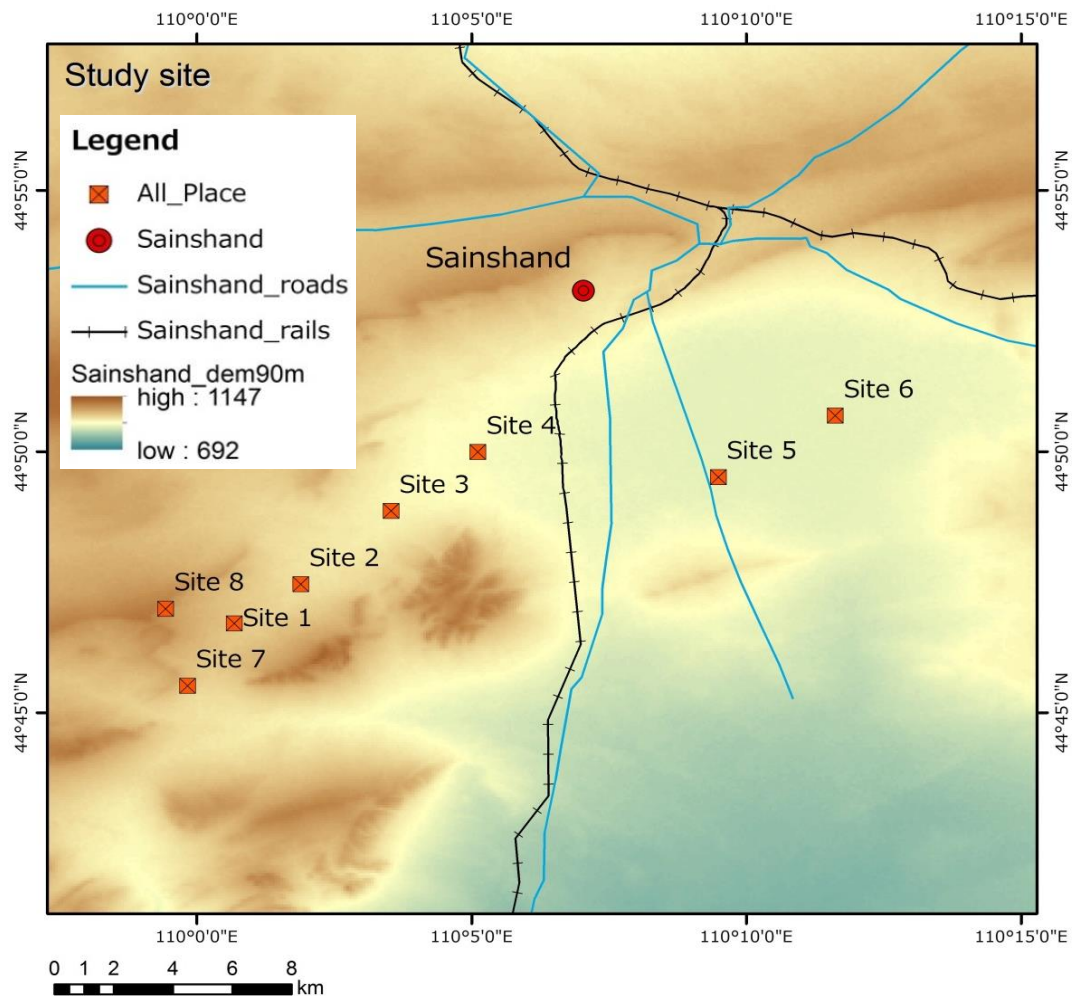


**Figure 10.** Location of the study area



Site	Latitude	Longitude
1	44°46'42.31"N	110° 0'41.20"E
2	44°47'26.99"N	110° 1'54.42"E
3	44°48'51.20"N	110° 3'32.00"E
4	44°49'58.90"N	110° 5'7.30"E
5	44°49'29.79"N	110° 9'29.92"E
6	44°50'40.83"N	110° 11'37.79"E
7	44°45'30.47"N	109° 59'49.91"E
8	44°46'58.81"N	109° 59'26.16"E

**Figure 11.** Study sites

## 2.3 Material and methods

### 2.3.1 Meteorological data

The meteorological data used in this the study were those from the Sainshand meteorological station, and provided by the National Agency for Meteorology, Hydrology and Environmental Monitoring of Mongolia (Table 1). This station was selected to represent the desert steppe vegetation types in the area.

**Table 1. Selected meteorological station**

	Station	Longitude	Latitude	Altitude (m)	Precipitation (mm)	Temperature (°C)
1	Sainshand	110.12°E	44.87°N	1101	116.7	3.7

Meteorological variables or ten-day precipitation, dust storm data and ten days mean air temperature data sets from June 2000 to August 2013 was obtained from that meteorological station.

### 2.3.2 Field survey

Pasture plant biomass has been measured with standard methods at the test plots located in the 8 selected sites during 2000- 2013 (Figure 12). The pasture plant biomass samples were collected during April 3d to 1st May 2013. Larger plot vegetation sampling was conducted on 5 plots (size 250x250 m).

We used Grasp of NDVI using ADC3 (Agricultural Digital Camera 3) and PixelWrench2 to image processing software, vegetation survey. Soil moisture measurement using HH2 moisture meter. Spectrum measurement (soil, plant, withered tree) utilized FieldSpec HandHeld2.

### 2.3.3 Satellite data

We used the 8-day Terra MODIS (Moderate Resolution Imaging Spectro-radiometer) MOD09Q1 product relative to the surface reflectance data. This product includes bands 1 and 2 corresponding to red (0.62-0.67  $\mu\text{m}$ ) and near-infrared (0.841-0.876  $\mu\text{m}$ ) wavelengths, respectively. The MOD09Q1 product includes all 8-day inputs at 250-meter resolution (Vermote et al., 2008). For this study, the MODIS images were acquired over a

period from January 2000 until October 2013. We calculate MODIS-NDVI during 2000–2013 for cross correlation analysis.

"Normalized Difference Vegetation Index" (NDVI) was calculated from the MOD09Q1 bands according to the following equation (Tucker, 1979):

$$NDVI = (NIR - RED) / (NIR + RED) \quad (1)$$

NDVI is generally recognized as a reliable index of ground vegetation cover. NDVI value is between -1 to +1. Negative value shows barren land or water surface, and when there's more vegetation cover then more positive value shows. NDVI anomaly shows drought years of location used for research. Negative values shows drought and positive value shows normal vegetation condition.

For the data processing the ERDAS IMAGINE 9.1, ArcGIS 10.3, ENVI/IDL, and Microsoft software were used.

## 2.4 Result

### 2.4.1 Changes in mean NDVI, dust storm and precipitation in study area during 2000-2013

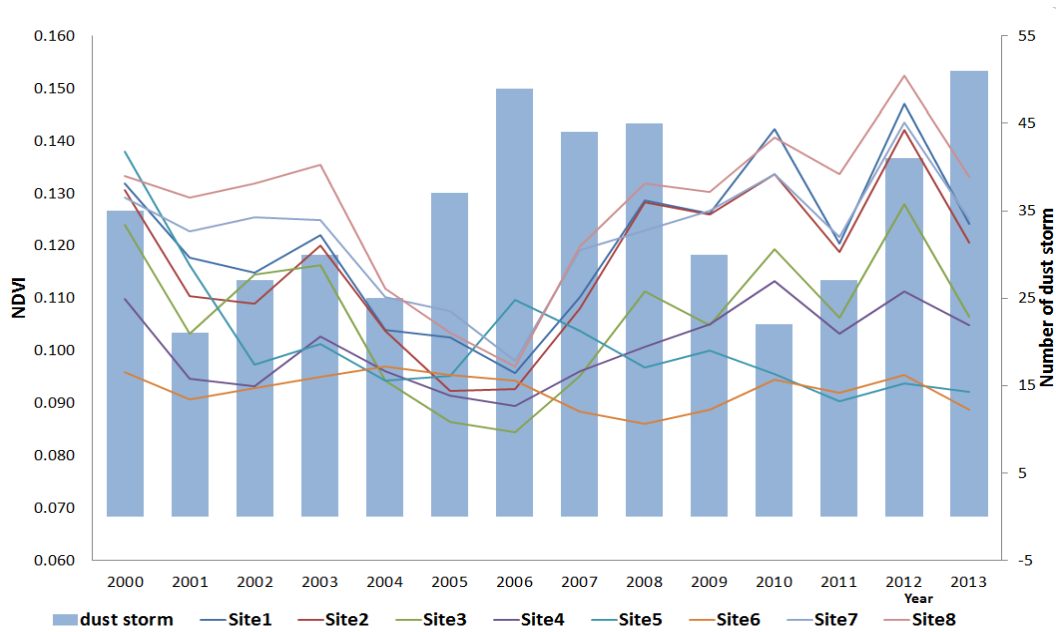


**Figure 12.** Relationship between mean NDVI and dust storm in spring 2000-2013

In all sites, the positive correlation was found between NDVI and precipitation between May to August, 2000-2013. But low correlation is observed in 5th and 6th sites. In places numbered 3, 4 and 8 sites, high correlation value was observed between dust storm events, and NDVI (Figure 12, Table 2).

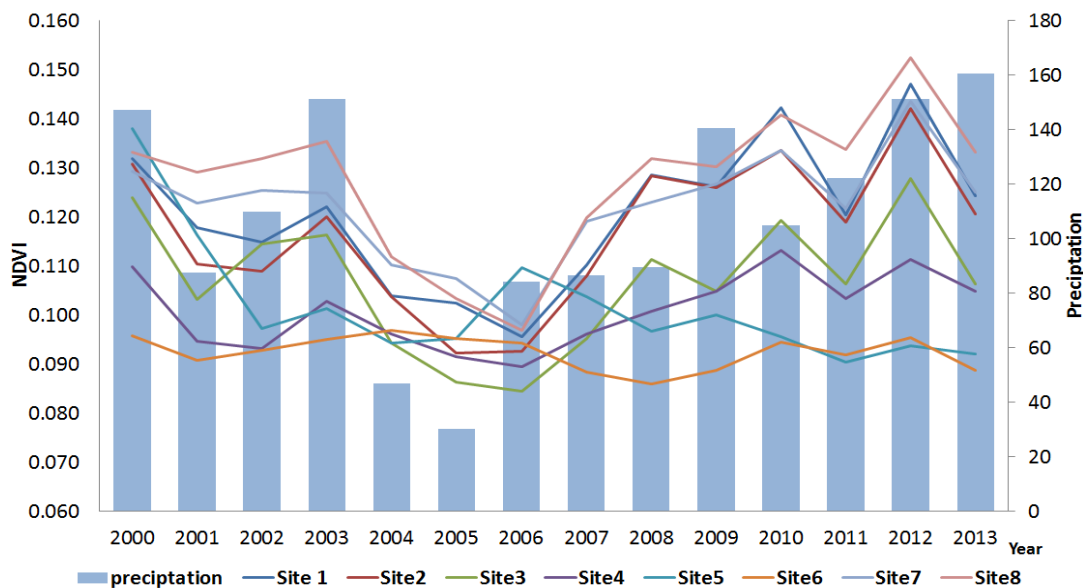


**Figure 13.** Relationship between mean NDVI and precipitation in spring 2010-2013

Dust storm occurrence had increased with decreasing of precipitation in spring. We found that the increase of NDVI was related with a relatively high amount of precipitation dropped in 2001, 2004 and 2006. Dust storm occurred to increasing next spring, NDVI value was high in next summer (2002, 2005, 2006) (Figure 13, Table 2).

**Table 2. Correlation coefficients various parameter (dust storm, precipitation, NDVI)**

Sites		1	2	3	4	5	6	7	8
Precipitation-NDVI	r	0.455	0.4427	0.4709	0.3689	0.0471	0.2648	0.4438	0.4517
	p	3.05E-09	8.96E-09	8.15E-09	2.50E-09	0.561	0.0009	8.17E-09	4.60E-09
Dust storm-NDVI	r	-0.689	-0.6907	-0.851	-0.727	0.0717	-0.500	0.693	-0.768
	p	0.0399	0.039	0.0035	0.026	0.854	0.170	0.039	0.0155

### 2.4.2 Relations between NDVI, Soil moisture and elevation in spring 2013

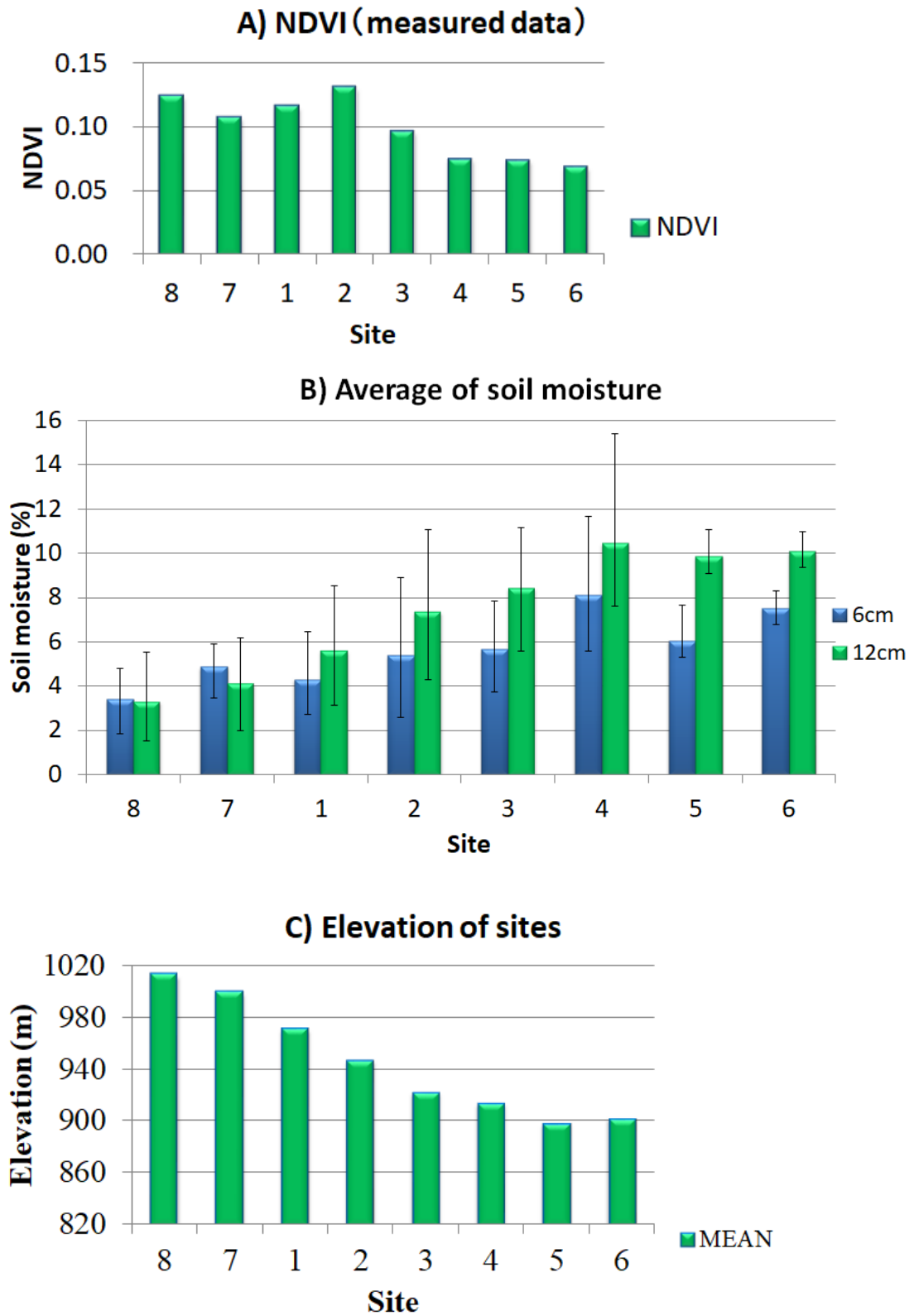


**Figure 14.** Comparison of NDVI (A), soil moisture measurements (B) and elevation (C) in Sainshand

The lower the elevation, the higher the soil moisture content. It is thought that precipitation mainly affects soil moisture content.

Figure 14a, b shows the elevation graph for each place, and the soil moisture measured in the field survey. From this, we expected that site 6 would have the highest NDVI, but site 6 (0.065) showed the lowest value when NDVI was measured.

Lowest values of NDVI were found in site 6 (0.065), and highest were in site 2 (0.13).

Soil moisture was highest in sites 4 and 5 were than 10.1 and 9.9 minimum value was in site 8 was 3.5 (Figure 14).

## 2.5 Conclusion

This study aims to examine the relationship between NDVI and dust storm observations in Gobi zone of Mongolia based on data from 8 sites based on 14 years of MODIS/NDVI data. We analyzed using meteorological parameters and of the NDVI derived from the satellite observations. The results reveal that a correlation between dust storm and vegetation cover was reasonable negative relationship, the correlation coefficient value was -0.5. For the analysis, we examined correlation between the precipitation and the NDVI. In all sites, there were positive correlation between NDVI and precipitation between May to August, 2000-2013. But low correlation is observed in sites 5 and 6. High correlation was observed in sites 3, 4 and 8 high correlation were observed between dust storm events, and NDVI. Dust storm occurrence had increased with decreasing of precipitation in spring. Dust storm occurrence had increased with decreasing of annual precipitation in spring. The most degraded area was southwest region of the Gobi with the least precipitations.

NDVI minimum value in sites 4, 5 and 6 were 0.065 and maximum value in site 2 was 0.13.

Soil moisture was highest in sites 4 and 5 were than 10.1 and 9.9 minimum value was in site 8 was 3.5 (Figure 14).

Comparison of springs NDVI and previous summer precipitation. We assume summer precipitation becomes the limiting factor for the vegetation growth.

The dust storm occurred during 2000-2013 are depended on precipitation of last summer and the vegetative cover.

## **Chapter 3 Overview of dust storms in Mongolia**

### **3.1 Introduction**

A dust storm is a meteorological phenomenon common in arid and semi-arid regions of the world. Dust storms that continue through several days in Mongolia are known as an “Ugalz” and the same storms are identified locally in different countries or regions by various specific term. For instance, it is called “Afganets” in Middle Asia. Sand storm is the term prevalent in Russia, Europe, Canada and USA. In Egypt and east regions of Sahara is named “hasmin”, in northern Sahara is “meheli”, in southern Sahara is “harmaton”, in Italy and northern regions of Africa – “sirroka”, in Sudan – “haboob”, in Iraq it’s known as “samoom”, in China identified as “huan fin”, which means “yellow dust” and “hin fin” which means “black dust.

According to report attempts to provide an overview of studies on dust storm that originate in Gobi areas of Mongolia. Dust storms frequently occur in the Gobi Desert in spring in association with strong winds, reduced vegetation coverage, and dry soil conditions. Dust storms happen in dry lands throughout the world, disrupting human life and economic activities and resulting in soil erosion. Dust storm have direct, indirect, and long-term effects. Dust storm are natural disaster phenomena that can have negative and direct consequences, including loss of life, delays to aviation, interruptions to rail and vehicular transport, and reductions in pasture for livestock. Dust storms can reduce the productivity of surface soil and have long-term effects regarding soil erosion, sand movement, and desertification processes (Natsagdorj et al., 2003).

According to P. S. Zaharov’s record about Russo-Japanese war fought from 1905 through 1906, the dust storm occurred in the Mongolian Gobi desert was carried to northeastward over the territories of China where it caused an interruption of the battle of Mukden.

In recent years, dust aerosols, originated from Mongolian Gobi and Northern China become familiar in East Asia as “Yellow dust storm” or “Yellow dust”. The dry soil particles contained in the dust passes over the Northeast Asia regions of China, Korea, and Japan, can stimulate significant environmental damages and affect human health. Recent written records show that the yellow dust of East Asia was found in the ice samples that were deposited nearly 45000 years ago in Greenland.

Dust and sand storms disrupt human life and economic activities and result in soil

erosion. One study showed that more than 70% of the pastureland area of Mongolia is under desertification, 22.1% is strongly overgrazed, and sand movement covers 7.9 million hectares of pasturelands (Jigjidsuren and Oyuntsetseg, 1998). According to the joint expedition by scientists of Mongolia and Russia, sand dunes with heights of 8–10 m move 15 m per year near the Ulaan-nuur Lake area, and sandy hills with heights of 5–6 m move 20 m per year near the Tavan Els area (Babaev et al., 1990). A Russian investigator (Nalivkin, 1963) showed that dust storms influence the formation of landscape and its variety and mentioned some study results of other scientists. A dust storm, which covered an area of 470,000 ha, was observed from 9 to 12 March 1901. At that time, it was discovered that 1.8 million tons of dust has been deposited. Mongolian scientist, Tuvdendorj studied climatology of dust storms and synoptic situations for the formation of dust storms using 10 years of data from 24 meteorological stations obtained between 1956 and 1965. This was the first published study of dust storms in Mongolia (Tuvdendorj, 1973, 1974). Researchers at the Institute of Geography and Permafrost in the Scientific Academy of Mongolia performed experiments on sand movement measurement near Zamyn-Uud city between 1982 and 1985, and the results are of special interest (Lomborenchin, 1983). Luvsandendeв and Jamiyanaа (1991) calculated dust and sand movements in Mongolia, using a turbulent diffusion equation. They compared calculated value of transported dust and sand with a measured value. In their study, the calculated value was 1990.7 tons and the experimental measured value was 1443.9 tons over a 0.5 km<sup>2</sup> of land field near Zamyn-Uud city.

In that study the frequency and distribution of dust storms over the territory of Mongolia investigated in detail. Using multiannual data, a dust storm prediction method that is being used for daily weather forecasting practice was developed (Jugder and Natsagdorj, 1992; Natsagdorj and Jugder, 1993).

### 3.1.1 Distribution of number days with dust storms and dusty day

Less frequency of dust storm has been identified in the Khangai region, due to weaker wind velocities, rich vegetation cover and long sustained snow cover. However, even with stronger wind power in steppe areas, considering the consequence of good vegetation cover and long sustained snow cover, the dust storms occur with less frequency in these areas. Sandstorm occurrences are more significant in urban areas where the soil erosion are caused by human-related activities. Figure has shown this in the certain places as in cities of Moron, Bulgan, Kharaa, Ulaanbaatar and Binder localities.

The geographical distribution of the number of days with drifting dust storms is shown on the Figure 15 and Figure 16. Geographical dispersion studies of annual average amount show that dust storm occurrences took place for less than 5 days a year in Khangai, Khovsgol and Khentii mountainous areas; in the desert areas, 30-37 days; and in the Great Lake Depression, 10-17 days (Figure 15 and 16). Three major regions, namely, Transaltai Gobi, Ulaan nuur of Umnugobi and Zamyn-Uud areas are identified as high frequency zones for dust storm occurrences. In addition to this, the dust storm occurrence and its geographical dispersion is closely related to geographical dispersion of days with massive wind and the surface soil characteristics of the country.

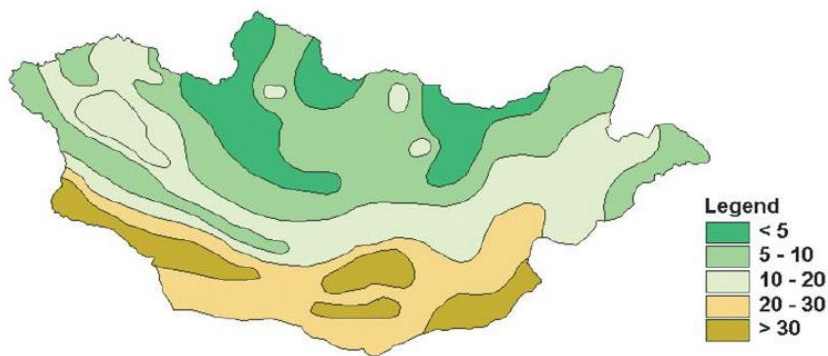


**Figure 15.** Distribution of number of days with dust storms observed in Mongolia  
(Source: L.Natsagdorj, D.Jugder, 2003)

The maximum number of days with drifting dust is 110 days over the Mongol Els area (the Durvuljin station's data), 60–70 days over the south side of the Altai Mountains and the Arts Bogd Mountain area (Figure 16).

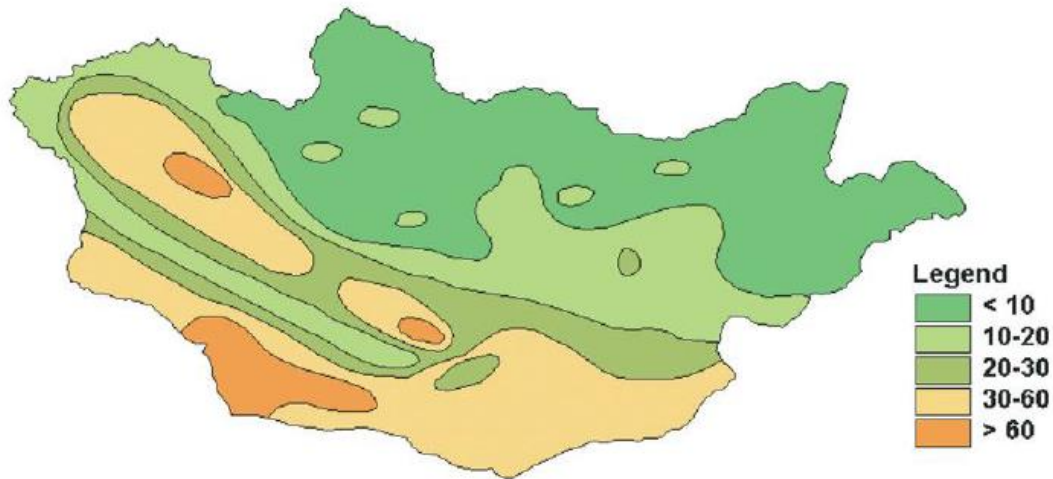


**Figure 16.** Distribution of number of days with drifting dust observed in Mongolia  
 (Source: L.Natsagdorj, D.Jugder, 2003)

### 3.1.2 Distribution of number of dusty days

The distribution of dusty days is shown in Figure 17. Remarkably, the amount of total number days both with sandstorm and blowing dust have identified less than 5 days in Khangai, Khentii, Khuvsgul mountainous areas, 71-125 days around Great Lake Hollow, 70-98 days within Transaltai Gobi area and nearly 80 days in the region of Arts Bogd. In other words, the significant occurrence of dust flowing arises over Mongol Sand desert area (Figure 17).

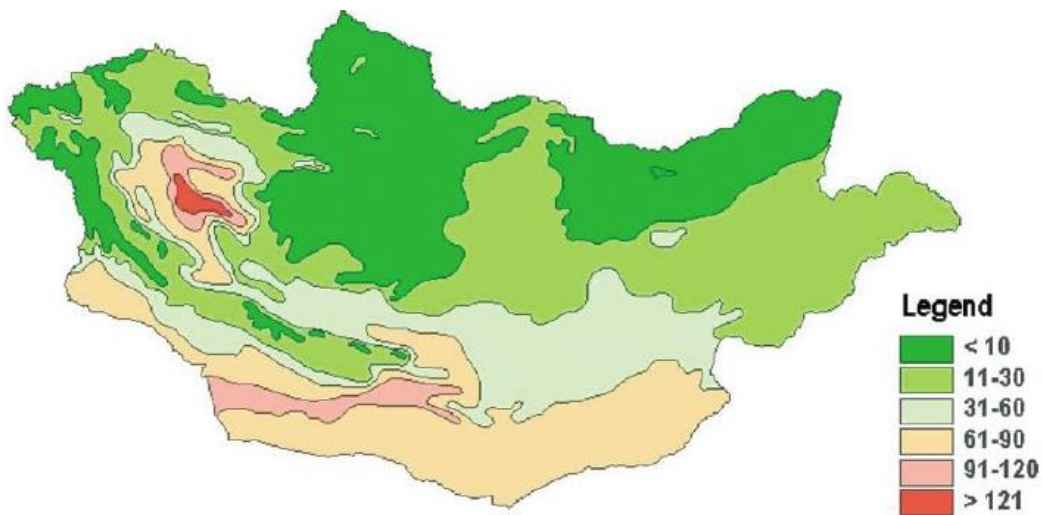


**Figure 17.** Distribution of number of dusty days observed in Mongolia.  
 (Source: L.Natsagdorj, D.Jugder, 2003)

### 3.1.3 Annual and daily variations of dust storms

There is a clear annual variation in dust storm occurrences in Mongolia. In association with the movement of the middle-latitude cold frontal belt, the highest frequency (61%) of dust storms occurs in spring and a second maximum frequency (22%) occurs in autumn (October and November) in Mongolia. The annual minimum frequency (7%) occurs in summer, a period when low-pressure fields with a weak pressure gradient predominates, and (10%) in winter, in which cyclonic activity is weak and the air is most stable. Annual variations in dust storm occurrences in the Gobi (station Dalanzadgad), steppe (station Baruun-Urt), and mountainous regions (station Muren) are shown in Figure 18.

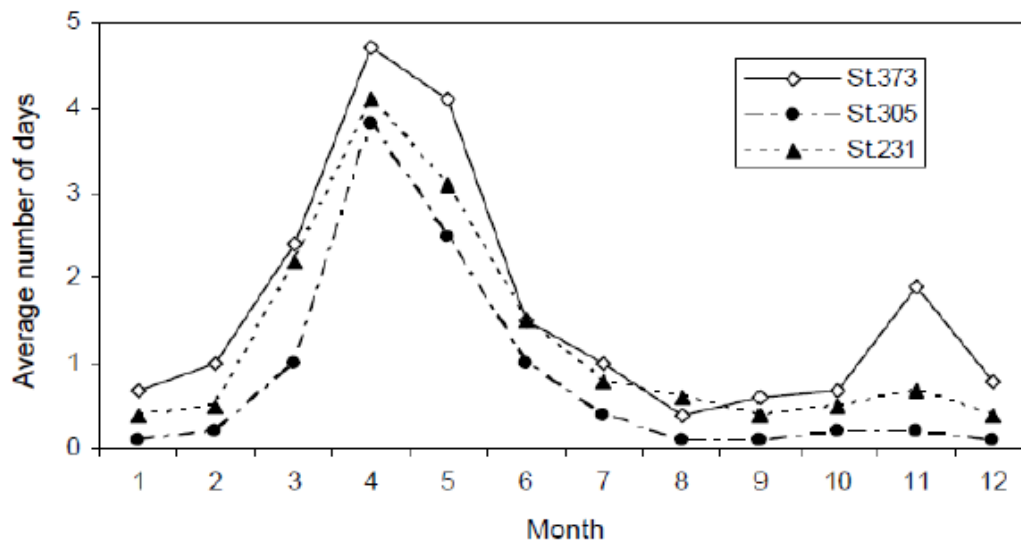


**Figure 18. Average number of days with dust storms between 1960 and 1989.**

(Source: L.Natsagdorj, D.Jugder, 2003)

From the top, St.373-Dalanzadgad station; St.305-Baruun-Urt station; St.231-Muren station.

The daily variation of dust storms for spring and highest frequency (65.5–91.0%) occurs in daytime and the lowest (9.0–34.5%) at night in the Gobi and steppe areas of each season.

### **3.1.4 Duration of dust storms**

For a study of the duration of dust storms, we used the beginning and ending times of dust storms obtained from 1975 to 1999. Monthly mean and annual mean durations of dust storms and drifting dust in the Gobi and the steppe area in Mongolia correlate well with the frequencies of dust storm occurrence. Where frequency is high there is a longer period of dust storms. The annual mean number of hours of dust storms is >100 h over the Gobi on the south of the Altai Mountains and the territory of Umnigobi Aimag.

The number of hours of dust storms is about 364 h at the Saikhan station in this Aimag. The maximum length of drifting dust is about 485 h around the Mongol Els area. The duration of the combinations of dust storms and drifting dust is longer than 200 h per year over the Gobi on the south of the Altai Mountains, Umnigobi Aimag and around the Mongol Els area. For example, it is about 493 h at the Tooroi station in the south of the Altai Mountains, about 614 h at the Saikhan station of Umnigobi Aimag, and about 508 h at the Durvuljin station in the Mongol Els area. We also calculated the average duration of a dust storm occurrence. This was done by first determining the duration of dust storm occurrences over 15 years (10458 h in the Zamyn-Uud). After that, the figure was divided by the total number of dust storm occurrence over the 15 years (233 cases over 15 years in Zamyn-Uud).

In this way, we obtained the average duration of dust storm occurrence at other stations in the Gobi (Table 3).

**Table 3. Average duration in a dust storm (a drifting dust) occurrence (h)**

(Source: L.Natsagdorj, D.Jugder, 2003).

Station	DS	DD
Baitag	3.5	3.4
Tooroi	4.0	3.1
Ekhiin gol	7.1	5.4
Tonkhil	4.6	4.8
Altai	3.3	3.3
Gurvantes	6.2	4.8
Saikhan	8.5	4.6
Tsogt-Ovoo	5.4	3.0
Dalanzadgad	4.6	3.2
Khanbogd	4.1	3.0
Bogd	2.9	3.6
Saikhan-Ovoo	2.8	2.4
Mandalgobi	3.9	2.4
Choir	5.3	4.6
Sainshand	3.3	2.1
Zamiin-Uud	4.7	4.3

DS—dust storm; DD—drifting dust

Figure 19 shows the average duration of a dust storm. A dust storm (also a drifting dust) lasts on average from 1.6 to 6.0 hour, sometimes more than 12 hour in the Gobi and 3 hour (60–80%) in the mountainous area. There is also a relationship between frequency and duration. If the average duration of a dust storm (also a drifting dust) occurrence is more than 6 hour then its frequency decreases. The duration of a dust storm occurrence is longer in spring and shorter in summer.

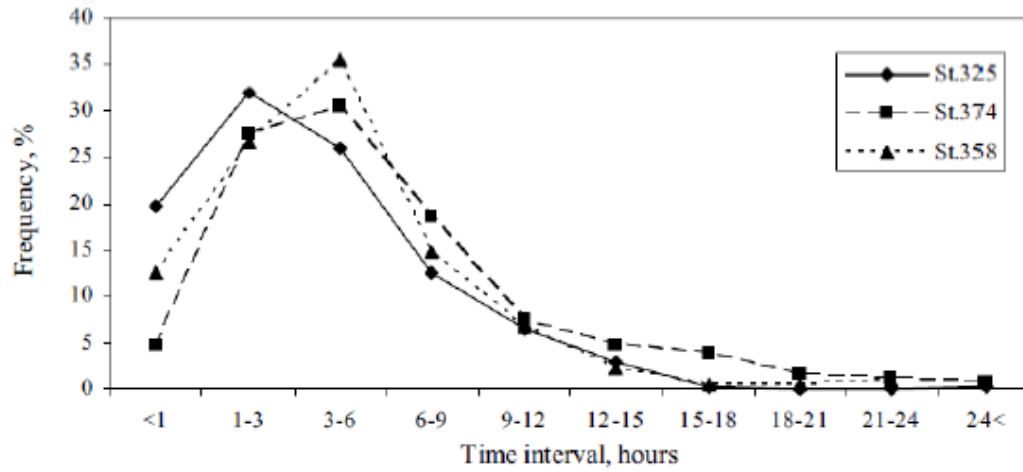


**Figure 19.** Average duration of a dust storm (time interval) in the Gobi.  
 (Source: L.Natsagdorj, D.Jugder, 2003)

### 3.1.5 Dust storm in Central Asia

Mongolian desert sandstorm has clear historical occurrences. Due to the cyclone impacts transferred southward and northward from mid-latitude, the peak frequency of sandstorm occurs during springtime (59%) and the second effective frequency - during autumn in September and October (10%). The least frequency occurrence in a year are during summer season, with lowest atmosphere pressure (7%). Secondly, it is at winter time, with sustained atmospheric high pressure (10%), when the impact of cyclone is weak. In other word, four extreme means of the annual occurrences of sandstorm have been presented during four seasons. Based on geographical dispersion of the annual average summary mean, the annual periodic duration of sandstorm has exceeded 100 h in South Gobi and Altai. Farther Gobi, particularly, it is 364 h in Saikhan. But, the maximum duration of blowing dust occurs within Altai farther Gobi (in Toroi) is 373 h a year. On average, the duration of an individual dust storm in desert areas is approximately 4.6 hours (Figure. 20 and MARCC2009).

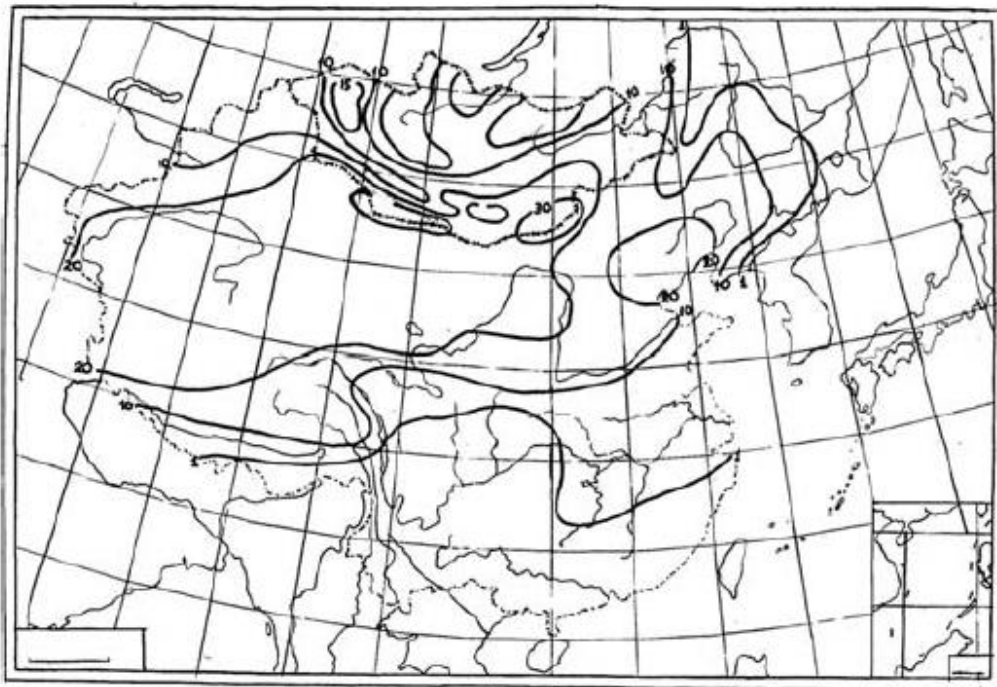


**Figure 20.** In order to indicate dust storm dispersion through desert zone of the Central Asia, a Map was developed by using data base on climate information of China Meteorological Administration and Meteorological Services of Mongolia.

## 3.2 Result

### 3.2.1 Duration of dust storm of Gobi area

#### 3.2.1.1 Data and methods

The meteorological data used in this the study was from Zamyn-uud meteorological station in Mongolia, and provided by the National Agency for Meteorology, Hydrology and Environmental Monitoring of Mongolia (Table 4).

**Table 4. Selected meteorological station (Gobi).**

	Station	Longitude	Latitude	Altitude (m)	Annual precipitation (mm)	Air average temperature (°C)
1	Zamyn-Uud	111.90°E	43.72°E	937	122.6	3.5

For a study of the maximum duration of dust storms, we used the beginning and end times of dust storms obtained March from 2000 to 2014 in Zamyn-Uud site of Mongolia.

Dusty days are defined the sum of days with dust storms and/or drifting dust. We counted the number of days corresponding to dust storm or drifting dust according to daily intervals of 24 hours from 20:00 (Ulaanbaatar local time, ULT, UTC+8). If a dust event (dust storm or drifting) persists past 20:00 ULT, the event is counting as occurring over two days. On the other hand, if there are several dust events in a day, the sum phenomenon is recording as only occurring over one day (Puntsagdorj, 2014). Dust storm days and dusty days are defined as those occurring in one month or one year.

A strong surface wind was defined as a velocity exceeding 6.5 m/s (a constant threshold), which is the threshold of dust emission for many dust storm numerical models (Tegen and Fung, 1995; Kurosaki and Mikami, 2003; Natsagdorj et al., 2003). Similarly, strong wind days are defined as the number of days of dust events.

The data were processed with R Studio, ERDAS IMAGINE 9.1, ArcGIS 10.3, MS Microsoft software.

### 3.2.2.2 Maximum duration day of dust storm

This study aims to examine the association maximum duration day of dust storms occurred in March from 2000 to 2014.

Maximum duration day of dust storm was at 12.04 hour from 29-30, 2012 in Zamyn-Uud station (Table 5).

**Table 5. Sum duration in a dust storm (a drifting dust) occurrence (hour), example 28-30 march in 2012.**

Year	Month	Day	WMO code	Power	Start time	End time	Duration time
2012	3	28	32	1	11:14	12:46	1:32
2012	3	28	32	1	17:10	18:06	0:56
2012	3	28	33	1	18:06	19:13	1:07
2012	3	28	32	1	19:13	20:00	0:47
2012	3	29	32	1	20:00	21:40	1:40
2012	3	29-30	32	1	00:46	12:50	12:04
2012	3	30	32	1	9:31	10:11	0:40
2012	3	30	33	1	10:11	18:20	8:09
2012	3	30	32	1	18:20	18:50	0:30

### **3.3 Discussion**

This chapter is focusing on spatial and temporal distribution of dust events over Mongolia based on the results of previous research (Natsagdorj et al., 2003).

According to climatology of dust storms in Mongolia it is compiled based on observational data of 49 meteorological stations from 1960 to 1999 and compared them with data between 1937 and 1989. Three different maps of the distribution of dust storms, drifting dust and the number of dusty days are presented. The results of the analysis show that the number of days with dust storms is 5 days, over the Altai, Khangai and Khentei mountainous regions and more than 20–37 days in the Gobi Desert and semi-desert area. The greatest occurrence of drifting dust arises around the Mongol Els area of west Mongolia. The number of dusty days, which is derived from the summary from number of days with dust storms and drifting dust is 10 days in the mountainous area and 61–127 days in the Gobi Desert and the Great Lakes hollow of west Mongolia (Natsagdorj et al., 2003). Dust storms occur more frequently in the city region and are accompanied by surface wind speeds usually from 6 to 20 m/s. Dust storms mostly occur when soil and air are dry, and 70% of dust storms occur in dry soil conditions. When dust storms occur, relative humidity averages 20–40% in Mongolia.

The highest frequency of dust storms happen in three areas in the Gobi Desert in Mongolia, such as the south side of the Altai Mountains and around Ulaan-nuur Lake and Zamiin-Uud. It should be noted that the distribution of dust storms coincides well with the distribution of strong wind (Natsagdorj, 1982; Jugder, 1999) and soil conditions.

### **3.4 Conclusion**

We examined the association maximum duration day of dust storms occurred in March from 2000 to 2014 in Gobi, Mongolia. Maximum duration day of dust storm was observed at 12.04 hour from March 29-30, 2012 in Zamyn-Uud station. Because of it we took it as our case study. Analysis on 4 different countries dust storm data was made and chose March 28 thru April 2<sup>nd</sup>, 2012 and studied it in Chapter 4 thoroughly.

## **Chapter 4 Northeast Asian dust transport: A case study of a dust storm event from 28 March to 2 April 2012**

### **4.1 Introduction**

Dust storms are a common phenomenon in the desert regions of Northeast Asia, especially in the Gobi desert in southern Mongolia, northern China, and Taklamakan desert in northwest China (Natsagdorj et al., 2003, Shao et al., 2003). Eastward and southeastward moving cyclones and the northwesterly wind often (transport large amounts of fine dust particles to the eastern parts of China, the Korean Peninsula, and Japan (Shao et al., 2003). Frequent Asian Dust vents in Japan during 2000–2002 followed severe dust outbreaks in East Asia (Kurosaki et al., 2003). Dust concentrations of PM<sub>10</sub> increase by at least double during severe dust events in comparison with normal atmospheric conditions (Judger et al., 2011, Judger et al., 2014). PM<sub>10</sub> dust particles are the primary source of the yellow dust phenomenon that spreads across Northeast Asia (Shao et al., 2008). Research has shown that Asian dust often reaches Korea (Lim et al., 2002, Chung et al., 1996, Kim et al., 2008, Uno et al., 2017), Taiwan (Tsai et al., 2013, Lin et al., 2004, Lui et al., 2004), and Japan (Kurosaki et al., 2003, Shao et al., 2003). The transport of desert dust from Asia to the North Pacific atmosphere has been well documented (Shaw et al., 1980, Parrington et al., 1983, Uematsu et al., 1983, Merrill et al., 1989, Bodhaine et al., 1995, Husar et al., 2001, Uno et al., 2009). The peak frequencies of dust storms occur from March to June and September (Natsagdorj et al., 2003). Dust storms are classified as a type of natural disaster, which can affect ecosystems, human life, and health (Natsagdorj et al., 2003, Kwon et al., 2002, Griffin et al., 2001, Garrison et al., 2003, Kellogg et al., 2004, Griffin et al., 2007, Higashi et al., 2014, Taylor et al., 2002). Researchers have included the use of radiative transfer, chemical transport, weather forecasting, and global, numerical, and regional climate models (Natsagdorj et al., 2003, Uno et al., 2003, Liu et al., 2001, Luo et al., 2003, Zender et al., 2003, Igarashi et al., 2011, Ishizuka et al., 2011, Sun et al., 2012) by using remote sensing (Husar et al., 2001, Prospero et al., 2002, Huang et al., 2007) such as light detection and ranging (LiDAR) (Shimizu et al., 2004, Sugimoto et al., 2005, Sugimoto et al., 2007) and climatology to understand the dust transport linked with dust storm events in Mongolia and China (Natsagdorj et al., 2003, Sun et al., 2001, Sun et al., 2003). Natsagdorj et al., (2003) have shown the number of dusty days has tripled from 1960 to 1999 (Natsagdorj et al., 2003). In Mongolia, the number of days with dust storms is less

than 10 days in the provinces of Altai, Khangai, Khuvsgul, and Khentii, more than 50 days in the Gobi desert region, and over 90 days in the southern part of Altai Gobi and far western regions of Mongolia (Chung et al., 2004, Mongolian national atlas book et al., 2009). The purpose of this study is to investigate the effects of long-distance transport from dust events occurring in Mongolia by cross-examining the elevated level of particulate matter in neighboring countries. With temporal variations and dust transport in Northeast Asia, we have used analyses of PM<sub>10</sub> concentration, back trajectory, and AD-Net LiDAR measurements at various locations during the period of 28 March to 2 April 2012.

## **4.2 Materials and methods**

### **4.2.1 Description of dust event**

Atmospheric dust phenomena includes widespread dust suspension in the air and dust or sand raised by the wind, i.e., a dust/sandstorm (DSS) caused by turbulent winds raising large quantities of dust or sand into the air and severely reducing visibility, dust whirls or sand whirls, and occasionally funnel clouds. The WMO (World Meteorological Organization) protocol has been used; dust events are classified according to visibility into the 4 categories as described below (WMO 407 et al., 1975)

- Dust storm: strong winds lift large quantities of dust particles, reducing visibility to between 200 m and 1 km.
- Drifting dust: dust is raised above the ground at eye level (<2m) locally through strong winds. The horizontal visibility may be reduced up to 10 km.
- Floating dust: raised dust or sand at the time of observation, reducing visibility to 1 to 10 km.
- Dust devils or dust whirls: local, spatially limited, columns of dust that neither travel far nor last long.

Dusty days are defined as the sum of days with dust storms and/or drifting dust. A strong surface wind was defined as a velocity exceeding 6.5 m/s (a constant threshold), which is the threshold of dust emission for many dust storm numerical models (Natsagdorj et al., 2003, Kurosaki et al., 2003). In this study, the DSS events are defined by above mentioned as the description of the dust events.

#### **4.2.2 Surface dust concentration data**

We used the hourly averaged data of PM<sub>10</sub> concentration measured by the KOSA Monitor of National Institute for Environmental Studies, Japan and National Agency for Meteorology and Environmental Monitoring, Mongolia, China and South Korea from March 28 to April 2, 2012 (Figure 21). In total 3 Mongolian, 9 Chinese, 11 Korean, and 9 Japanese dust monitoring stations were used in the study (Figure 21, Table 6-9)

**Table 5. Dust monitoring stations in Mongolia. (Source: National Agency for Meteorology and Environmental Monitoring, Mongolia)**

	<b>Name of station</b>	<b>Latitude (degree °N)</b>	<b>Longitude (degree °E)</b>	<b>Height (m) above sea level</b>	<b>Kind of station</b>
1	Dalanzadgad	43.57°N	104.42°E	1465	Urban
2	Sainshand Zamyn-	44.87°N	110.12°E	1101	Urban
3	Uud	43.72°N	111.90°E	937	Urban

**Table 6. Dust monitoring stations in China. (Source: China National Environmental Monitoring Center)**

	<b>Name of station</b>	<b>Latitude (degree °N)</b>	<b>Longitude (degree °E)</b>	<b>Height (m) above sea level</b>	<b>Kind of station</b>
1	Chifeng	42.27°N	118.97°E	649	Urban
2	Hohhot	40.82°N	111.68°E	1047	Urban
3	Yan'an	36.60 °N	109.05°E	981	Urban
4	Datong	40.10°N	113.13°E	162	Urban
5	Dalian	38.90°N	121.63°E	10	Urban
6	Jinan	36.68°N	116.98°E	44	Urban
7	Jinzhou	41.13°N	121.12°E	25	Urban
8	Shenyang	41.77°N	123.43°E	51	Urban
9	Qingdao	36.18N	120.39°E	27	Urban

**Table 7. Dust monitoring stations in Korea (Source: Korea Meteorological Administration)**

	<b>Name of station</b>	<b>Latitude (degree °N)</b>	<b>Longitude (degree °E)</b>	<b>Height (m) above sea level</b>	<b>Kind of station</b>
1	Donghae	37.52°N	129.11°E	30	Urban
2	Gwangju	35.16°N	126.85°E	72.4	Urban
3	Daegu	35.87°N	128.60°E	57.3	Urban
4	Busan	35.18°N	129.08°E	21	Urban
5	Incheon	37.46°N	126.71°E	116	Urban
6	Seoul	37.57°N	126.98°E	42	Urban
7	Mokpo	34.81°N	126.39°E	29	Urban
8	Jeonju	35.82°N	127.15°E	50	Urban
9	Jeju	33.50°N	126.53°E	65	Island
10	Seosan	36.78°N	126.45°E	41	Urban
11	Cheongju	36.64°N	127.49°E	50	Urban

**Table 8. Dust monitoring stations in Japan. (Source: Ministry of the Environment, Japan)**

	Name of station	Latitude (degree N)	Longitude (degree E)	Height (m) above sea level	Kind of station
1	Rishiri	45.12°N	141.21°E	40	Island
2	Ochiishi	43.16°N	145.50°E	49	Urban
3	Tappi	41.25°N	140.35°E	106	Urban
4	Sado-seki	38.25°N	138.40°E	136	Island
5	Happo	36.70°N	137.80°E	1850	Mountain
6	Ijira	35.57°N	136.69°E	140	Urban
7	Banryu	34.68°N	131.80°E	53	Urban
8	Yusuhara	33.38°N	132.83°E	790	Urban
9	Hedo	26.87°N	128.25°E	60	Urban

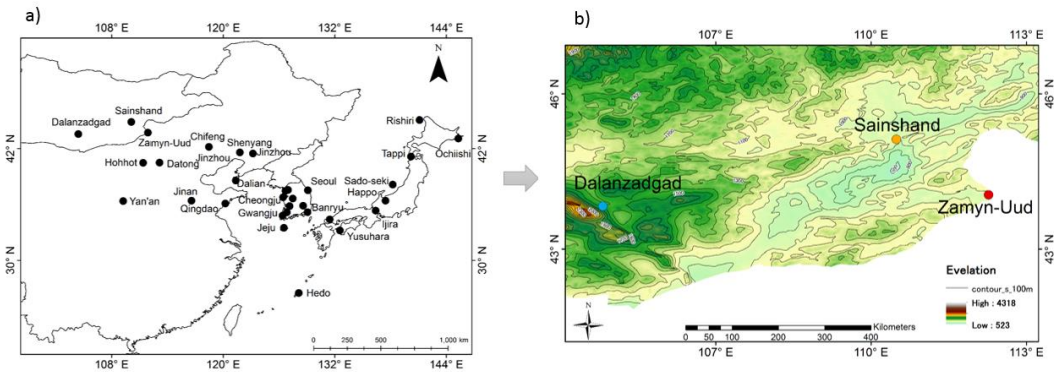


**Figure 21.** (a) Dust monitoring stations in Northeast Asia and (b) DEMs (digital elevation models) in the southern part Mongolia retrieval using NASA’s Shuttle Radar Topography Mission (STRM Data product)

According to PM<sub>10</sub> data sites were obtained by KOSA monitors which measure light scattering and are fitted with cyclone-type sizers. (KOSA Monitor; TOA-DKK Co., Tokyo, Japan) (Nishikawa et al., 2011)

The instrumentation of dust monitoring stations in Japan was sourced from the Ministry of the Environment in Japan.

The instrumentation of dust monitoring stations in China and Korea are available from the China National Environmental Monitoring Center and Korea Meteorological Administration, respectively.

### 4.2.3 LiDAR Monitoring data for AD-Net (The Asian Dust and Aerosol Lidar Observation Network)

Data from Mie scattering LiDAR measurements at Sainshand (44.87°N, 110.12°E), Seoul (37.57°N, 126.98°E), and Hedo (26.87°N, 128.25°E) were obtained from the AD-Net (The Asian Dust and Aerosol Lidar Observation Network) (STRM Data product et al., Mongolian DEMs et al., 2016) (Figure 22).

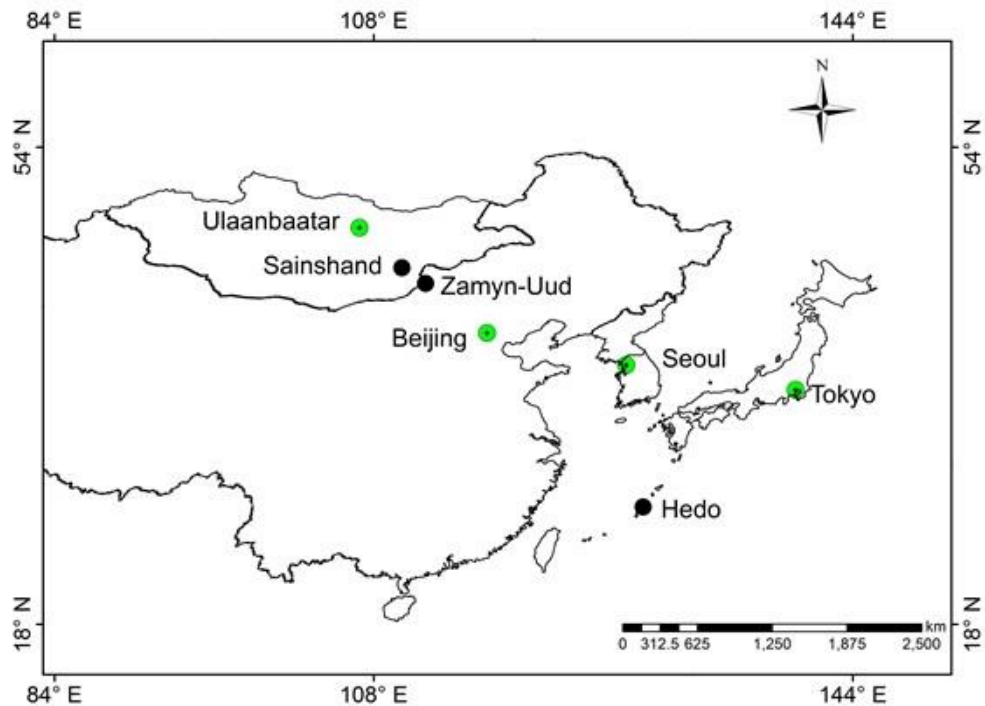


**Figure 22.** Locations of the AD-Net light detection and ranging (LiDAR) stations

These LiDARs are operated by the National Institute for Environmental Studies (NIES), Japan and the National Agency for Meteorology and Environmental Monitoring (NAMEM), Mongolia. The AD-Net LiDAR measurements used in the study have two wavelengths (532 nm, 1064 nm), the pulse repetition rate is 10 Hz, and the pulse energy is 50 mJ. The polarization of backscatter light is measured at a wavelength of 532 nm. The main parameters of the Mie-scattering LiDARs are the depolarization ratio, attenuated backscattering coefficient and extinction coefficient. They are operated automatically and the five-minute averaged LiDAR profiles are recorded every 15 minutes in the continuous observation mode (Judger et al., 2011, Sugimoto et al., 2005, Sugimoto et al., 2007, Mongolian DEMs et al., 2016)

#### **4.2.4 Meteorological data**

The hourly measurements of wind speed, visibility, weather conditions from the daily surface and 500-hPa upper level charts produced by NAMEM were used.

Synoptic observations, including wind speed, present weather and archive data (such as the number of dusty days and duration of dust storms) were obtained from three meteorological stations in Mongolia. The period during 1999 to 2016 was used for climatological analysis. ERA-Interim (ERA-Interim is a dataset, showing the results of a global climate reanalysis from 1979, continuously updated in real time) (Sugimoto.N et al., 2008) data is used for wind at 10 m and pressure at sea surface level.

#### **4.2.5 Trajectory method**

We have used forward and backward trajectories of air mass movements using the reanalysis HYSPLIT (The Hybrid Single Particle Lagrangian Integrated Trajectory) Model from the NOAA (National Oceanic and Atmospheric Administration) (Dee et al., 2011) and archived meteorological data of NOAA.

## 4.3 Result

### 4.3.1 Number of dusty days, its trend and PM<sub>10</sub> concentration of spring season at Dalanzadgad, Sainshand and Zamyn-Uud stations, Mongolia

There is a clear annual variation in dust storm occurrence in Mongolia. In association with the movement of the mid-latitude cold frontal belt the highest frequency (61%) of dust storms in Mongolia occurs in spring, and the second maximum occurrence (22%) of dust storms occurred in fall (October and November). The annual minimum frequency (7%) occurs in summer, which is a period when low-pressure fields with small pressure gradients predominate across the country and in winter (10%), when cyclonic activity is weak and the air is largely stable (Draxler et al., 2003). We analyzed daily meteorological data for a period of 18 years between 1999 and 2016.

In previous study (Judger et al., 2014), they have frequency and trends of sand/dust storm at the Dalanzadgad, Sainshand and Zamyn-Uud stations between 1960-2012 have been described. In this study, we extended the data of sand/dust storms up to 2016.

The numbers of dusty days at Dalanzadgad, Sainshand and Zamyn-Uud, located in the Gobi Desert. Only Zamyn-Uud has an increasing trend (Figure 23).

Dust storm frequency is higher during March and April months than other months in Mongolia (Natsagdorj et al., 2003). Monthly average concentration of PM<sub>10</sub> at Dalanzadgad, Sainshand and Zamyn-Uud were higher in March and April in 2009-2017. The results are shown in Figure 24. This study is a continuation previous studies (see (Judger et al., 2011, Judger et al., 2014) and included the latest data of PM<sub>10</sub>. The higher dust storm frequencies and higher concentrations of PM<sub>10</sub> are most likely correlated. In 2013, from summer to winter an instrument was disabled so measurements of PM<sub>10</sub> concentration couldn't be collected. The monthly average concentration of PM<sub>10</sub> varied from 36 to 46  $\mu\text{g}/\text{m}^3$  at Dalanzadgad in March and April between 2009-2017 except for in 2010, in which concentrations were as high as 60  $\mu\text{g}/\text{m}^3$ . According to climate data, precipitation was small, and for Dalanzadgad, 2010 was a drought year (Draxler et al., 2003). Conversely, the year 2017 was with higher precipitation and higher vegetation (Draxler et al., 2003). These climate conditions can influence the sand/dust storm frequencies at Dalanzadgad in those years.

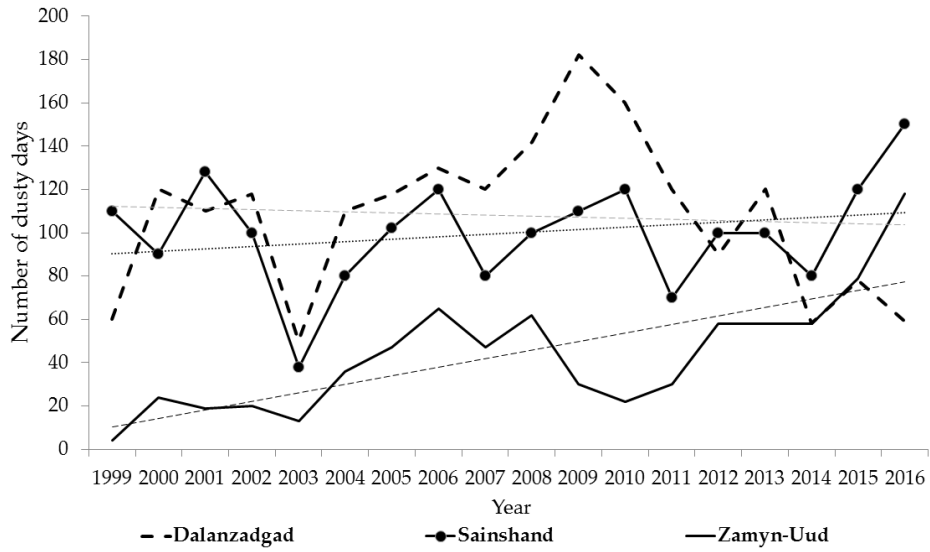


**Figure 23.** Number of dusty days at Dalanzadgad, Sainshand and Zamyn-Uud between 1999-2016

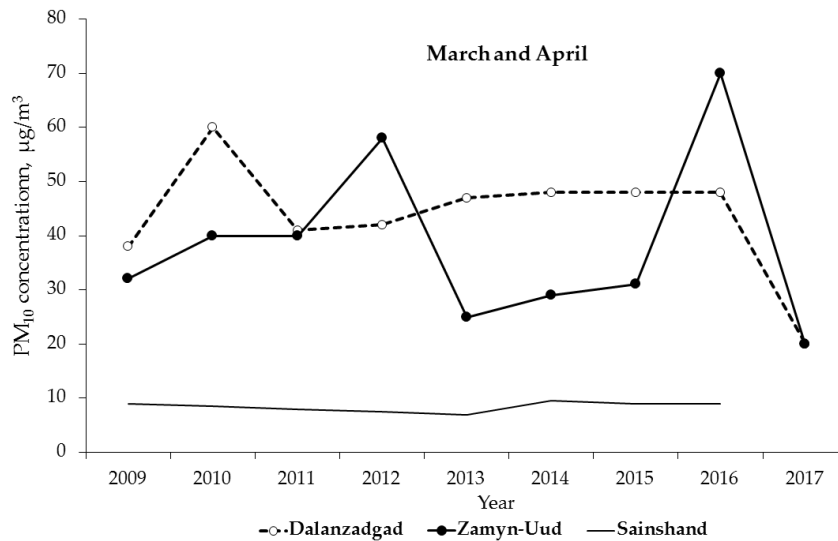


**Figure 24.** Monthly average datasets of PM<sub>10</sub> at Dalanzadgad, Sainshand and Zamyn-Uud in March and April between 2009-2017

Monthly average concentration of PM<sub>10</sub> at Zamyn-Uud in March to April was between 30-40 µg/m<sup>3</sup> in 2009-2011 and 25-30 µg/m<sup>3</sup> in 2013-2015 and as high as 60 µg/m<sup>3</sup> in 2012 and 71µg/m<sup>3</sup> in 2016 (Figure 24). Climate data shows that precipitation was higher and vegetation growth was good around 2013-2015 and 2017. These climate conditions may influence the lower frequencies of sand/dust storms, causing low concentrations of PM<sub>10</sub>.

Concentrations was as low as 19-21 $\mu\text{g}/\text{m}^3$  at those two sites in 2017. The monthly average concentration of  $\text{PM}_{10}$  at Sainshand was less than 10 $\mu\text{g}/\text{m}^3$  in March to April in 2009-2017.

## 4.3.2 North East Asian dust transport: A case study

### 4.3.2.1 Meteorological condition

A cyclonic circulation formed at sea level height, its wind speed increased and travelled from central Mongolia to east Mongolia on 28 March, 2012 (Figure 25a). The low-pressure system moved eastward with the high wind speed through northeast China, the Korean Peninsula and Japan from 28 March to 2 April, 2012 (Figure 25b, 25c).

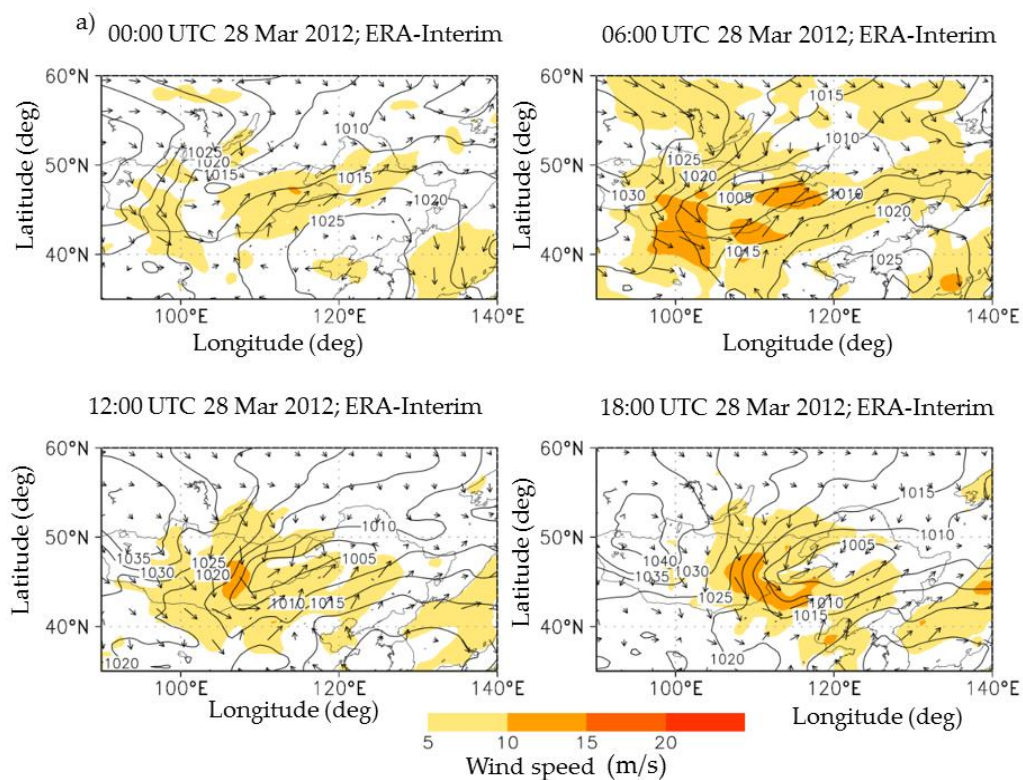


**Figure 25.** Sea level pressure (hPa) by contour and 10-m wind vectors using the ERA-Interim from 00:00 to 18:00 UTC on (a) 28 March 2012, (b) 29 March 2012, and (c) 30 March 2012 over Mongolia

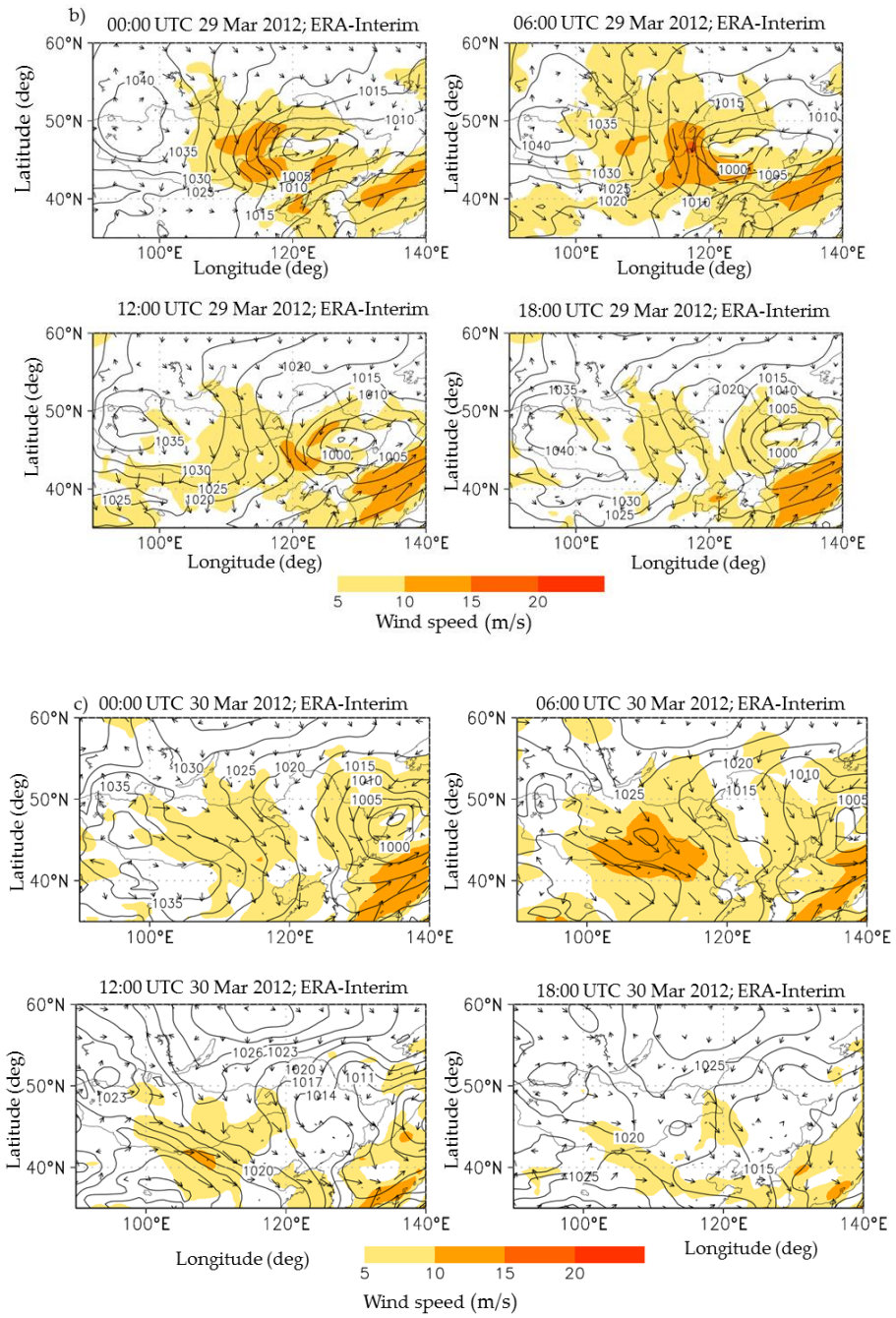


Figure 25. cont

Wind speeds increased in the dust source area including the Gobi Desert regions in southern Mongolia and northern China due to the cyclonic pressure system. For example, daily maximum wind speeds varied at Dalanzadgad, Sainshand and Zamyn-Uud stations from 10 to 14 m/s. Maximum wind speed reached 14 m/s and duration of the dust storm was around 12 hours in Zamyn-Uud in 29-30 March, 2012. Relative humidity was measured at 7-12% at these sites during the dust storm period. High wind speeds in the Gobi Desert regions produced sufficient dust concentration of PM<sub>10</sub> in the source areas.

Dust concentrations of PM<sub>10</sub> increased by two times at observation stations in Mongolia and China during 28-30 March, 2012. The reason is related to the atmospheric cold and warm fronts that passed through the Gobi Desert areas of the two countries. Higher dust concentrations of PM<sub>10</sub> in 28-30 March were in conjunction with the passage of the atmospheric cold and warm fronts, respectively.

#### **4.3.2.2 Dust concentrations of PM<sub>10</sub> in the source areas**

**Mongolia:** The instrument measuring PM<sub>10</sub> was disabled at Dalanzadgad during the peak dust storm period due to a cut in the power supply. Historically, PM<sub>10</sub> concentrations are lower at Sainshand (Judger, D et al., 2011, Judger et al., 2014) a topic that should be explored in future studies. For these reasons, these two sites could not provide reliable data on PM<sub>10</sub>. However, PM<sub>10</sub> dust concentrations at Zamyn-Uud showed the dust event perfectly. Hourly mean dust concentrations of PM<sub>10</sub> were as high as 404 µg/m<sup>3</sup> at Zamyn-Uud during the dust event period (Figure 26). Dust concentrations of PM<sub>10</sub> at Zamyn-Uud reached the threshold values of the onset of dust events (Judger et al., 2014).

**China:** Hourly mean dust concentrations of PM<sub>10</sub> were higher than usual, 999 µg/m<sup>3</sup>, at Hohhot and 1387 µg/m<sup>3</sup> at Chifeng in 28-29 March 2012, while concentrations at Hohhot measured 1724 µg/m<sup>3</sup> on 30 March and around 599 µg/m<sup>3</sup> in Qingdao and Dalian on 31 March, respectively (Figure 27). Concentrations fluctuated under 400 µg/m<sup>3</sup> at the other stations during the study period.

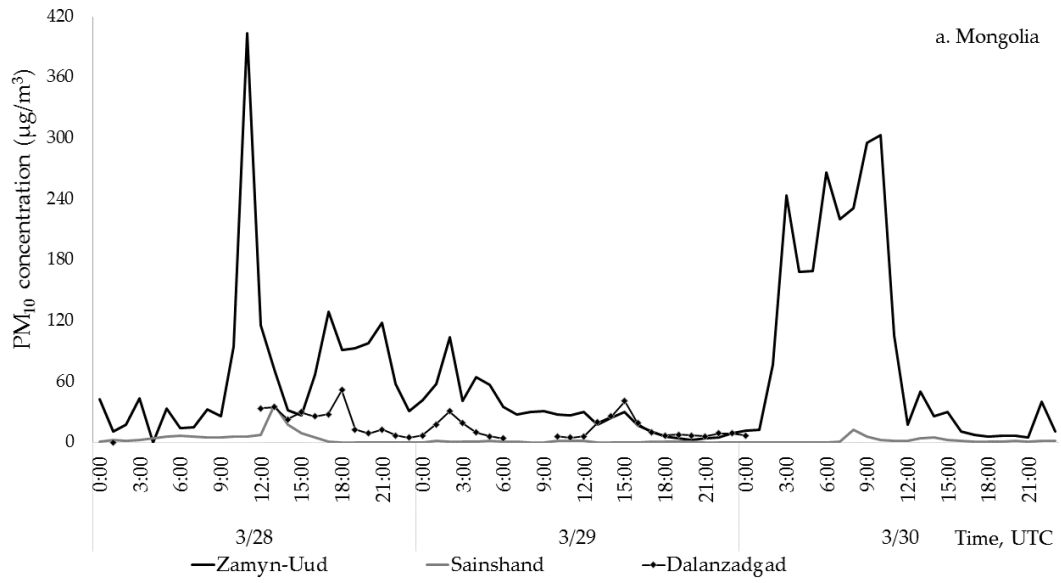


**Figure 26.** Time series variations of dust concentration of PM<sub>10</sub> at stations in Mongolia, 2012

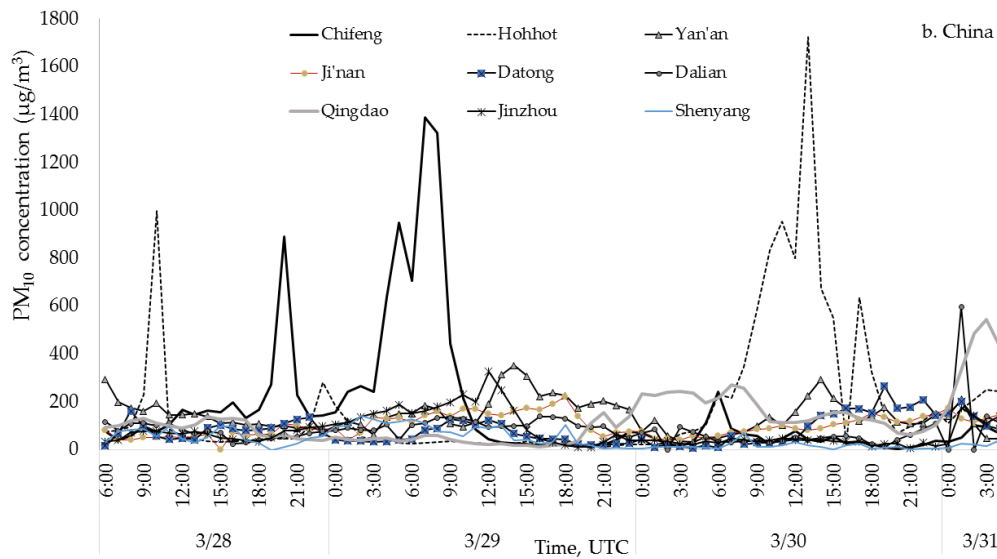


**Figure 27.** Time series variations of dust concentration of PM<sub>10</sub> at stations in China, 2012

### 4.3.2.3. Dust concentrations of PM<sub>10</sub> in downwind areas

**South Korea:** Maximum values of hourly mean dust concentrations of PM<sub>10</sub> were between 225 and 266  $\mu\text{g}/\text{m}^3$  in Jeju, Incheon and Cheongju on 31 March and varied from 147 to 182  $\mu\text{g}/\text{m}^3$  at the other stations between 31 March and 2 April, 2012 (Figure 28).

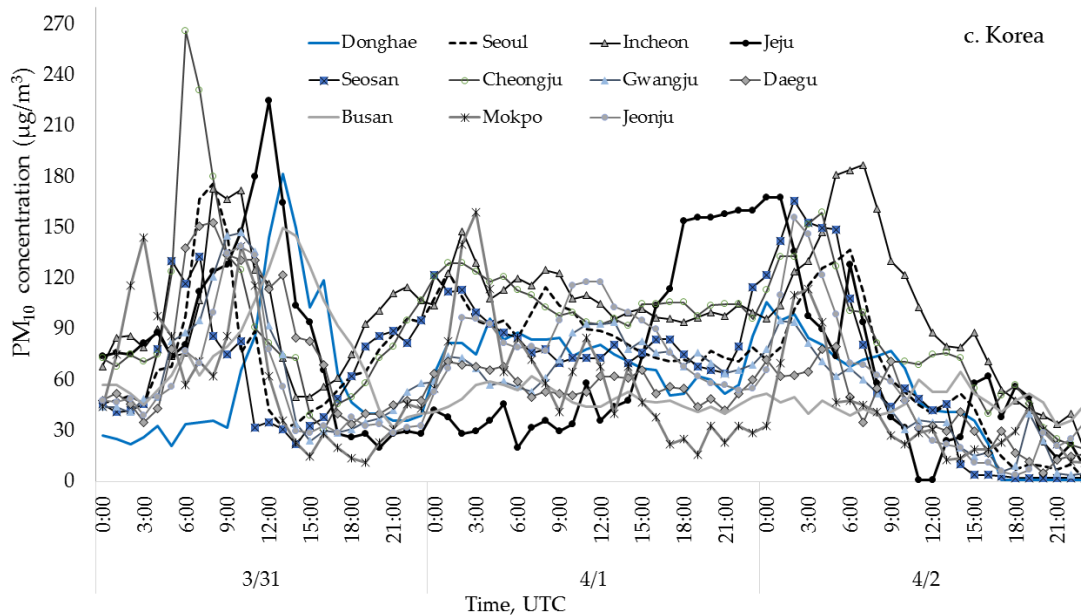


**Figure 28.** Time series variations of dust concentration of PM<sub>10</sub> at stations in Korea, 2012

**Japan:** Dust concentrations of PM<sub>10</sub> were higher at Hedo station (compared to all other stations), which is located on the north side of the island of Okinawa, Japan. Hourly mean dust concentrations of PM<sub>10</sub> were higher, 104-207  $\mu\text{g}/\text{m}^3$ , at Hedo station from 31 March to 1 April, 2012 (Figure 30). Concentrations increased at Banryu station in Yamaguchi Prefecture in northwest Japan and in Yusuhara station in Ehime Prefecture, Japan during the same days. Hourly mean dust concentrations of PM<sub>10</sub> increased slightly to 100  $\mu\text{g}/\text{m}^3$  at other stations in Japan on 2 April (Figure 29). Dust concentrations of PM<sub>10</sub> near the surface were higher in the source area during the dust storm period and decreased in the downwind areas.

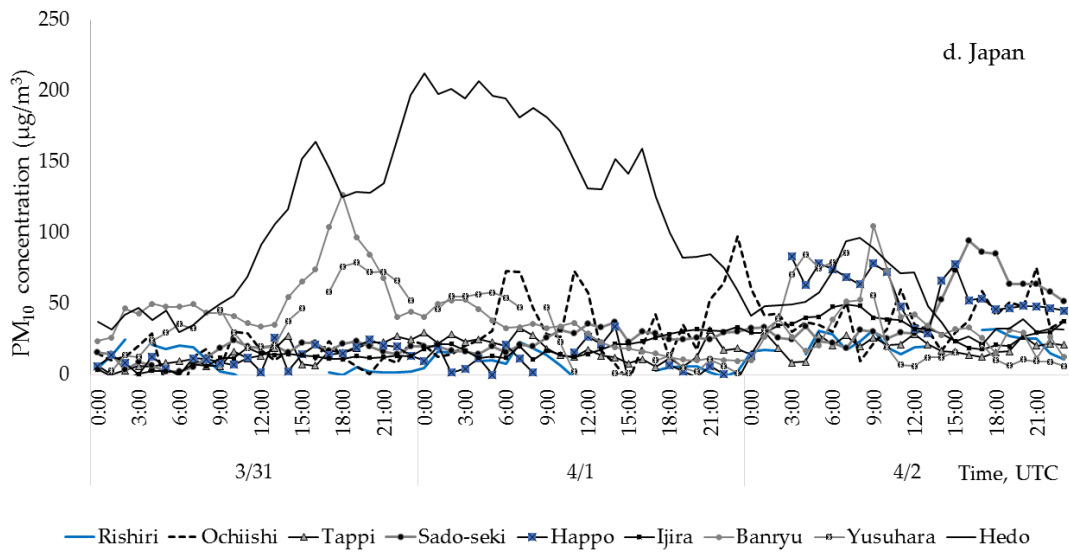


**Figure 29.** Time series variations of dust concentration of PM<sub>10</sub> at stations in Japan, 2012

#### **4.3.2.4 Vertical distribution of dust by LiDAR measurements and transport trajectories**

Dust vertical spread was measured by LiDAR in Mongolia, Korea and Japan during the dust storm period. Figure 30 shows time-height indications of extinction coefficients of non-spherical aerosols (mostly mineral dust) and spherical aerosol (mostly anthropogenic particles) derived from LiDAR measurements (MARCC et al., 2014, Sugimoto et al., 2014). LiDAR measurements show that the soil dust (upper panel) that was recorded at Sainshand between March 28-29 (Figure 30a) and at Seoul and Hedo stations from between 31 March to 1 April (Figure 30b, c). The heights of dust vertical spread were around 0.7 km in Sainshand between 28-29 March 2012 and around 1.2 km in Seoul, Korea and around 1.5 km around Hedo, Japan between 31 March and 2 April, respectively.

Our paper's discussion goal is soil dust event so we didn't describe detailed anthropogenic dust. But on Figure 30 (lower panels) we can very distinctly see anthropogenic dust (air pollution, red, green, blue colors). Between dates March 27<sup>th</sup> and April 2<sup>nd</sup> anthropogenic dust or air pollution (spherical particles) reached almost daily up to 800 meters (Figure 30a, lower panel) in Sainshand and Hedo stations. On the other hand, Seoul station's anthropogenic dust (spherical particles) between dates of March 27<sup>th</sup> and 30<sup>th</sup> distributed 1.5 km high (Figure 30b, lower panel).

LiDAR measurements showed that vertical diffusion of dust in the atmosphere was lower in the source area during the dust storm period and increased with distance in the downwind areas. PM<sub>10</sub> concentration sources originated in Mongolia, which we confirmed with the NOAA HYSPLIT model.

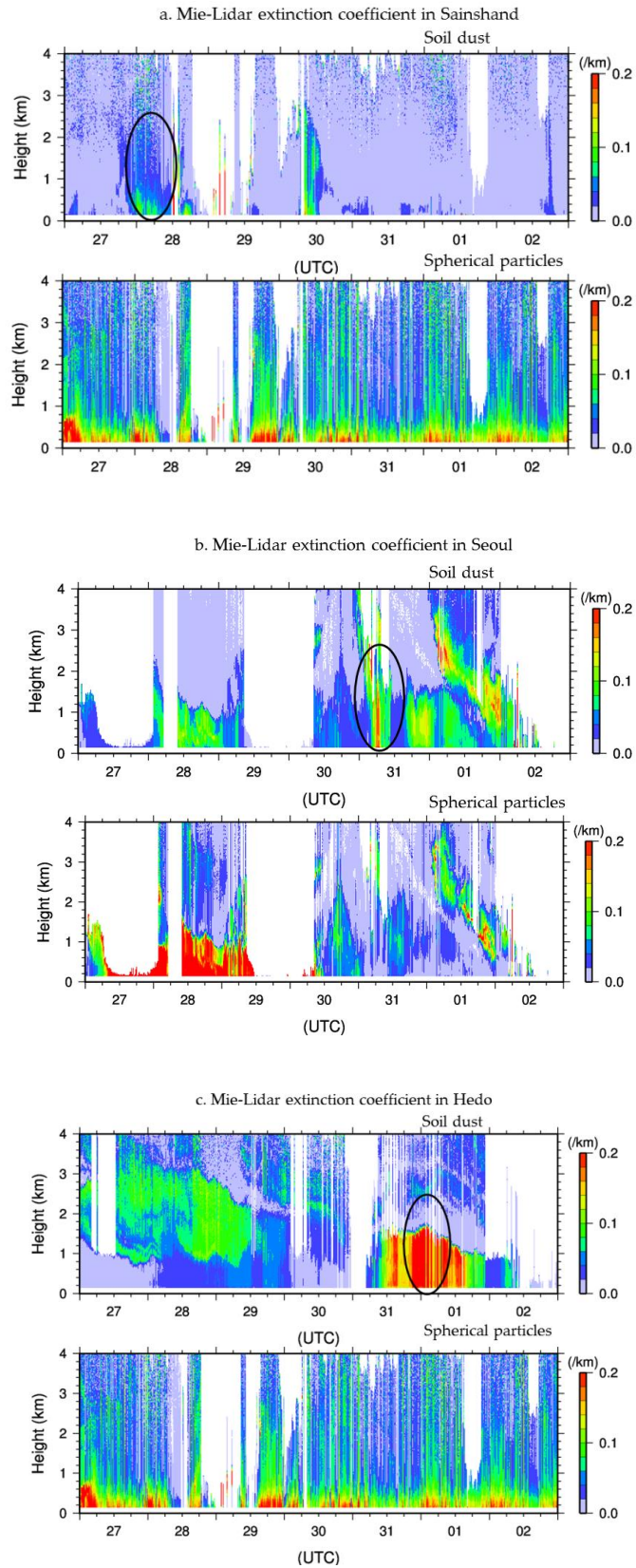


**Figure 30.** The Mie LiDAR extinction coefficients of non-spherical aerosol (dust) and spherical aerosol in Sainshand (a), Seoul (b), Hedo (c) from 28 March to 2 April, 2012 (Note: Time (UTC) in the horizontal axis and height in the vertical axis. The black circles indicate suspected dust observation)

#### **4.3.2.5 Dust transport by Air Mass Trajectories**

Forward and backward trajectories from the NOAA HYSPLIT model were used for air mass movements in North East Asia during the dust storm period from 29 March to 2 April, 2012 (Figure 31). To create the trajectories, we set the geographical coordinates of 4 stations in Northeast Asia including Zamyn-Uud, Hohhot, Seoul, and Hedo. A forward trajectory from Zamyn-uud, Mongolia ending at 00:00 UTC on 30 March and backward trajectories from Hohhot ending at 00:00 UTC on 31 March and Seoul and Hedo ending at 00:00 UTC on 1 April, 2012 were created at heights of 1500, 2000 and 2500 m, respectively (Figure 31).

The air mass movements at these heights mainly confirm the far transfer of air mass impurities at regional and global scales (Sugimoto et al., 2016).

In addition, the average heights of dust layers during the dust storm event were around 2.2 km at Zamyn-Uud and 2.0 km at Sainshand (Judger et al., 2011). Trajectories had a window of 48 hours.

The episode of forward trajectories of air mass movement from Zamyn-Uud, Mongolia (30 March 2012) is presented (Figure 31a) for illustration. Apparently, from (Figure 31), air mass from the Mongolian Gobi Desert passed over the eastern territories of China, the Korean Peninsula and Japan.

The results of the calculation of air mass backward trajectories show air mass transported from the Gobi Desert areas in southern Mongolia and in northern China to the eastern parts of China, the Korea peninsula and Japan (Figure 31b, c, d). These trajectories of air mass confirmed that dust was transported from the source areas downwind through Northeast Asia.

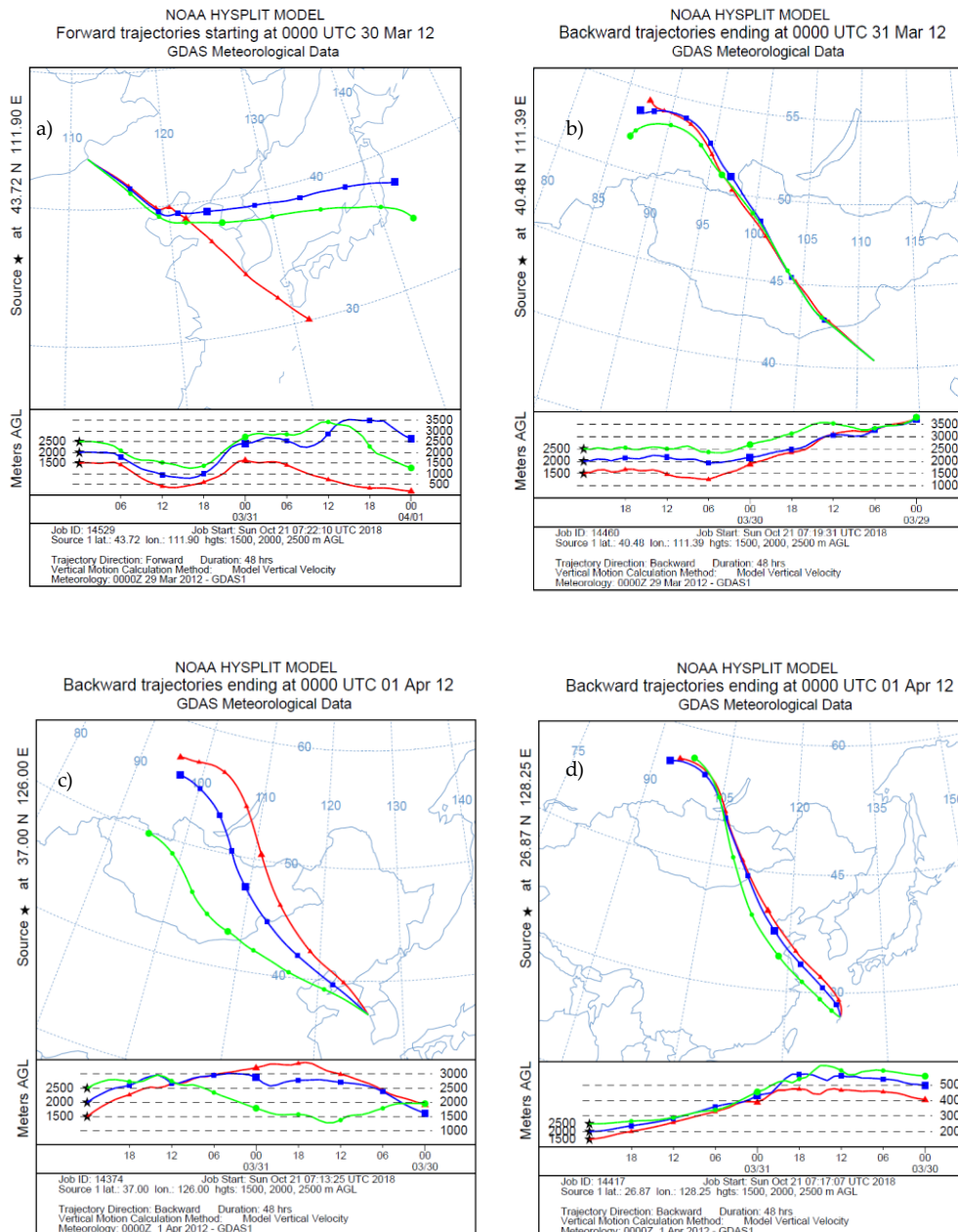


**Figure 31.** Forward and backward air mass trajectories using the NOAA HYSPLIT model: a) forward from Zamyn-Uud, Mongolia, b) backward from Hohhot, China, c) backward from Seoul, Korea d) backward from Hedo, Japan

## 4.4 Discussion

NOAA HYSPLIT model was used to analyze air mass movements which moved from Russia to Mongolia on March 30 and then travelled through southern to eastern Mongolia, eastern China and the Korean Peninsula on April 1 then through Japan to the Pacific Ocean (Figure 31).

The Sainshand station on March 28-29, Seoul station on March 31, and the Hedo station on April 1 all had dust movement that were observed by LiDAR measurements. We analyzed each station's dust transportation by NOAA HYSPLIT.

The Hedo station's PM<sub>10</sub> concentration was the highest value to come from Mongolia, as shown in Figure 31a. Along with the Hedo station's backward trajectory, PM<sub>10</sub> concentrations were observed higher than the 150 µg/m<sup>3</sup> value at the Hohhot and Qingdao stations.

Although there were observations of some fluctuations of dust concentration at Datong station which is situated 150 km and Yanan station that located 513 km from Hohhot respectively, that values slightly exceeded 150µg/m<sup>3</sup> standard value.

At the Seoul station, dust movement was observed higher than 100 µg/m<sup>3</sup> standard value from the north-west as it moved through the Chifeng station.

Highest dust fluctuation has been observed at the Incheon station located 33km from Seoul station. Also, a low increase of dust concentration to 90 µg/m<sup>3</sup> standard value was observed at Banryu station 544 km from Seoul station. That increase was slightly more than the country standard value. Dust movements observed at Tappi station located 1273 km and at Sado-Seki station situated 1003 km from Seoul station respectively, however, these values did not differ from regular meanings.

The PM<sub>10</sub> concentration maximum value in Mongolia was 404 µg/m<sup>3</sup> on March 28, and 999 µg/m<sup>3</sup> was observed in China, respectively. In Korea PM<sub>10</sub> concentration maximum value was observed on March 30-31 as 266 µg/m<sup>3</sup>. Lastly the Mongolian Gobi area's dust storm was active as it moved to Japan on April 1 with a PM<sub>10</sub> concentration maximum value of 212 µg/m<sup>3</sup>.

## 4.5 Conclusions

An Asian dust event occurring from 28 March to 2 April, 2012 was analyzed by ground observations of PM<sub>10</sub>, dust vertical spread by AD-Net LiDAR measurements and dust transport by air mass trajectories using the NOAA HYSPLIT model. The main results are summarized as follows:

1. Climatological data of dusty days show that the number of dusty days at only Zamyn-Uud, Mongolia has an increasing trend.
2. A low-pressure system and its cold front resulted in strong winds that transported dust from the source area across Northeast Asia at the end of March and the beginning of April, 2012. The dust storm also created an increase in PM<sub>10</sub> particles in the dust source area as well as in the downwind areas. Dust concentration of PM<sub>10</sub> near the surface is higher in the source areas of the Gobi Desert in Mongolia and China and less in the downwind areas during transport such as in Korea and Japan.
3. LiDAR measurements showed that dust vertical diffusion in the atmosphere is lower in the source area during the dust storm period and increases in the downwind areas especially when transported across far distances.
4. The trajectories of air mass confirmed that dust can be transported from the dust source areas in Mongolia and China to the Korean Peninsula and Japan.

## **Chapter 5 Overview of Regime shift**

### **5.1 Introduction**

Regime shifts refer to sudden and rapid changes in the structure or function of system due to the presence of forces/pressures (Scheffer et al., 2001; Holling et al., 1973; Folke et al., 2004). A regime is a characteristic behavior of a system which is maintained by mutually reinforced processes or feedbacks. Regimes are considered persistent relative to the time period over which the shift occurs. The change of regimes, or the shift, usually occurs when a smooth change in an internal process (feedback) or a single disturbance (external shocks) triggers a completely different system behavior (Scheffer et al., 2001; Scheffer et al., 2003; Folke et al., 2004; Beisner et al., 2003). Although such non-linear changes have been widely studied in different disciplines ranging from atoms to climate dynamics, (Feudel et al., 2008) regime shifts have gained importance in ecology because they can substantially affect the flow of ecosystem services that societies rely upon, (Biggs et al., 2009; Millennium Ecosystem Assessment et al., 2005) such as provision of food, clean water or climate regulation. Moreover, regime shift occurrence is expected to increase as human influence on the planet increases– the Anthropogenic (Steffen et al., 2007) including current trends on human induced climate change and biodiversity loss (Rockström et al., 2009). This occurs because systemic change alters feedback processes that maintain a system in a particular regime (Mayer et al., 2004). Second, hysteresis greatly enhances the role of history in a system, and demonstrates that the system has memory in that its dynamics are shaped by past events. Conditions at which a system shifts its dynamics from one set of processes to another are often called thresholds. In ecology for example, a threshold is a point at which there is an abrupt change in an ecosystem quality, property or phenomenon; or where small changes in an environmental driver produce large responses in an ecosystem (Groffman et al., 2006).

Vegetation in arid and semi-arid regions is highly dependent on precipitation and inter annual variation of vegetation is greater than in humid regions. Dependence on rainfall by annual plants is greater than by perennial plants. On the other hand, once perennial plants die, they take a very long time to recover. Ecosystem changes do not always occur in a continuous fashion. A regime shift is defined as a phenomenon that is irreversible or difficult to return to the original state when it exceeds a certain threshold (Nakashizuka et al., 2015). In the Inner Asian dry steppe, precipitation is the limiting factor (driving force)

for plant growth, and thus, knowledge of the relationship between precipitation and vegetation is important for efficient natural resource management and prevention of desertification (Otto et al., 2016). The relationship between precipitation and the Normalized Difference Vegetation Index (NDVI) as an indicator of plant growth has been thoroughly investigated in arid and semiarid regions. Since this period, the degradation of vegetation in pastureland has been observed more frequently. Annual plants in Gobi area of Mongolia might also have been affected by overgrazing and decreased precipitation. Recently, the frequency of Asian dust storm occurrence has increased in degraded pasturelands (Demura et al., 2015; Hoshino et al., 2014). The main environmental factors that affect the probability of Asian dust storm occurrences, are not only generated by atmospheric stability (such as wind speed, low pressure) but are also affected by ground surface heating, soil moisture content and surface vegetation coverage (roughness). Recognition of the importance of land-use history and its legacies in most ecological systems has been a major factor driving the recent focus on human activity as an essential subject of ecosystem regime shifts (Foster et al., 2003).

A study (Kurosaki and Mikami, 2004) defines the effect of snow cover on the threshold wind velocity of dust outbreak using data from 1988-2003. A threshold wind velocity for dust emission increases with the snow cover fraction (Kurosaki and Mikami, 2004). Small amounts of precipitation and snow cover in the Gobi Deserts influence spring soil moisture and cause dry soil conditions. Dry land surface plays a great role on the dust emission. The soil moisture index and the Thornthwaite precipitation evaporation index were less than 0.30 and 20 in the Gobi Desert area, respectively (MARCC, 2014). The spring drying was between April and May (Nandintsetseg, Shinoda, 2010) and this soil drying period coincided well with dust frequencies. Vegetation cover can influence dust emissions. A study used NDVI data from NOAA satellite in 1982-2003 (Bayasgalan, 2005) determined that NDVI was less than 0.29 in the Gobi region and less than 0.06 in the Desert region in Mongolia. Pasture production has decreased by 20-30% in the past 40 years based on pasture observation data. About 90% of pasture has changed in certain aspects. (MARCC, 2014). Pasture plants composition has changed, ecosystem zones have shifted and plants tolerant to droughts have become dominant. Soil fertility and quality has degraded (Wang, et. al., 2014).

### **5.2.1 The study area**

The study area was located in Gobi and the desert area over the southern part of Mongolia and in the northern part of China. Gobi is classified as a dry and semi-arid land with an average annual rainfall of around 100-200 mm. In this study, we focused on the area located between 40° N - 47.5° N latitude and 90° E - 117.5° E longitude.

### **5.2.2 Methods and Materials**

#### **5.2.2.1 Normalized Difference Vegetation Index (NDVI)**

The Normalized Difference Vegetation Index (NDVI) is a numerical indicator that uses the visible red and near-infrared bands of the electromagnetic spectrum to characterize surface vegetation conditions. The NDVI expressed as (1).

$$\text{NDVI} = (\rho\text{NIR} - \rho\text{R}) / (\rho\text{NIR} + \rho\text{R}) \quad (1)$$

Where,  $\rho\text{R}$  and  $\rho\text{NIR}$  stand for the spectral reflectance (GIMMS) in the visible red and near-infrared regions, respectively. In this study, we used NOAA AVHRR 15 day composite images with a resolution of 8 km. The atmospherically corrected reflectance product data (data sources from Goddard Space Flight Center, GSFC) was used to calculate the NDVI from 1985 to 2013 for the May to September season.

#### **5.2.2.2 Hovmoller diagrams**

Hovmoller diagrams are great for displaying large amounts of data in a meaningful and understandable form (Hovmöller, 1949). As show in Figure 32, Hovmoller diagrams were generated to summarize and examine the space time features of seasonal evolution and the anomaly patterns for the entire monthly time series from 1985 to 2013 (Sofue et al., 2017; 2018).

#### **5.2.2.3 Identification of vegetation growth period**

Using vegetation cover data and monthly rainfall data, monthly average images for 29 years were created using ArcGIS 10.2. For the vegetation cover data, the maximum value was selected from bi-monthly data and an NDVI image of monthly maximum value was

created. Using these images, Hovmoller diagram were created using the open source software R. By comparing the resulting Figure.32, we identified the growth period (growing season: GS) of major vegetation in Gobi.

### 5.3 Results and Discussion

From the Hovmoller diagrams, NDVI values were found to increase with increase in precipitation, during the VGP. This showed a high response to precipitation by vegetation. We focused on longitude distribution of precipitation and NDVI since as shown in Figure 5, during the VGP, different distribution of precipitation in this area has been strongly affected by monsoon. Vegetation in eastern region (longitude is  $>E100.00$ ) that has more precipitation than other regions responded well to the precipitation.

Figure 5 shows the comparison of precipitation anomaly and NDVI anomaly in VGP of longitude E900-E117.50 between 1985 and 2013.

In the Figure 32, the region highlighted with a dashed rectangle is an area where there was minimal response by vegetation to precipitation. There is a possibility that regime shift of vegetation had occurred in this area.

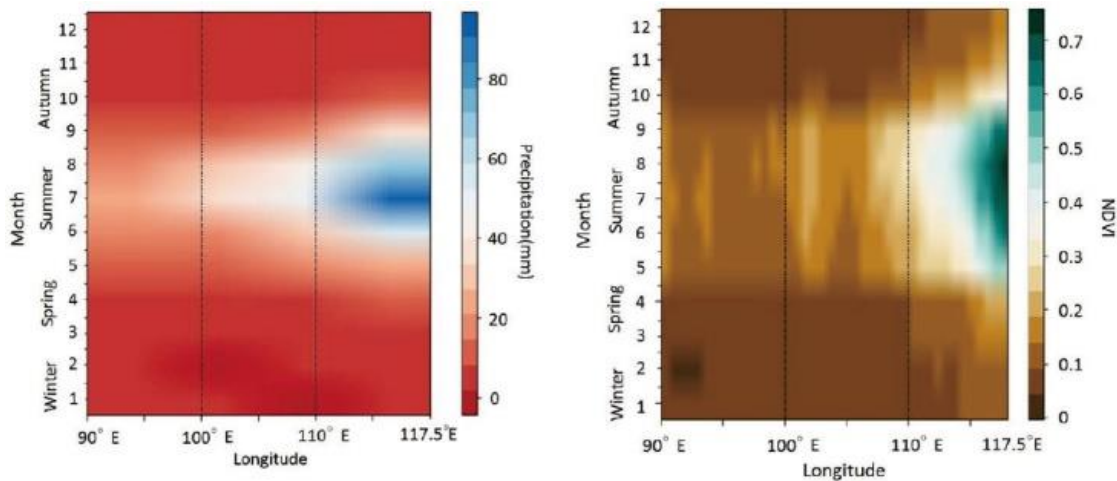


**Figure 32.** Hovmoller diagrams of monthly precipitation (left) and monthly NDVI (right) VGP along the E90° – E117.5° longitude

### 5.3.1 Detection environmental regime shift

The environmental regime shifts real world systems occasionally undergo substantial changes triggered by minor disturbances. According to a major theoretical finding when it comes to regime shifts is that ecosystems recover slowly from small perturbations in the vicinity of tipping points (Figure 33b). However, indicators of critical slowing down are not manifested in all cases where regime shifts occur, because not all regime shifts are associated with tipping points. In recent years, this challenge has gained importance as it is unclear how grassland ecosystems will respond to current trends in climate patterns and anthropogenic pressures (Dakos et al., 2015).

It is difficult to know if regime shift is happening. The provided water such as rainfall is one of the most important factors for vegetation especially in arid regions (Figure 33a). As shown in Figure 33, the areas highlighted with the circle and square respectively, are situated in China, such as Gansu, Xinjiang Uygur and Bayannaoer. Previous study showed that there was a decline trend in Bayannaoer in Inner Mongolia during 1999-2012 (Buhe, 2015).

In 2001 and 2002, very low precipitation with anomaly value of  $-40\%$  or less was found and vegetation tendency changed around the same time, after that, the negative trend continued (Figure 33c, d). From these results, it is considered that one cause of vegetation degeneration is likely to be change in precipitation. In semi-arid ecosystems, water soil respiration (Yan et al., 2011).

Water availability moderates the effects of other, factors such as temperature and substrate supply, on soil respiration. It's interannual variations are directly linked to both the intensity and the frequency of precipitation. Shifts in precipitation regime will alter not only the size of individual rainfall events, but also the length of the dry-spell duration and thus the antecedent soil water condition (Yan et al., 2014).

Droughts, which result from irregularities in annual or season precipitation, can negatively affect land and lead to ecological degradation. Ecosystem degradation can lead to deforestation and desertification.

Desertification, in combination with high-speed wind, leads to sand and dust storms (Abdi, Glover and Luukkanen, 2013).

When the pasture land undergoes desertification, the seed bank in the soil disappears and the soil layer is destroyed. It was suggested from 2003 that vegetation no longer responds

to precipitation in  $F_2$  region. Variation of vegetation showed a decreasing trend with increase in precipitation, (Sofue et al., 2017, 2018; Hoshino et al., 2018)

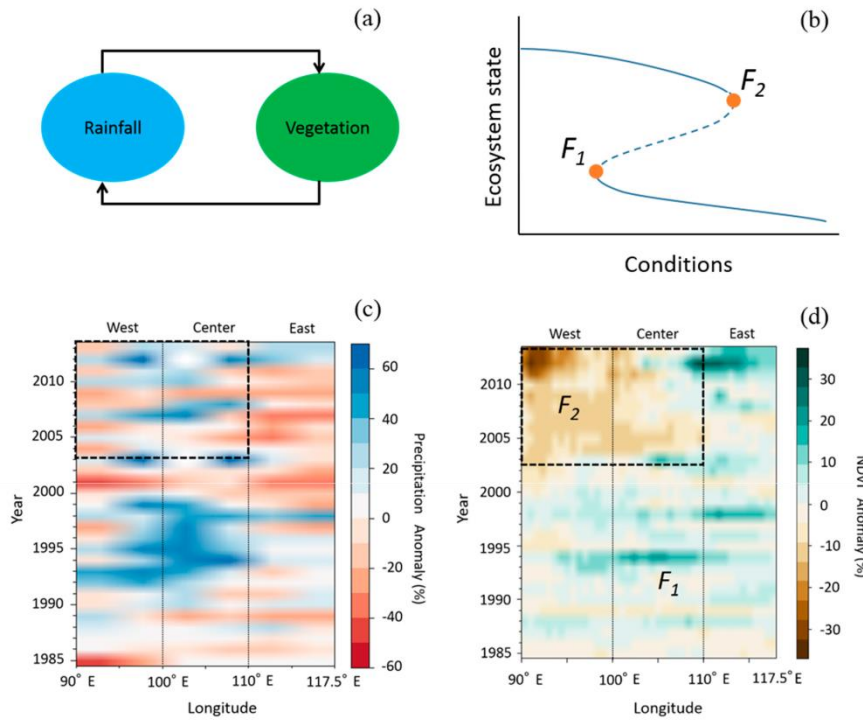


**Figure 33.** Environmental regime shifting in North China, during 2003-2013. (a) shows that the concept of relationship between precipitation and vegetation, (b) shows that the concept of regime shift, (c) precipitation anomaly and (d) NDVI anomaly of the study area

Previous study showed that there were empirical evidences of the links between desertification by overgrazing, drought and dust storms from the Gobi Desert of Mongolia. The country’s mobile pastoralism traditions stretch back more than a thousand years, but overgrazing of rangeland by pastoralists has been the most commonly cited cause of desertification in global dry lands for more than 30 years. Although overgrazing, desertification and dust storms are frequently connected, drought was found to be an important driver of vegetation cover change in and around the Gobi Desert. Vegetation cover adversely affected by drought was further reduced by grazing; the combined conditions led to loss of livelihood opportunities and increased household poverty (Middleton, 2016).

According to the drought conditions and changes are calculated based on satellite data, therefore the Normalized Drought Difference Index (NDDI), which is a MODIS data standard index, was analyzed. Comparative analyses of drought changes in the years 2000 and 2010 indicate significant increases of drought in the Great Lake Depression, Lake

valley and Southern parts of Gobi. (Mongolian desertification atlas, 2013). One of the signs that land is degraded is the occurrence of dust storms, which are for many reasons explained as a driver of the soil degradation and desertification process. The impact of wind on soil surfaces has various forms, but dust storm should be understood as the most severe form of erosion. Although the impact of wind on soil and vegetation cover has to be an integral part of desertification research, such survey has been abandoned in Mongolia. The only research to address this is by L.Natsagdorj, who researched the erosive impact of wind and wind velocity, and attempted to explain it in relation to current climate conditions.

The wind erosion for the entire territory of Mongolia was assessed for the first time using the wind erosion equation. Other hand soil erosion maps for the years 2000 and 2010, calculated using these factors, demonstrate that there is a high degree of wind erosion along the desert zone, Great Lakes Depression, and the Lakes Valley. Especially soil around the Baruun Khuurain Khotgor, Southern Altai Govi, Ulaan Nuur Lake, Mandal-Ovoo territories has the highest degree of wind erosion. These areas have a limited vegetative cover, a slight surface slope, and limited barriers and etc., which play a role in the wind erosion process (MARCC, 2014).

However, over long periods, wind-blown dust contributes to the creation of soils (Pye, 1987). According to a joint expedition by Mongolian and Russian scientists, sand dunes with heights of 8–10 m can move up to 15 m/a near the Ulaan-nuur Lake area, and sandy hills with heights of 5–6 m can move 20 m/a near the Tavan Els area (Babaev et al., 1990). Luvsandendev and Jamiyanaa (1991) calculated the movement of dust and sand in Mongolia using a turbulent diffusion equation. They compared their calculated value of dust and sand transport with a measured value. Their calculated value was 1990.7 tons and the experimentally measured value over a 0.5-km<sup>2</sup> field near Zamyn-Uud rural community was 1443.9 tons. This study showed that about 3 tons of sand/dust was blown from a 1-km<sup>2</sup> area of the Zamyn-Uud region.

Total dust emissions from the source region in East Asia was estimated at 10.4 million tons/a for PM<sub>10</sub>, 27.6 million tons/a for PM<sub>30</sub>, and 51.3 million tons/a for PM<sub>50</sub> (Huan et al., 2004).

A study by Igarashi et al. (2011) showed that the specific activities of the 137 Cs and 90 Sr radionuclides as well as the 137 Cs/90 Sr ratio in the surface soil were well correlated with the annual average precipitation in the Mongolian desert-steppe zone. Higher specific

activities and a higher  $^{137}\text{Cs}/^{90}\text{Sr}$  ratio were found in those grassland regions that experienced greater precipitation. These findings suggest that the increased specific activities and the activity ratio detected in atmospheric depositions in Japan during years with frequent Asian dust transport events in the 2000s are signs of grassland degradation.

### **5.3.2 Dust emission and transportation effects on Regime shift**

In Chapter 2, this study examines the relationship between Normalized Difference Vegetation Index (NDVI) and dust storm observations in Gobi zone of Mongolia based on data from 8 sites for 14 years of MODIS/NDVI. We analyzed using meteorological parameters and of NDVI derived from the satellite observations. Our results reveal that a correlation between dust storm and vegetation cover was reasonable negative relationship, the correlation coefficient value was -0.5. On all sites, there were positive correlation between NDVI and precipitation between May to August months, of 2000-2013 years. Dust storm occurrences had increased with decreasing of annual precipitation in spring. We found that the increase of NDVI was related with a relatively high amount of precipitation dropped in 2001, 2004 and 2006. Dust storm occurrence increased to next spring then NDVI value was high in next summer (2002, 2005, 2006).

In Chapter 4, we analyzed daily meteorological data for a period of 18 years between 1999 and 2016. In previous study (Judger et al., 2014), they have frequency and trends of sand/dust storm have been described at the Dalanzadgad, Sainshand and Zamyn-Uud stations between 1960-2012. In our study, we extended data used of sand/dust storms up to 2016 year. The numbers of dusty days at Dalanzadgad, Sainshand and Zamyn-Uud, located in the Gobi Desert. Only Zamyn-Uud has an increasing trend (Figure 23).

This result shows us direct relation between rainfall and vegetation growth to dust storm frequency from previous year. When there's environmental regime shift happens, then there's much higher chance of dust storm events. Dust storm frequency is higher during March and April months than other months in Mongolia (Natsagdorj et al., 2003)

Chapters 2 and 4 results proves to us of regime shift happening in Gobi region of Mongolia, especially it points in our calculations to previous year's decrease of precipitation is the cause of next year's dust storm increase or reverse is true.

With dust storm occurrence increasing negative impacts on Mongolian economy, human health, agriculture, livestock even wild animals.

With this in mind we put our study purpose in chapter 4 to prevent and decrease of loss in economy, natural environment, human health and more in the form of dust emission, distribution and transportation of PM<sub>10</sub> to Mongolia and beyond, China, Korea and Japan. Arid, semi-arid areas have soil degradation, soil moisture loss which aids dust storm frequency and intensity, in return effects negatively health of population living in these. In Mongolia one of the leading concerns of negative effect to general population's health is dust sand storm, related to climate change. When compared with dust free weather condition to dusty, dust transfers large scale fine dust particles, microelements, mold spores, bacteria to the damaging point for human respiratory system (Claiborn et al., 2000; Fan et al., 2002; Shinn et al., 2003; Cook et al., 2005; Prospero et al., 2005; Xie et al., 2005; Kellogg and Griffin 2006). But present time researches didn't statistically proven yet correlation between Asian dust storm impacts and sickness rate in Canada, Taiwan clinics (Chen and Tang 2005; Yang et al., 2005a; Bennett et al., 2006).

On the other hand, local governments level, there are facts of rising death numbers in especially heart infarctions and respiratory system failures, after dust storm days (Kwon et al., 2002; Chen et al., 2004).

## **5. 4. Conclusion**

Semi-arid Gobi region has two kinds of plants, annual plant and perennial plants. Annual plants are highly dependent on rainfall and are susceptible to overgrazing, while perennial plants are relatively stable and can live even in extreme drought conditions. However, once perennial plants such as shrubs die, they need a very long time to recover. This is a contributory factor to the occurrence of regime shift (Sofue et al., 2017).

In this region, precipitation supports the fragile ecosystem. Limited precipitation is one of the most influential driving forces on Gobi's environmental condition. In this region, precipitation is concentrated in the period from May to September. The NDVI values, which represent vegetation mass levels, responded well to the precipitation in this period. The distribution patterns of precipitation have indicated the decreased amount and shifted location from east to west region. The areas with lower precipitation were more sensitive to the dynamics of precipitation than the areas with higher precipitation. The most degraded area was a south west region of Gobi with the least precipitation. The NDVI

values responded to precipitation over many regions including Inner Mongolia, China. In some areas, we propose the ecosystem is destroyed and regime shift of ecosystem has been occurring. In the mountainous area, it is also possible that the amount of snowfall, the timing of snow melting in spring, the fall of groundwater and the accompanying soil moisture amount are changing due to global warming (Sofue et al., 2018; Hoshino et al., 2018).

## Chapter 6 Summary

Chapter 6 shows main summary of precipitation was a determinant of vegetation productivity in arid regions and a driving force for ecosystem change. The frequency of dust storms is increasing in the spring when annual average precipitation is decreasing, and it is found that the occurrence of dust storms in spring is highly dependent on the summer precipitation in the previous year. In the Gobi Desert, where dust storms occur, the frequency of dust storms increases as the wind speed increases, and critical wind speed is 6.5 m/s (a constant threshold). It was also confirmed that the dust storm generated in the Gobi Desert reached the Japan in just two days via Seoul in northern China, and the PM<sub>10</sub> concentration reached more than twice the normal level. The main results are summarized as follows:

- On all sites, there were positive correlation between NDVI and precipitation between May to August months, of 2000-2013 years. Dust storm occurrences had increased with decreasing of annual precipitation in spring. We found that the increase of NDVI was related with a relatively high amount of precipitation dropped in 2001, 2004 and 2006. Dust storm occurrence increased to next spring then NDVI value was high in next summer (2002, 2005, 2006).
- In the Chapter 3, focusing on spatial and temporal distribution of dust events over Mongolia based on the results of previous research.
- Maximum duration day of dust storm was observed at 12.04 hour from March 29-30, 2012 in Zamyn-Uud station.
- Climatological data of dusty days show that the number of dusty days at only Zamyn-Uud, Mongolia has an increasing trend.
- A low-pressure system and its cold front resulted in strong winds that transported dust from the source area across Northeast Asia at the end of March and the beginning of April, 2012.
- The dust storm also created an increase in PM<sub>10</sub> particles in the dust source area as well as in the downwind areas. Dust concentration of PM<sub>10</sub> near the surface is higher in the source areas of the Gobi Desert in Mongolia and China and less in the downwind areas during transport such as in Korea and Japan.

- LiDAR measurements showed that dust vertical diffusion in the atmosphere is lower in the source area during the dust storm period and increases in the downwind areas especially when transported across far distances.
- The trajectories of air mass confirmed that dust can be transported from the dust source areas in Mongolia and China to the Korean Peninsula and Japan.
- In the Chapter 5, shown the previous study result of ecosystem regime shifting of Mongolian plateau. According to the major theoretical finding when it comes to regime shifts is that ecosystems recover slowly from small perturbations in the vicinity of tipping points. The provided water condition such as rainfall is one of the most important factors for vegetation especially in arid regions.

## Acknowledgments

I would like to offer my sincerest gratitude to my supervisor, Professor Buho Hoshino, for his enormous help and guidance to complete this Ph. Sc. Degree. He guided and directed, supervised and helped in every step to my goal, for this I thank you professor.

I'm indebted most to Dr Jugder Dulam, Dr. Baba Kenji and Dr. Sumiya Ganzorig who constantly advised and helped me to successfully complete this work. Thank you Dr Jugder Dulam and Dr. June Noda for your support and encouragement that enabled me to accomplish my goal.

The three members of my committee, Professor Katsuro Hagiwara, Associate Professor June Noda, Professor Kenji Baba were very helpful and supportive throughout all stages of my research.

Further, I would like to express my thanks to my colleagues at the National Agency for Meteorology, Hydrology and Environmental Monitoring of Mongolia.

I would like to thank Dr. L. Natsagdorj (IRIMH), S. Enkhtuvshin (NAMEM), Dr. D. Dagvadorj (MNET), Professor Kenji Kai (Ibaraki University), Dr. Kei Kawai (Kyoto University), J. Erdenetsetseg (IRIMH), G. Chuluunchimeg (IRIMH), G. Batkhishig (IRIMH), E. Enkhbat (IRIMH), N. Enkhmaa (Dornogovi), E. Zoljargal (Dornogovi), Sh. Amarbileg (Dornogovi), G. Uuganbayar (HNP), N. Narangerel (HNP) my father Ch.Tsedendamba, my mother B. Javzmaa, my dear husband, my sister Ts. Lkhagvasuren, brother N. Bayaraa (Altanbulag soum), my younger sister Ts. Nyamsuren, Ts. Namuundari, my younger brother Ts. Lkhagvajav, also D. Munkhjargal, G. Ochbayar, T. Naranbaatar, B.Tuvshinbayar, Yuta Demura, Yuki Sofue, Sorgog, Tian Ying, Shima Keita, B. Bilguun, D. Myagmarnaran, Yuki Murashma and the staff of the Laboratory of Environmental Remote Sensing, Rakuno Gakuen University.

Thanks to the workplace staff, drivers and friends for their hard work.

## References

- Abdi, O. A., Glover, E. K., & Luukkanen, O. Causes and Impacts of Land Degradation and Desertification: Case Study of the Sudan. *International Journal of Agriculture and Forestry*, 3 (2), 40-51, **2003**.
- Anyamba and C.J. Tucker, “Analysis of Sahelian vegetation dynamics using NOAA-AVHRR NDVI data from 1981–2003,” *Journal of arid environments*, 63, pp.596–614, **2005**, 10.
- Aston, S.R, R. Chester, L.R. Johnson, R.C. Padgham; Eolian dust from the lower atmosphere of the eastern Atlantic and Indian Oceans, China Sea and Sea of Japan; *Marine Geology 14, Issue 1, p. 15-28; 1973*.
- Bagnold, R.; The Physics of Blown Sand and Desert Dunes; *Proceedings of the Royal Society A 225 49; 1954*
- Bao. G, Z. Qin, Y. Bao, Y. Zhou, W. Li, and A. Sanjjav, “ NDVI-based long-term vegetation dynamics and its response to climatic change in the Mongolian Plateau,” *Remote Sensing*, vol. 6, no. 9, pp. 8337-8358, **2014**.
- Bayasgalan M, Drought monitoring in Mongolia, Dissertation, Ulaanbaatar, Mongolia **2005.3**
- Bodhaine, B . A. Aerosol absorption measurements at Barrow, Mauna Loa and the South Pole, *J. Geophys. Res.* **1995**, *100*, 8967–8975, <https://doi.org/10.1029/95JD00513>.
- Biggs, R., et al. Turning back from the brink: Detecting an impending regime shift in time to avert it. *P Natl Acad Sci Usa* 106, 826–831, **2009**.
- B. Buhe, PhD Thesis, *Chiba university 2015*.
- Buho HOSHINO, Yuki SOFUE, Yuta DEMURA, Tsedendamba PUREVSUREN, Morine KURIBAYASHI, Kenji BABA, Enkhtuvshin ZOLJARGAL, Katsuro HAGIWARA, Jun NODA, Keiichi KAWANO, Olaf KARTHAUS, Kenji KAI, Detection of dry lake beds formation and estimate of environmental regime shift in semi-arid region, 28-S, 109-113 *Journal of Arid Land Studies*, **2018**.
- Buho HOSHINO, Yuki SOFUE, Yuta DEMURA, Tsedendamba PUREVSUREN, Morine KURIBAYASHI, Kenji BABA, Enkhtuvshin ZOLJARGAL, Katsuro HAGIWARA, Jun

- NODA, Keiichi KAWANO, Olaf KARTHAUS, Kenji KAI (2018), Detection of dry lake beds formation and estimate of environmental regime shift in semi-arid region 沙漠研究 28-S, 109-113 *Journal of Arid Land Studies*
- Buseck, P.R, M. Pósfai; Airborne minerals and related aerosol particles: Effects on climate and the environment; *Proceedings of the National Academy of Sciences* 96(7), p. 3372-3379; **1999**.
- Chun, Y.; Boo, K.; Kim, J.; Park, S.; Lee, M “Synopsis, transport, and physical characteristics of Asian dust in Korea,” *J. Geophys. Res.* **2001**.106, 18461–18469.
- Chung, Y.S.; Kim, H.S.; Natsagdorj, L.; Jugder, D.; Chang, S.J. On yellow sand occurred during 1997-2000 *Journal of Meteorological Society* . 4, **2004**, pp.305-316.
- Chung, Y.S.; Yoon M.B On the occurrence of yellow sand and atmospheric loading *Atmos. Environ.* **1996**, 30pp.2387-2397.
- T. Claquin, M. Schulz, Y. Balkanski; Modeling the mineralogy of atmospheric dust sources; *Journal of Geophysical Research* 104(22), p. 243-256; **1999**.
- Collie, J., et al. Regime shifts: can ecological theory illuminate the mechanisms *Prog. Oceanogr.* 60, 281–302 , **2004**.
- V. Dakos, S. R. Carpenter, E. H. van Nes, M. Scheffer, Resilience indicators: prospects and limitations for early warnings of regime shifts, *Philosophical Transactions of the Royal Society B: Biological Sciences*, 370, 1659, 20130263 , **2005**.
- D. P. Dee, et al., The ERA-Interim Reanalysis: Configuration and Performance of the Data Assimilation system. *Quarterly Journal of Royal Meteorological Society.* **2011**, 137. 553-597.
- Demura Y., Hoshino B., Sofue Y., Kai K., Purevsuren Ts., Baba K., Chen J., Mori K. (2015): Estimates of critical ground surface condition for Asian dust storm outbreak in Gobi desert region based on remotely sensed data, *IEEE IGARSS*, **2015**(1): 870-873.
- Demura Y., Hoshino B., Baba K.; McCarthy C., Sofue Y., Kai K.; Purevsuren T., Hagiwara K., Noda J.: Determining the frequency of dry lake bed formation in Semi-Arid Mongolia from satellite data, *Land*, 6(88): 1-10,**2017**.

- Draxler R.R.; Rolph G.D. HYSPLIT (HYbrid Single-Particle Lagrangian Integrated Trajectory) Model access via NOAA ARL READY Website (<http://ready.arl.noaa.gov/HYSPLIT.php>). NOAA Air Resources Laboratory, **2003**.
- Dulam Jugder, Enkhbaatar Davaanyam and Tsedendamba Purevsuren, Temporal and Spatial Characteristics of Dust Storms Observed in Mongolia during 1986-2016, Third JSPS Seminar in Ulaanbaatar, Mongolia, **2017**.
- Feudel. U, Complex dynamics in multistable systems. *Int J Bifurcat Chaos* 18, 1607–1626 , **2008**.
- Folke, C., et al. (2004) Regime Shifts, Resilience, and Biodiversity in Ecosystem Management. *Annu. Rev. Ecol. Evol. Syst.* 35, 557–581
- Garrison, V.H.; Shinn, E.A.; Foreman, W.T; Griffin, D.W.; Holmas, C.W.; Kellogg, C.A.; D. W. Griffin. Atmospheric movement of microorganisms in clouds of desert dust and implications for human health. *Clin Microbiol rev.* **2007**, 20(3); 459-77.
- A.S. Goudie, N.J. Middleton; Desert Dust in the Global System; ISBN-10 3-540-32354-6 Springer Berlin Heidelberg New York
- L. Gomes, G. Bergametti, G. Coudé-Gaussen, P. Rognon; Submicron desert dusts: A sandblasting process; *Journal of Geophysical Research* 95 13, p. 927–13; **1990**.
- Griffin, D. W.; Garrison,V. H.; Herman, J. R.; Shinn E. A. African desert dust in the Caribbean atmosphere. *Microbiology and public health. Aerobiologia.* **2001**, 17, 203-213.
- Grimi. A, C.S. Zender, P. Colarco; Saltation sandblasting behavior during mineral dust aerosol production; *Geophysical Research Letters* 29(18), p. 1868; **2002**.
- Groffman, P., et al. Ecological thresholds: The key to successful environmental management or an important concept with no practical application? *Ecosystems* 9, 1–13 , **2006**.
- Guneralp, B., and Barlas, Y. Dynamic modelling of a shallow freshwater lake for ecological and economic sustainability. *Ecological Modelling* 167, 115–138, **2003**.
- Jickels, T.D; L.J. Spokes; Atmospheric Iron Inputs to the Oceans; *The Biogeochemistry of Iron in Seawater*; editor: D.R. Turner; K.A. Hunter; chapter 4, pp. 85-121, Wiley,

Chichester, UK; **2001**.

- Higashi, T.; Kambayashi, Y.; Ohkura, N.; Fujimura M.; Nakanishi, S.; Yoshizaki, T.; Saijoh, K.; Hayakawa, K.; Kobayashi, F.; Michigami, Y.; Hitomi, Y.; Nakamura, H. Exacerbation of daily cough and allergic symptoms in adult patients with chronic cough by Asian dust: A hospital-based study in Kanazawa. *Atmos. Environ.* **2014**, *97*, 537–543.
- Hoshino B., Nawata H., Baba K., Ganzorig S., Purevsuren T., Demura Y., Sofue Y., Noda J., Hagiwara K., Batdorj D. Comparative characteristics of the home ranges of domestic and wild animals in arid and sub-arid Afro-Eurasia, and watering places as hot spot for the pasture degradation, *Journal of Arid Land Studies*, 24(1): 51-56, **2014**.
- E. Hovmöller, “The Trough-and-Ridge Diagram,” *Tellus*, vol. 1, no. 2, pp. 62–66, **1949**.
- Huang, J.; Ge, J.; Weng, F. Detection of Asia Dust Storms Using Multisensor Satellite Measurements. *Remote Sens. Environ.* **2007**, *110*, 186–191.
- Husar, R. B.; Tratt, D. M.; Schichtel, B. A.; Falke, S. R.; Jaffe, F. Li, D.; Gassó, S.; Gill, T.; Laulainen, N. S.; Lu, F.; Reheis, M. C.; Chun, Y.; Westphal, D.; Holben, B. N.; Gueymard, C.; McKendry, I.; Kuring, N.; Feldman, G. C.; McClain, C.; Frouin, R. J.; Merrill, J.; DuBois, D.; Vignola, F.; Murayama, T.; Nickovic, S.; Wilson, W.E.; Sassen, K.; Sugimoto, N.; Malm, W. C. Asian dust events of April 1998. *J. Geophys. Res.* **2001**, *106*, 18317–18330.
- Igarashi, Y.; Fujiwara, H.; Jugder, D. Change of the Asian dust source region deduced from the composition of anthropogenic radionuclides in surface soil in Mongolia, *The Journal of Atmospheric Chemistry and Physics*. **2011**, *11*, 7069–7080.
- Ishizuka M.; Mikami, M.; Yamada, Y.; Kimura, R.; Kurosaki, Y.; Jugder, D.; Gantsetseg, B.; Cheng, Y Shinoda M. Does ground surface soil aggregation affect transition of the wind speed threshold for saltation and dust emission, *SOLA*. **2012**, *Vol. 8*, 129-132, ISSN:1349-6476.
- Jugder D, Shinoda M Intensity of a Dust Storm in Mongolia during 29–31 March 2007. Online Journal of the Science Online Letters on the Atmosphere *SOLA*. **2011**, *7A*, 029–03.1.

- Jugder, D.; Sugimoto, N.; Shinoda, M.; Matsui, I.; Nishikawa, M. Dust, biomass burning smoke, and anthropogenic aerosol detected by polarization-sensitive Mie LiDAR measurements in Mongolia. *The International Journal of Atmospheric Environment*. **2012**, *54*, pages 231-241.
- Jugder, D.; Shinoda, M.; Kimura, R.; Batbold, A.; Amarjargal, D. Quantitative analysis on windblown dust concentrations of PM<sub>10</sub> (PM<sub>2.5</sub>) during dust events in Mongolia. *Aeolian Research*. **2014**, *14*, 3–13.
- Kalashnikova, O.V.; Sokolik I.N. Modeling the radiative properties of nonspherical soil-derived mineral aerosols; *Journal of Quantitative Spectroscopy and Radiative Transfer* *87*, Issue 2, 15, p. 137-166; **2004**.
- Karunanithi, A.T., et al. Detection and Assessment of Ecosystem Regime Shifts from Fisher Information. *Ecol. Soc.* *13*, *15*, **2008**.
- Kellogg, CA.; Griffin, DW.; Garrison, VH.; Peak, HK.; Royal, N.; Smith, RM.; Shinn, EA. Characterization of aerosolized bacteria and fungi from desert dust events in Mali, West Africa. *Aerobiologia*. **2004**, *20*, 99-110.
- Kim, J. Transport routes and source regions of Asian dust observed in Korea during the past 40 years (1965–2004). *Atmos Environ*. **2008**, *42*, 4778e4789.
- Kok, K. The potential of Fuzzy Cognitive Maps for semi-quantitative scenario development, with an example from Brazil. *Global Environmental Change* *19*, 122–133, **2009**.
- Kurosaki, Y.; and M. Mikami, Recent frequent dust events and their relation to surface wind in East Asia, *Geophys. Res. Lett.* **2003**, *30* (14), 1736, doi:10.1029/2003GL017261.
- Kwon, H. J.; Cho, S. H.; Chun Y.; Lagarde F.; Pershagen, G. Effects of the Asian dust events on daily mortality in Seoul, Korea. *Environ. Res.* **2002**, *90*, 1–5. 01023-3.
- Lewontin, R. Meaning of Stability. *Brookhaven Sym Biol*, *13*, **1969**.
- Lim, H.; Choi, G. Seasonal and interannual variability of Asian desert aerosols from Nimbus 7/TOMS Data, *IEEE Trans. Geosci. Remote Sens.* **2002**, *5*, 2945–2947, doi: 10.1109/IGARSS. 2002.1026830.

- Lin, C.Y.; Liu, S.C.; Chou, C.C. K.; Liu, T.H.; Lee, C.T.; Yuan, C.S, et al. Long-range transport of Asian dust and air pollutants to Taiwan. *Terrestrial, Atmospheric and Oceanic Sciences*. **2004**, 15:759-784.
- Liu, G. R. .; Lin T. H. Application of geostationary satellite observations for monitoring dust storms of Asia. *TAO*. **2004**, 15, 825–837.
- Ludwig, D., et al. Qualitative-Analysis of Insect Outbreak Systems - Spruce Budworm and Forest. *J. Anim. Ecol.* 47, 315–332 , **1978**.
- Luvsandendev, B. and Jamiyanaa, D., 1991. Hydrodynamic model for sand transportation. Brief report of symposium on Nature and environment in the Gobi (in Mongolia), Ulaanbaatar, pp-20
- Majewski, M.S.; Richardsan, L.L.; Ritchie, K.B.; Swith, G.W. African and Asian dust: from desert soils to coral reefs. *Bio Science*. **2003**, 53, 469-480.
- MARCC (Mongolia Second Assessment Report on Climate Change). **2014**, Ministry of Environment, Nature and Tourism, Mongolia. Ulaanbaatar.
- May, R.M. (1977) Thresholds and Breakpoints in Ecosystems with a Multiplicity of Stable States. *Nature* 269, 471–477 , **1977**.
- Mayer, A., and Rietkerk, M. The dynamic regime concept for ecosystem management and restoration. *BioScience* 54, 1013–1020 , **2004**.
- Merrill, J. T.; M. Uematsu, and R. Bleck, Meteorological analysis of long range transport of mineral aerosols over the North Pacific, *J.GeophysR. es*.**1989**, 94, 8584-8598.
- Millennium Ecosystem Assessment (2005) Ecosystems and human well-being:biodiversity synthesis. 87 , **2005**.
- Mongolian national atlas,book **2009**, p.108.
- Moulin.C., C.E. Lambert, U. Dayan, V. Masson, M. Ramonet, P. Bousquet, M. Legrand, Y.J. Balkanski, W. Guelle, B. Marticorena, G. Bergametti, F. Dulac; Satellite climatology of African dust transport in the Mediterranean atmosphere; *Journal of Geophysical Research*103(11), p. 13,137-13,144; **1998**.
- Natsagdorj, L.; Jugder, D.; Chung, Y.S. Analysis of dust storms observed in Mongolia during 1937–1999. *Atmos. Environ.* **2003**, 37, 1401–1411, doi: 10.1016/S1352-

2310(02)

- Nandintsetseg, B. and M. Shinoda, 2010: Seasonal change of soil moisture in Mongolia: its climatology and modeling. *International Journal of Climatology*, 31, 1143-1152. doi:10.1002/joc.2134
- M. Otto and C. Höpfner and J. Curio and F. Maussion and D. Scherer, “Assessing vegetation response to precipitation in northwest Morocco during the last decade: an application of MODIS NDVI and high resolution reanalysis data,” *Theor Appl Climatol.*, 123, pp. 23–41, 2016. [
- Nickovic.S., M. Vujadinovic, A. Vukovic, G. Pejanovic, V. Djurdjevic, M. Dacic; Database of mineral composition in arid soils and its application in atmospheric transport of iron embedded in dust;, *EGU General Assembly, Geophysical Research Abstracts 13, EGU2011-13029-2, 2011.*
- Nishikawa. M.; I Matsui; D.Batdorj; D.Juger; I.Mori; A. Shimizu; N.Sugimoto; K. Takahashi. Chemical composition of urban airborne particulate matter in Ulaanbaatar *Atmos. Environ.* **2011**, 45, 5710-5715.
- Noymeir, I. (1975) Stability of Grazing Systems - Application of Predator-Prey Graphs. *Journal of Ecology* 63, 459–481
- Parrington, J. R.; Zoller W. H.; Aras, N. K. Asian dust: Seasonal transport to the Hawaiian Islands, *Science*, **1983**. 20, 195-197.
- Prospero, J.M.; Ginoux, P.; Torres, O.; Nicholson, S.E.; Gill, T.E. Environmental Characterization of Global Sources of Atmospheric Soil Dust Identified with the NIMBUS 7 Total Ozone Mapping Spectrometer (TOMS) Absorbing Aerosol Product. *Rev. Geophys.* **2002**, 40:1002, doi: 10.1029/2000RG000095.
- Purevsuren Tsedendamba, Jugder Dulam, Kenji Baba, Katsuro Hagiwara, Jun Noda, Kei Kawai, Ganzorig Sumiya, Christopher McCarthy, Kenji Kai and Buho Hoshino (2019) Northeast Asian Dust Transport: A Case Study of a Dust Storm Event from 28 March to 2 April 2012, *Journal of MDPI-Atmosphere*.
- Puntsagdorj. C, 2014: Meteorological Observations Manual 14 (in Mongolian). NAMHEM, Ulaanbaatar, pp-8.
- Pye, K. 1987: Aeolian Dust and Dust Deposits. Academic Press, London, 334 pp.

- Qian, W. H.; Quan, L. S.; Shi, S. Y. Variations of the dust storm in China and its climatic control, *J. Clim.* **2002**, *15*(10), 1216– 1229.
- Rockström, J., et al. A safe operating space for humanity. *Nature* 461, 472–475 , **2009**.
- Saysel, A.K., and Barlas, Y. A dynamic model of salinization on irrigated lands. *Ecological Modelling* 139, 177–199 , **2001**.
- Scheffer, M., et al. Catastrophic shifts in ecosystems. *Nature* 413, 591–596 , **2001**.
- Scheffer, M., and Carpenter, S. Catastrophic regime shifts in ecosystems: linking theory to observation. *Trends Ecol. Evol.* 18, 648–656 , **2003**.
- Shaw, G. E. Transport of Asian desert aerosol to the Hawaiian Islands, *J. Appl. Meteorol.* **1980**, 19, 1254-1259.
- Shimizu, A.; Coauthors. Continuous observations of Asian dust and other aerosols by polarization LiDARs in China and Japan during ACE-Asia. *J. Geophys. Res.***2004**. *109*, D19S17. doi:10.1029/2002JD003253.
- Shao, Y.; M. Raupach; Effect of saltation bombardment by wind; *Journal of Geophysical Research* 98,12, p. 719–12; **1993**.
- Shao, Y.; Wang, J.A. Climatology of Northeast Asian dust events. *Meteorol. Z.* **2003**, *12*, 187–196. doi: 10.1127/0941-2948/2003/0012-0187.
- Sugimoto, N.; Matsui, I.; Nishikawa, M.; Park, SU.; Chun, YS.; Park, MS. Spatial and temporal variations of dust concentrations in the Gobi Desert of Mongolia. *The Journal of the Global and Planetary Changes.* **2011**, *78*, 14–22.
- Shao, Y. Physics and Modelling of Wind Erosion. Springer Science & Business Media, New York. 2008.
- Shao, Y; C.H. Dong; A review on East Asian dust storm climate, modelling and monitoring;*Global and Planetary Change* 52, p. 1–22; **2006**.
- Sofue, Y, B. Hoshino, Y. Demura, E. Nduati, and A. Kondoh, “The Interactions Between Precipitation, Vegetation and Dust Emission Over Semi-Arid Mongolia,” *Atmos. Chem. Phys. Discuss.*, in review, **2017**.
- Sofue Y., Hoshino B., Demura Y., Kai K., Baba K., Nduati E., Kondoh A., Sternberg, T.:

Satellite monitoring of vegetation response to precipitation and dust storm outbreaks in Gobi Desert Regions, *Land*, 7(1): 19, **2018**.

Sofue Y., Hoshino B., Nduati E., Kondoh A., Kai K., Purevsuren Ts., Baba K.: Remote sensing methodology for detection of environmental regime shifts in semi-arid region, IEEE IGARSS, 2017(1), 2153-7003, **2017**.

Steffen, W., et al. (2007) The Anthropocene: Are humans now overwhelming the great forces of nature. *Ambio* 36, 614–621, **2007**.

STRM Data Product; *Mongolian DEMs (Digital Elevation Models)*. **2016**

<https://marine.rutgers.edu/~cfree/mongolian-dems-digital-elevation-models/>

Sugimoto, N.; Shimizu, A.; Matsui, I.; Uno, I.; Arao, K.; Dong, X.; Zhao, S.; Zhou, J.; Lee, C.H. Study of Asian Dust Phenomena in 2001-2003 Using a Network of Continuously Operated Polarization LiDARs. *Water Air Soil Pollut. Focus*. **2005**, 5: 145–157.

Sugimoto, N.; Hara, Y.; Shimizu, A.; Yumimoto, k.; Uno, I.; Nishikawa, M. Comparison of Surface Observations and a Regional Dust Transport Model Assimilated with LiDAR Network Data in Asian Dust Event of March 29 to April 2, *SOLA*. **2007**, 7A, 013-016.

Sugimoto; N., I. Matsui; A. Shimizu; T. Nishizawa; Y. Hara; C. Xie, I. Uno; K. Yumimoto; Z. Wang; and S. C. Yoon. LiDAR network observations of tropospheric aerosols. *Proc. SPIE*, **2008**, **7153**, 71530A, doi:10.1117/12.806540.

Sugimoto. N; T. Nishizawa; A. Shimizu; I. Matsui.; Assurance of Data Quality of Aerosol LiDARs and a Method for Obtaining Consistency of Observations with Different Types of LiDARs, *Eaorozoru Kenkyu ..* 29 (3), **2014**, pp.166-173.

Sugimoto.N; A. Shimizu; I. Matsui; T. Nishizawa..A method for estimating the fraction of mineral dust in particulate matter using PM<sub>2.5</sub>-to-PM<sub>10</sub> ratios. **2016**. *Particuology* 29, 114-120

Sun, L.; Zhou, X.; Lu J.; Kim, Y.-P.; Chung, Y.-S. Climatology, trend analysis and prediction of sandstorm and their associated dust fall in China. *Water Air Soil Pollut. Focus*. **2003**, **3**, 41–50.

- Sun, J. M.; Zhang, M. Y.; Liu T. S. Spatial and temporal characteristics of dust storms in China and its surrounding regions, 1960 – 1999: Relations to source area and climate, *J. Geophys. Res.* **2001**. *106* (D10), 10,325–10,333.
- Sun, H.; Pan, Z. T.; Liu, X. D.; Numerical simulation of spatial-temporal distribution of dust aerosol and its direct radiative effects on East Asian climate, *J. Geophys. Res.* **2012**, 117, <https://doi.org/10.1029/2011JD017219>.
- Sun, J.; M. Zhang.; Liu, T. Spatial and temporal characteristics of dust storms in China and its surrounding regions, 1960–1999: Relations to source area and climate. *J. Geophys. Res.* **2001**, *106*, 10 325–10 333.
- Taylor, D. A. Dust in the wind, *Environ. Health Perspect*, **2002**, 110, A80–A87.
- Tegen. I., I. Fung; Modeling of mineral dust in the atmosphere: Sources, transport, and optical thickness; *Journal of Geophysics* *99*, p. 22,897-22,914; **1994**.
- Todd M.C, R. Washington, J. Vanderlei Martins, O. Dubovik, G. Lizcano, S. M. Bainayel, Engelstaedter. S.; Mineral dust emission from the Bodélé Depression, northern Chad, during BoDEx 2005; *Journal of Geophysical Research* *112*; **2007**.
- Tsai, F. J.; Fang Y, S.; Huang S, J. Case study of Asian dust event on March 19-25, 2010 and its impact on the marginal sea of China. *Journal of Marine Science and Technology*. **2013** . 21.3, 353-360.
- Tuvdendorj, D., **1973**. Frequency statistics of dust storms over the territory of Mongolia. Geographical problems in Mongolia, Issue, No.11, 136pp.
- Tuvdendorj, D., **1974**. Dust storms over the territory of Mongolia. Thesis for the Ph.D. in Geography, Moscow, 190pp.
- Uematsu, M.; Duce, R. A.; Prospero, J. M.; Chen, L.; Merrill, J. T.; McDonald R. L. Transport of mineral aerosol from Asia over the North Pacific Ocean, *J. Geophys. Res.* **1983**, *88*, 5343-5352.
- Uno, I.; Osada, K.; Yumimoto, K.; Wang, Z.; Itahashi, S.; Tahashi, S.; Pan, X.; Hara, Y.; Yamamoto, S.; Nishizawa, T. Importance of long-range nitrate transport based on long-term observation and modeling of dust and pollutants over East Asia, *Atmos. Chem. Phys.* 2017, *17*, 14181–14197. <https://doi.org/10.5194/acp-17-14181-2017>.

- Uno, I.; Eguchi, K.; Yumimoto, K.; Takemura, T.; Shimizu, A.; Uematsu, M.; Liu, Z.; Wang, Z.; Hara, Y.; Sugimoto, N. Asian dust transported one full circuit around the globe. *Nat. Geosci.* 73.**2009**.
- Uno, I.; and Coauthors, Regional chemical weather forecasting system CFORS: Model descriptions and analysis of surface observations at Japanese island stations during the ACE-Asia experiment, **2003**. *Journal of Geophysical Research Atmospheres* 108(23) DOI:10.1029/2002JD002845.
- Vermote, E.F.; Kotchenova, S.Y. *MOD09 (Surface Reflectance) User's Guide*; MODIS Land Surface Reflectance Science Computing Facility: College Park, MD, USA, Kassas, M. Desert: (1995) A general review. *J. Arid Environ.* 30, 115±128 , **2008**.
- WMO No. 407, 1975 edition, International cloud atlas, Volume 1, Manual on the Observation of Clouds and other Meteors.
- Wooldridge, S., et al. Precursors for resilience in coral communities in a warming climate: a belief network approach. *Mar Ecol-Prog Ser* 295, 157–169 , **2005**.
- Xuan, J.; Sokolik I.N.; Hao, J.; Guo F.; Mao, H.; Yang, G. Identification and characterization of sources of atmospheric mineral dust in East Asia, *J. Atmos. Environ.* **2004**. 38, 6239–6252.
- Yan. L, S. Chen, J. Huang, G. Lin, Water regulated effects of photosynthetic substrate supply on soil respiration in a semiarid steppe, *Global Change Biology*, vol. 17, no. 5, pp. 1990-2001, **2011**.
- Yan. L, S. Chen, J. Xia, Y. Luo, Precipitation regime shift enhanced the rain pulse effect on soil respiration in a semi-arid steppe, *PloS one*, 9(8), e104217 , **2014**.
- Yue. X, H. Wang, Z. Wang, K. Fan; Simulation of dust aerosol radiative feedback using the Global Transport Model of Dust: 1. Dust cycle and validation; *Journal of Geophysical Research* 114; 2009
- Yuta Demura, Buho Hoshino, Yuki Sofue, Kenji Kai, Ts. Purevsuren, Kenji BABA, Jun Noda (2016) Estimates of ground surface characteristics for outbreaks of the Asian Dust Storms in the sources region *ProScience* , 21-30
- Yuki Sofue, Buho Hoshino\*, Eunice Nduati, Akihiko Kondoh, Kenji Kai, Ts. Purevsuren, Kenji Baba (2017) Remote sensing methodology for detection of environmental regime

shifts in semi-arid region *Journal of GISS IEEE*.

Zender, C. S.; Bian, H.; Newman, D.; Mineral Dust En-102 JOURNAL OF CLIMATE  
VOLUME 19rainment and Deposition (DEAD) model: Description and 1990s dust  
climatology. *J. Geophys. Res.* **2003**, *108*, 4416, doi:10.1029/2002JD002775.

Zhou, Z. J.; Zhang, G. C. Typical severe dust storms in northern China during 1954– 2002.  
*Chin. Sci. Bull.*; **2003**, *48* (21), 2366– 2370.

Zubler, E. M, D. Folini, U. Lohmann, D. Lüthi, A. Muhlbauer, S. Pousse-Nottelmann, C.  
Schär, M. Wild; Implementation and evaluation of aerosol and cloud microphysics in  
a regional climate model; *Journal of Geophysical Research* *116*; **2011**.

## 北東アジアにおけるダスト輸送について——ゴビ砂漠地域における ダストの発生、分布とその輸送の事例研究

TSEDENDAMBA PUREVSUREN (食生産利用科学)

モンゴル国は南部にゴビ・砂漠の乾燥地が広がり、北部と西部に寒冷半湿潤の山地生態系が成り立っている。南部のゴビ・砂漠の乾燥・半乾燥地域はアジア内陸のダストストームの主な発源地域として知られている。本研究はまず2000年～2013年間の正規化植生指数(NDVI)と各地の気象ステーションで観測されたダストストームの記録データを用いて、ダストストームの発生と地上植被率との相関を調べた。その結果、ダストストームの発生と植被率の間は負の相関が認められた( $r = -0.5$ )。更に、サイト毎の降水量とNDVIの相関を調べたところ、全サイトにおいて両者に正の相関があることが認められた。更に、ダストストームの発生頻度は年平均降水量が減少傾向を示す春季においては増加傾向にあることが判明された。特にこの傾向はゴビ・砂漠の南西部では著しくであることが示唆された。また北東アジア地域におけるダストストームの輸送経路とダスト粒子の沈着を明らかにするために、地上観測PM<sub>10</sub>と上空18キロまでの大気垂直断面を観測可能なLiDAR観測装置を用いて、2012年3月28日～4月2日かけてのダストイベントの分析を行った。その結果、2012年3月27日から28日にかけてゴビ・砂漠から発生したダストストームは中国北部を經由して、30日から31日にかけてソウルの上空に到達し、31日から4月1日にかけて辺戸の上空に到達した。また、PM<sub>10</sub>の濃度が通常の2倍以上に到達したことも確認された。今回のイベントの場合、発源地域から日本列島に到達するまで僅か2日間しかかからなかったことも分かった。LiDAR測定によるダストの垂直分布の高度は、地上では1～2 kmの厚さがあり、ソースエリアから遠く離れるほど高くなる傾向を示した。

第1章では、序論として、モンゴル国のゴビ・砂漠地帯の特徴と気候変動への応答について述べた。過去60年間に年平均気温は1.56℃上昇し、その中で特に春秋の気温が1.4–1.5° 上昇したことに對して、冬季の気温は3.61° も上昇した；1940年から1998年までのモンゴル国平均降水量が6%増加しているが、ダストストームの発生季節である春の降水量は逆に17%減少した。春の乾燥は植物が芽

生える時期である5月に主に発生していた。急激な気温の上昇と春季の降水量の大幅な減少は、ダストストームの発生に拍車をかけることとなった。

第2章では、モンゴル国のゴビ・砂漠地区における2000年～2013年の13年間の植生指数NDVIと気象データの相関性を調べた。その結果、全サイトにおいて2000年～2013年間の5月～8月にかけてNDVIと降水量の間に正の相関が認められた。降水量はこうした乾燥地域の植生生産力の決定要素であり、生態系変動の駆動力であることが改めて確認された。春の降水量の減少は、ダストストームの発生の増加に繋がる。春季のNDVIと前夏の降水量との関連の解析結果から、前年度の夏季の降水量が翌春の植生の成長を制限する要因になっていて、2000年～2013年の間に発生したダストストームは、前年度の夏の降水量への依存度が高いことが示唆された。

第3章では、モンゴル国上空で発生するダストイベントの時・空間的分布パターンを研究し、ゴビ・砂漠を発生源とするアジアダストストームは2000年～2014年の14年間の記録では、最大継続日（ダスティデー）は中国との国境の町であるザミンウド(Zamyn-Uud)で観測された2012年3月29～30日にかけて発生したイベントの最大連続12.04時間だったことが確認された。

第4章では、近隣諸国における高レベルの粒子状物質を調査することにより、モンゴル国ゴビ・砂漠から発生するダストイベントの長距離輸送の影響を明らかにした。事例研究として、本研究は2012年3月28日～4月2日間に発生したアジアのダストイベントに関して、PM<sub>10</sub>の地上観測、AD-Net LiDAR測定によるダスト垂直拡散、NOAA HYSPLITモデルを用いたダスト気団 (air mass) の軌道追跡によるダストストームの長距離輸送シミュレーションを行った。結果として、1) 気象観測データの解析からダスティデーは、モンゴルのザミン・ウード (Zamyn-Uud) の観測点のみは増加傾向を示した； 2) 低気圧とその寒冷前線により、2012年3月末～4月初めにゴビ・砂漠を発生源とし、北東アジアを横断したダストイベントは強風とより強い関連があることが示された；ダストストームが発生時に、発生源エリアと風下エリアのPM<sub>10</sub>粒子濃度は著しく増加する；地表面近くのPM<sub>10</sub>の濃度は、モンゴルと中国北部のゴビ砂漠の発源地域で最も高く、通常の2倍以上の値を示し、風下地域の韓国や日本などでは若干少ないことも示唆された； 3)

LiDAR測定により、大気中のダストの垂直拡散は、ダストストーム期間中は発生源エリアで低く、特に遠距離に輸送される場合は風下エリアで増加する傾向が確認された。ダスト発生時の気団(air mass)軌跡は、発生源のモンゴル国と中国国境地帯のゴビ・砂漠から下風の朝鮮半島と日本列島の上空を通過して太平洋へ輸送されることがモデルで確認された。

第5章では、環境変動と人為活動などによる生態系のネットワークの崩壊がエコシステムレジームシフトを招かれない事実を述べた。

第6章 結論として、降水量は乾燥地域の植生生産力の決定要素であり、生態系変動の駆動力であった。ダストストームの発生頻度は年平均降水量が減少傾向を示す春季においては増加傾向で、春季のダストストームの発生は前年度の夏の降水量への依存度が高いことがわかった。ダストストームの発生地であるゴビ砂漠では、ダストストームの発生頻度は風速が速くなるほど増加して、その臨界風速は6.5m/sであった。またゴビ砂漠で発生したダストストームは中国北部、ソウルを経由して、僅か二日間で日本列島に到達して、PM<sub>10</sub>の濃度が通常の2倍以上に到達したことも確認された。

## 7. Publication and Presentation

### 7.1 Publication

1. Purevsuren Tsedendamba, Jugder Dulam, Kenji Baba, Katsuro Hagiwara, Jun Noda, Kei Kawai, Ganzorig Sumiya, Christopher McCarthy, Kenji Kai and Buho Hoshino (2019) Northeast Asian Dust Transport: A Case Study of a Dust Storm Event from 28 March to 2 April 2012, *Journal of MDPI-Atmosphere*.
2. Tsedendamba Purevsuren, Buho Hoshino, Sumiya Ganzorig, (2012) “Spatial and temporal patterns of NDVI response to precipitation and temperature in Mongolian Steppe”, 沙漠研究 22-1, 243 -246, *Journal of Arid Land Studies*
3. Tsedendamba Purevsuren, Buho Hoshino, Sumiya Ganzorig, Ts.Tserendulam, (2011) “Spatial and temporal patterns of NDVI response to precipitation in Mongolian Steppe”, *Journal of Rakuno Gakuen University* Vol.35, No.2.
4. Marie SAWAMUKAI, 2013. Buho HOSHINO, Sumiya GANZORIG, Tsedendamba PUREVSUREN, Mitsuhiro ASAKAWA, Kenji KAWASHIMA (2012) “Preliminary results on surface and soil characteristics of Brandt’s vole (*Microtus brandti*) habitat in Central Mongolia using satellite data”, 沙漠研究 22-1, 291 -294, *Journal of Arid Land Studies*
5. Buho HOSHINO, Hiroshi NAWATA, Kenji KAI, Hiroshi YASUDA, Kenji BABA, Sumiya GANZORIG, SURIGA, Manayeva KARINA, Tsedendamba PUREVSUREN, Miki HASHIMOTO, Kenji KAWASHIMA, Jun NODA, Katsuro HAGIWARA, Yuka SHIBATA, (2014) “Comparative Characteristics of the Home Ranges of Domestic and Wild Animals in Arid and Semi-Arid Afro-Eurasian Watering Places as Hot Spots for Pasture Degradation” 沙漠研究 24-1, 51-56, *Journal of Arid Land Studies*
6. SURIGA, Miki HASHIMOTO, Buho HOSHINO, Sumiya GANZORIG, SAIXIALT, YONG-HAI, Karina MANAYEVA, Tsedendamba PUREVSUREN, (2014) “Grazing Behavior of Livestock in Settled and Nomadic Herders Households in Mongolian Plateau”, 沙漠研究 24-1, 187-189, *Journal of Arid Land Studies*
7. YONG-HAI, Buho HOSHINO, Sumiya GANZORIG, SURIGA, Tsedendamba PUREVSUREN, Karina MANAYEVA, (2014) “Studies on Long-term Changes in Herders Household and Land Use in Inner Mongolia, China”, 沙漠研究 24-1, 191-194, *Journal of Arid Land Studies*
8. Yuta Demura Buho Hoshino Yuki Sofue Kenji Kai Purevsuren Tsedendamba et al., (2015) “Estimates of critical ground surface condition for Asian dust storm outbreak in Gobi

- desert region based remotely sensed data” *Journal of GISS IEEE*
9. Buho HOSHINO, Yuki SOFUE, Yuta DEMURA, Tsedendamba PUREVSUREN, Morine KURIBAYASHI, Kenji BABA, Enkhtuvshin ZOLJARGAL, Katsuro HAGIWARA, Jun NODA, Keiichi KAWANO, Olaf KARTHAUS, Kenji KAI (2018), Detection of dry lake beds formation and estimate of environmental regime shift in semi-arid region 沙漠研究 28-S, 109-113 *Journal of Arid Land Studies*
  10. Yuta Demura, Buho Hoshino, Yuki Sofue, Kenji Kai, Ts. Purevsuren, Kenji BABA, Jun Noda (2016) Estimates of ground surface characteristics for outbreaks of the Asian Dust Storms in the sources region *ProScience* , 21-30
  11. Yuki Sofue, Buho Hoshino\*, Eunice Nduati, Akihiko Kondoh, Kenji Kai, Ts. Purevsuren, Kenji Baba (2017) Remote sensing methodology for detection of environmental regime shifts in semi-arid region *Journal of GISS IEEE*.
  12. Yuta Demura, Buho Hoshino, Kenji Baba, Christopher McCarthy, Yuki Sofue, Kenji Kai Tsedendamba Purevsuren, Katsuro Hagiwara and Jun Noda (2018) Determining the Frequency of Dry Lake Bed Formation in Semi-Arid Mongolia From Satellite Data *Journal of MDPI-Land*
  13. Morine Kuribayashi, Keiichi Kawano, Yuta Demura, Kenji Baba, Yuki Sofue, Purevsuren Tsedendamba, Tamaki Matsumoto, Katsuro Hagiwara, Olaf Karthaus, Kenji Kai, Buho Hoshino\* (2019) Imaging of micro-organisms on topsoil particles collected from different landscape in the Gobi Desert. *E3S Web of Conferences 99, 01011, CADUC 2019*

## 7.2. Presentation

### 7.2.1 Present presentation:

1. Tsedendamba Purevsuren, Buho Hoshino, Sumiya Ganzorig, Ts.Tserendulam (2011)  
Spatial and temporal patterns of NDVI response to precipitation in Mongolian Steppe,  
日本写真測量学会北海道支, February 18, 2011 Sapporo, Hokkaido
2. Tsedendamba Purevsuren, Buho Hoshino, Sumiya Ganzorig, Ts.Tserendulam (2011)  
Spatial and temporal patterns of NDVI response to precipitation in Mongolian Steppe,  
Arid, Semi-arid Land Eco-system and Civilization in a Changing World, February 27-  
28, 2011 Rakuno Gakuen University

### 7.2.2 Poster presentation:

3. Tsedendamba Purevsuren, Buho Hoshino, Sumiya Ganzorig (2011) Spatial and  
temporal patterns of NDVI response to precipitation in Mongolian Steppe, 58th Annual  
Meeting of Ecological Society of Japan, March 8-12, 2011 Sapporo, Hokkaido
4. Tsedendamba Purevsuren, Buho Hoshino, Sumiya Ganzorig (2011) Spatial and  
temporal patterns of NDVI response to precipitation and temperature in Mongolian  
Steppe, The 1<sup>st</sup> International Conference on Arid Land (ICAL1), May 24-28, 2011  
Narita-Tokyo
5. Purevsuren Tsedendamba, Buho Hoshino, Yuki Sofue, Sumiya Ganzorig, Jugder  
Dulam Kenji Kai, Relationship between vegetation coverage and dust storms over the  
Gobi area Third JSPS Seminar of “Collaborative Research between Mongolia, China  
and Japan on Outbreaks of Asian Dust and Environmental Regime Shift, 8-12 August  
2016, Ulaanbaatar, Mongolia